STABILITY OF ZONED EARTH DAM COUPLED WITH UNSTEADY DRAWDOWN

A Thesis

Submitted to the College of Engineering of the University of Babylon in Partial Fulfillment of the Requirements for the Degree of Master of Science in Civil Engineering

By

Imad Habeeb Obiad

October *Shaaban* ١٤٢٣

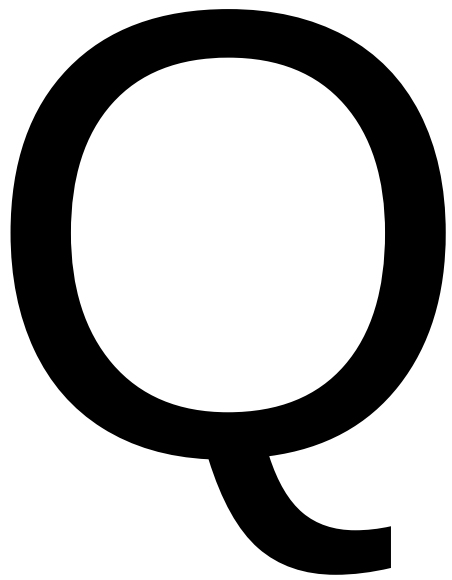

هُوَ الَّذِي بَعَثَ فِي الْأُمِّيِّينَ رَسُولًا مِنْهُمْ يَتْلُو عَلَيْهِمْ آيَاتِهِ وَيُزَكِّيهِمْ
وَيُعَلِّمُهُمُ الْكِتَابَ وَالْحِكْمَةَ وَإِنْ كَانُوا مِنْ قَبْلُ لَفِي ضَلَالٍ مُبِينٍ

صدق الله العلي العظيم

سورة الجمعة، الآية ٢

أستقرارية السد الممنطق المصاحبة للهبوط غير المستقر

الخلاصة

يتطلب تحليل إستقرارية السدود الترابية الأخذ بنظر الاعتبار التأثير المزدوج للقوى الخارجية المؤثرة على السد بالإضافة إلى القوى الناتجة عن حالة التسرب المستقر أو حالة التسرب غير المستقر خلال جسم السد.لقد بينَت العديد من البحوث والدراسات أهمية ، بل ضرورة دراسة وبحث إستقرارية السدود تحت ظروف حالة التسرب غير المستقر نتيجة لهبوط الماء في بحيرة السد.

يتضمن الجزء الأول من هذا البحث طريقة العناصر المحددة كأسلوب تحليل لإيجاد موقع السطح الحر المعتمد زمنياً ، كذلك إيجاد كل من قيمة شحنة التسرب وضغط ماء المسام داخل جسم السد . تم دراسة حالات الهبوط ألأني والمتدرج لماء بحيرة السد باستخدام هذه الطريقة ، وتبَين أن هذه الطريقة تمتاز بإستقرارية جيدة لكنها تتطلب عدد كبير من الخطوات الزمنية للوصول إلى الحالة المستقرة ، مقارنة النتائج المستحصلة مع نتائج الحلول التحليلية أظهر توافق جيد .

الجزء الثاني من هذا البحث يتضمن طريقة إيجاد موقع سطح الانزلاق الحرج ، وقيمة أقل معامل أمان مرافق لهذا السطح ، استخدمت طريقة (M orgenstern-Price) لتحليل استقرارية الميول و السدود ، حيث لا توجد محددات لهذه الطريقة من حيث شكل و موقع سطح الانزلاق ، كما إنها تحقق جميع شروط الموازنة . لقد بينَت المقارنات التي أجريت بين النتائج المستحصلة وتلك المتوفرة ضمن البحوث السابقة تقابل وتوافق جيد .

تم تطبيق الطرق أعلاه لتحليل التسرب والاستقرارية على أحد السدود العراقية الممنطقة ولحالات مختلفة من شروط الماء الخارجي في بحيرة السد ، وقد بينت النتائج المستحصلة من التحليل آن السد بصورة عامة أمن تحت تلك الظروف .

CERTIFICATION

We certify that this thesis titled "**Stability of Zoned Earth Dam Coupled with Unsteady Drawdown**", was prepared by "**Imad Habeeb Obiad**" under our supervision at Babylon University in partial fulfillment of the requirements for the degree of Master of Science in Civil Engineering.

Signature: **Signature:**

Name: Dr. Karim K. Al-Jumaily **Name: Dr. Abdul-Hassan K. Shukur**

Date: **Date:**

CERTIFICATION

We certify that we have read this thesis, titled (**Stability of Zoned Earth Dam Coupled with Unsteady Drawdown**), and as examining committee examined the student **Imad Habeeb Obiad** in its contents and in what is connected with it, and that in our opinion it meets the standard of thesis for the Degree of Master of Science in Civil Engineering (Water Resources).

Signature:
Name: Asst. Prof. Dr. Salah Taofeek Ali
(Member)
Date: / / ٢٠٠٢

Signature:
Name: Asst. Prof. Nameer A. Alwash
(Member)
Date: / / ٢٠٠٢

Signature:
Name: Prof. Dr. Rafa H.S.Al-Suhaili
(Chairman)
Date: / / ٢٠٠٢

Signature:
Name: Asst. Prof. Dr. Karim K.Al-Jumaily
(Supervisor)
Date: / /٢٠٠٢

Signature:
Name: Asst. Prof. Dr.Abdul-Hassan K.Shukur
(Supervisor)
Date: / /٢٠٠٢

Approval of the Civil Engineering Department
Head of the Civil Engineering Department

Signature
Name: **Asst. Prof. Dr. Nameer A. Alwash**
Date: / / ٢٠٠٢

Approval of the Deanery of the College of Engineering
Dean of the College of Engineering

Signature
Name :**Prof. Dr. Abdul Amir S. Resen**
Dean of the College of Engineering
University of Babylon

Date: / /

ACKNOWLEDGEMENT

All the thanks for GOD who lightened my way during the critical times.

Sincere thanks go in particular to my supervisors **Asst. Prof. Dr.Karim K. Al-Jumaily** and **Asst. Prof. Dr. Abdul-Hassan K. Shukur** for their valuable guidance and constructive suggestions during the preparation of this thesis.

It is with pleasure, I would like to thank the Dean of the College of Engineering, the Head of the Civil Engineering Department in University of Babylon for Their co-operation and assistance.

Finally, gratitude goes to my family for their encouragement and support during the course of this thesis.

Imad H. Obiad

٢٠٠٢

ABSTRACT

Stability analysis of earth dams and slopes requires consideration of the coupled effects of external loads and seepage forces due to the steady or transient flow of water. A sufficient number of failures of earth dams under unsteady drawdown conditions have been reported in the literature to demonstrate that is important if it is not critical, to investigate the stability of dams under these conditions [**Sherard *et al.***, ١٩٦٣].

The first part of this work therefore presents a finite element procedure for determination of the time dependent locations of free surface, seepage heads and pore pressures within the dam body. The seepage analysis is based on **Galerkin** method involving saturated and unsaturated zones in which the original mesh remains invariant during unsteady flow and iterations. The cases of the sudden and gradual (linear) drawdown conditions are studied by this method. The method is stable but requires a large number of time steps to reach the steady state, comparison with analytical results indicate that the maximum percentages of absolute differences are insignificant (less than ٢٪).

The second part presents a computation procedure by which the most critical slip surface and its relevant minimum factor of safety are obtained. The procedure adopts the more general **Morgenstern – Price** method of slope stability, no restrictions are imposed on the shape and location of the slip surfaces and the analysis satisfies all equilibrium conditions. Comparison between the present analysis results and those reported in the literature shows a fair correspondence, but in every case a more critical slip surface with lower factor of safety is found.

The present procedures are then utilized to re-analyze the stability of upstream side slope of a zoned earth dam. The results indicate that the dam is safe under the different water conditions that have been studied.

LIST OF CONTENTS

منسّق
منسّق
منسّق
منسّق

منسّق

منسّق

منسّق

منسّق

NOTATION

Most of the commonly used symbols are listed below; other are defined where they appear in the research.

Item	Description
C	Cohesion.
D	The problem domain.
$[D]$	Assemblage permeability matrix.
$[D^e]$	Element matrix.
E	Normal stress component of interslice force.
E_j	Maximum relative error.
$f(t)$	Function specifying variation of water level.
$f(x)$	Function variation with respect to x.
F	Factor of safety.
F_f, F_m	Safety functional.
$\{F\}$	Forcing vector.
h	Head.
H^e	Head within the element.
H_i	Height of slice (i).
H_d	Drawdown head at given time.
H_e	Head of exit point of slope.
i	Hydraulic gradient.
I	Modified Bessel function.
J_s	Bessel function of first kind of orders.
$[J]$	Jacobian matrix.
$[J]^{-1}$	Inverse of Jacobian matrix.
K	Coefficient of permeability.
$[\bar{K}]$	Permeability matrix.
K_x, K_y	Permeability in x and y directions respectively.
l_i	Portion of a boundary.
$[L]$	Transformation matrix
m	Total number of elements in the flow domain.
$[M]$	Assemblage mass matrix.

Item	Description
$[M^e]$	Mass matrix.
n	Porosity.
N_i	Shape function of the element.
P^x, P^y	Forces in x and y direction per slice, respectively.
P_i^w	Force due to pore water pressure.
q_n	Flux normal to the boundary.
R	Residual.
R^E	Element residual.
S	Distance between two points.
S_S	Specific storage.
T	Time.
U	Pore water pressure.
V	Seepage velocity of fluid.
V_X, V_Y, V_Z	Velocities in the directions of three axes x,y,z.
$[\bar{V}]$	Velocity vector.
$\{V_P\}$	Particle velocity vector.
W	Weighting function.
X, Y, Z	Global coordinate system.
α_I	Angle of inclination of slice base.
α, β	Angles of slope inclination.
ΔT	Time step.
ε_O, ε,	Tolerances.
ϕ	Angle of internal friction.
γ	Bulk density of fill.
γ_W	Water density.
λ	Constant.
Φ	Potential head.
$\lambda(T)$	Parameter.
θ_I	Angle of inclination of interslice forces.
σ	Normal stress.
χ	Shear components of interslice forces.
ζ, η	Local coordinates system.
τ	Shear stress.

G

Appendix A

SHAPE FUNCTION

The shape functions for a four-nodded quadrilateral with corner nodes where $\eta = \pm ١$, and $\zeta = \pm ١$, takes the form:

$$N_1 = \frac{1}{4}(1-\zeta)(1-\eta) \quad \text{..... (A-١)}$$

$$N_2 = \frac{1}{4}(1-\zeta)(1+\eta) \quad \text{..... (A-٢)}$$

$$N_3 = \frac{1}{4}(1+\zeta)(1+\eta) \quad \text{..... (A-٣)}$$

$$N_4 = \frac{1}{4}(1+\zeta)(1-\eta) \quad \text{..... (A-٤)}$$

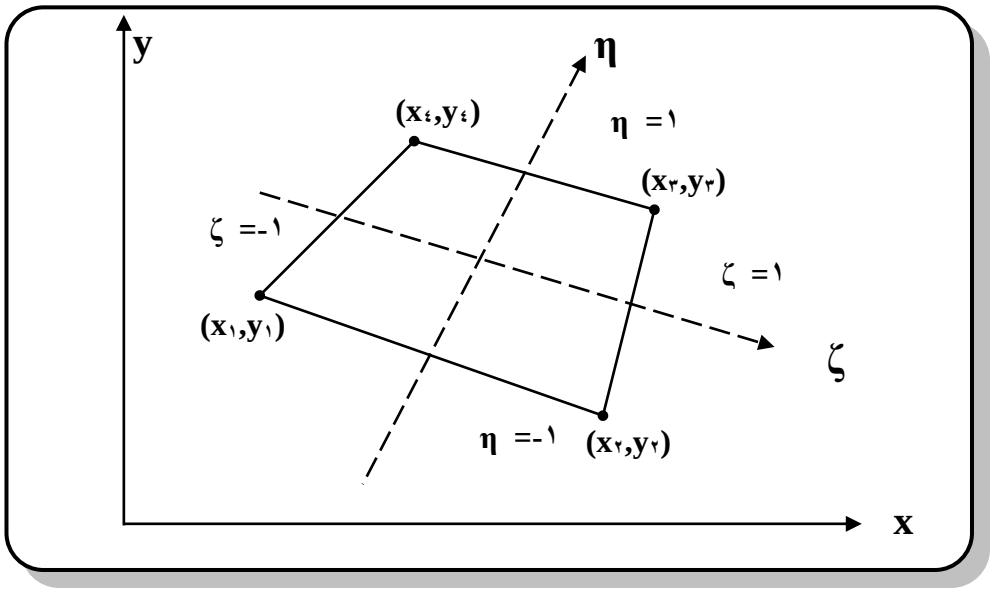

Figure (A-١): Typical quadrilateral finite element

Appendix B

EXPLANATION OF PROGRAMS

B

B-١ General

The following paragraph presents a brief explanation of the various parts of the plane free surface flow program and slope stability program used in this thesis. Some of the subroutines are extracted from I.M. Smith (١٩٨٨) and from R. Baker (١٩٨٠), while the others are modified in this work.

B-٢ Divisions of Plane Free Surface Flow Program

The main program includes a number of major subroutines as shown in Figure (٣.٥). The major subroutines are:

١. Geometry Subroutine

This subroutine forms the coordinates and steering vector for four-node quadrilaterals element, numbering in x-direction. Generating invariant mesh, ١-freedom per node as shown in Figure (B-١).

٢. FORMLN Subroutine

This subroutine forms the shape functions and there derivatives for four noded quadrilateral element in local coordinates (η, ζ). Gaussian integration points needed in this subroutine specified from GASS subroutines as shown in Figure (B-٢).

٣. MATMUL Subroutine

This subroutine forms Jacobian matrix by multiplication of shape function derivatives matrix by coordinate matrix, as this routine calls another subroutine as follows.

(a) JACOB Subroutine

This subroutine forms the inverse of Jacobian matrix and its determinant as shown in Figure(B-٣).

٤. FSURF Subroutine

This subroutine is used to determine the coordinate of free surface nodes for each time level during drawdown process as shown in Figure (B.٤).

٥. CHECON Subroutine

This subroutine is used to perform convergence criterion by set converged to "false" if relative change in HEAD and OLHEAD is greater than tolerance and updates OLD HEAD, as shown in Figure (B-٥).

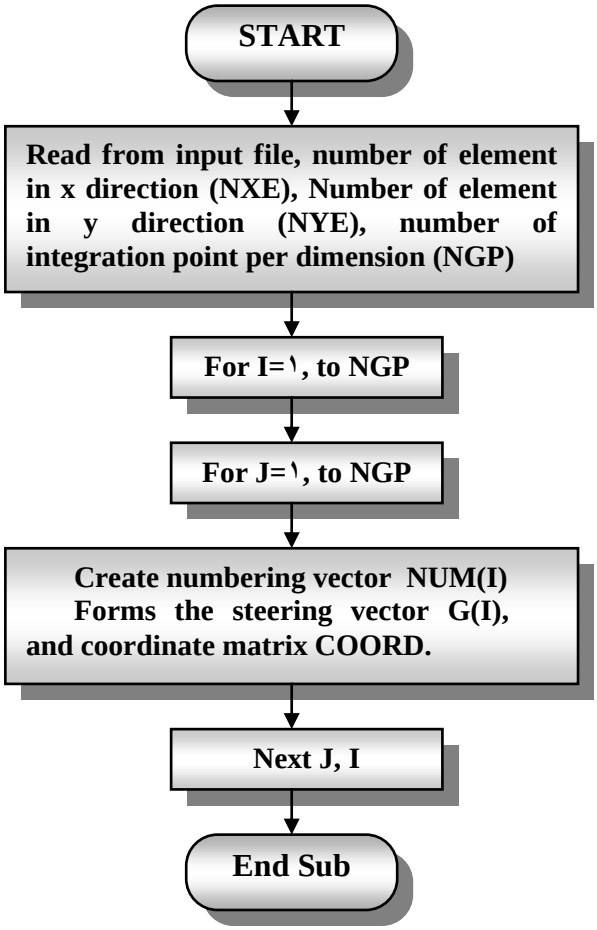

Figure (B-١): Geometry subroutine flowchart

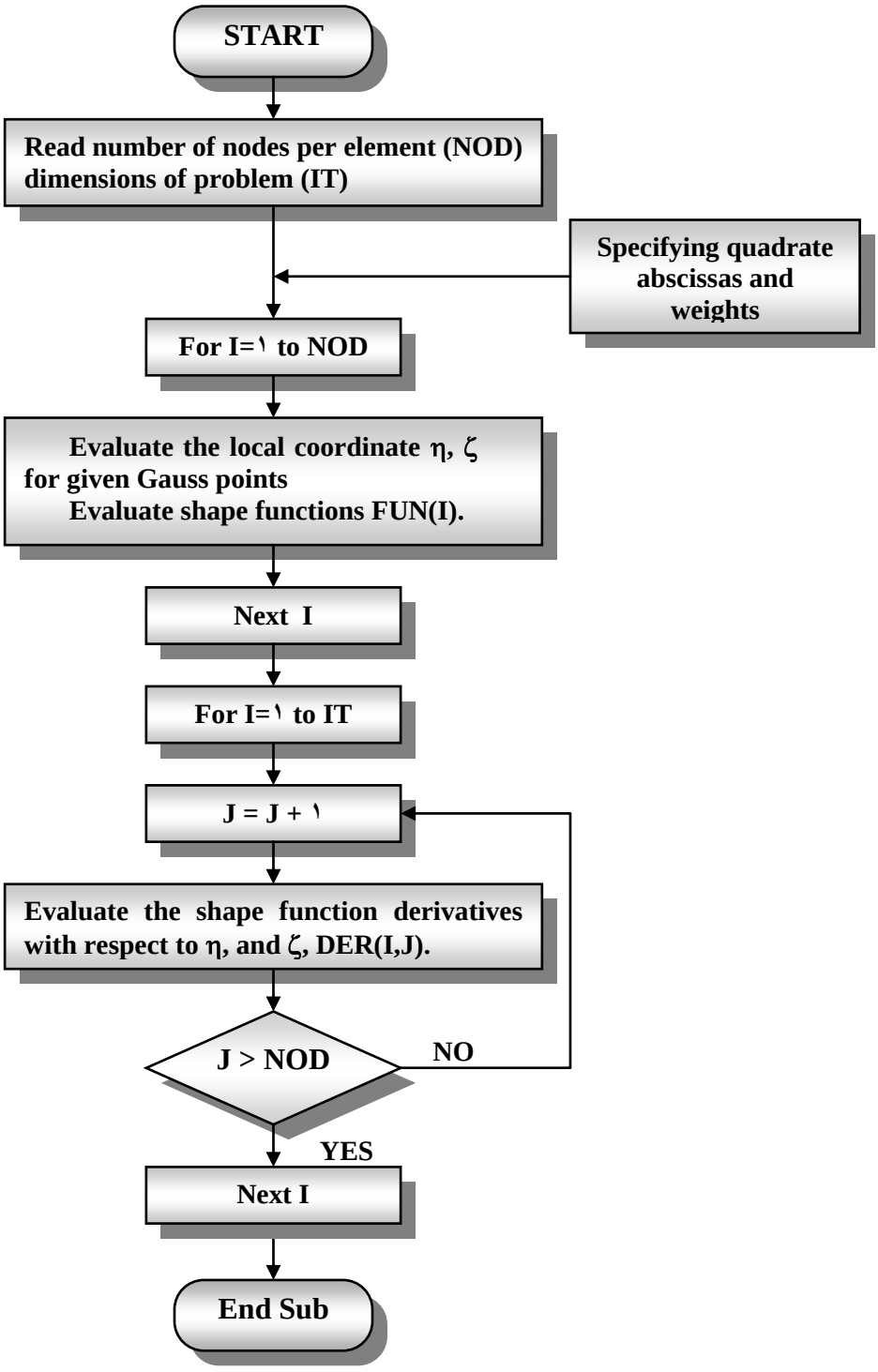

Figure (B-٢): FORMLN subroutine flowchart

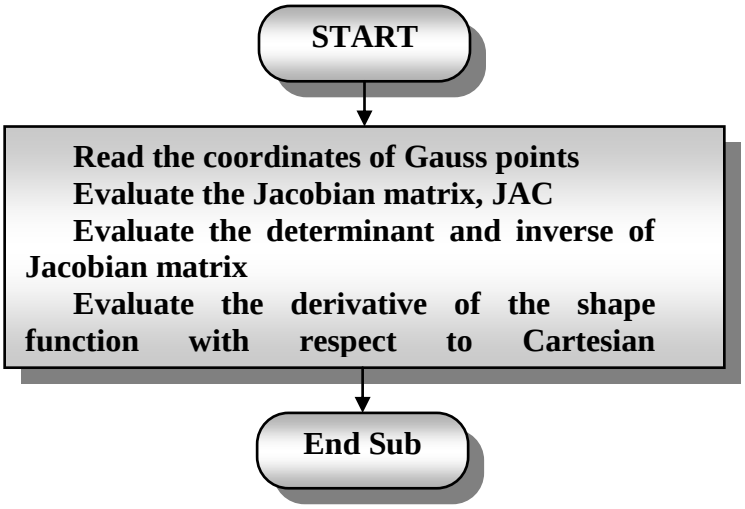

Figure (B-٣): JACOB subroutine flowchart

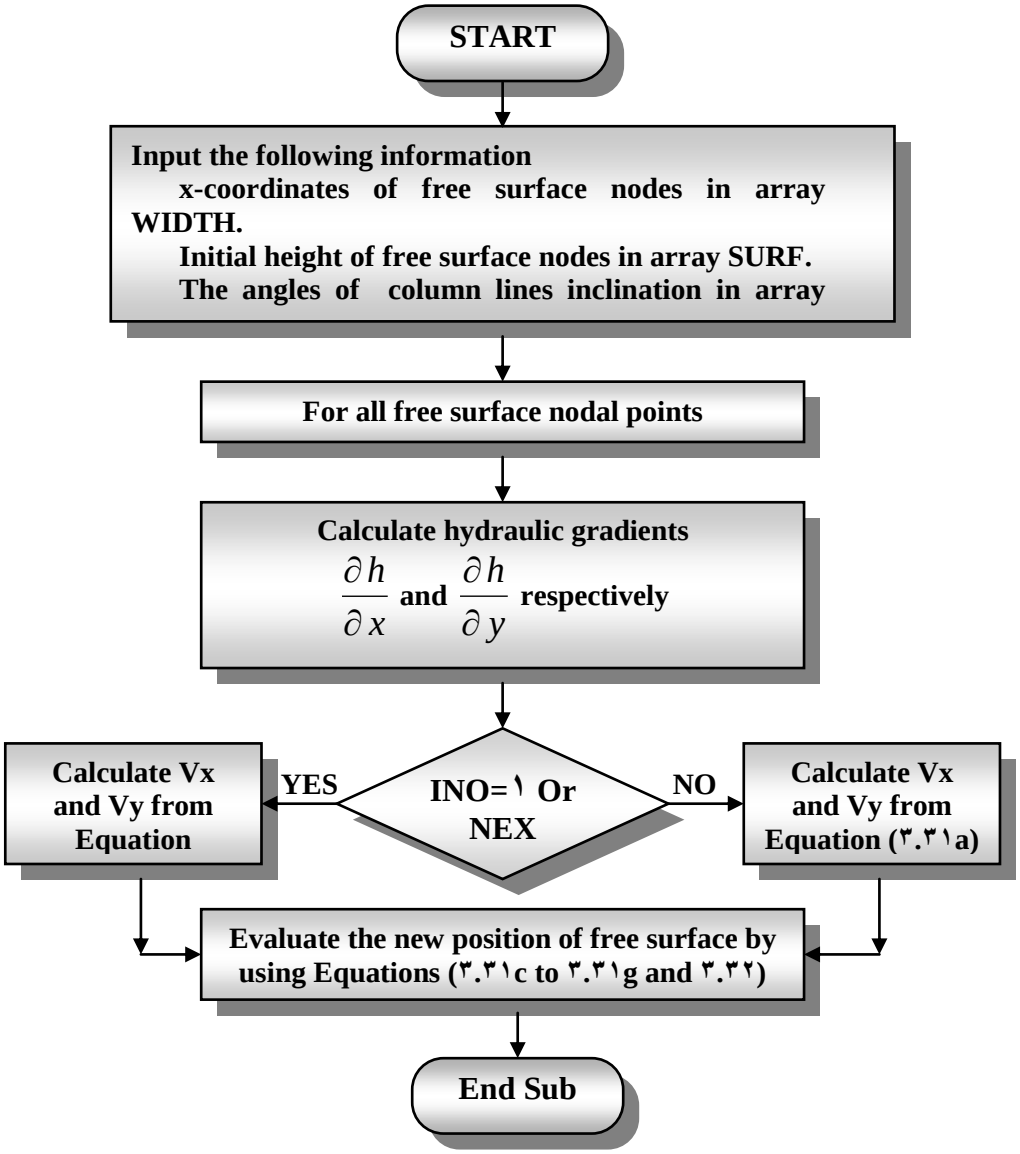

Figure (B-٤): FSURF subroutine flowchart

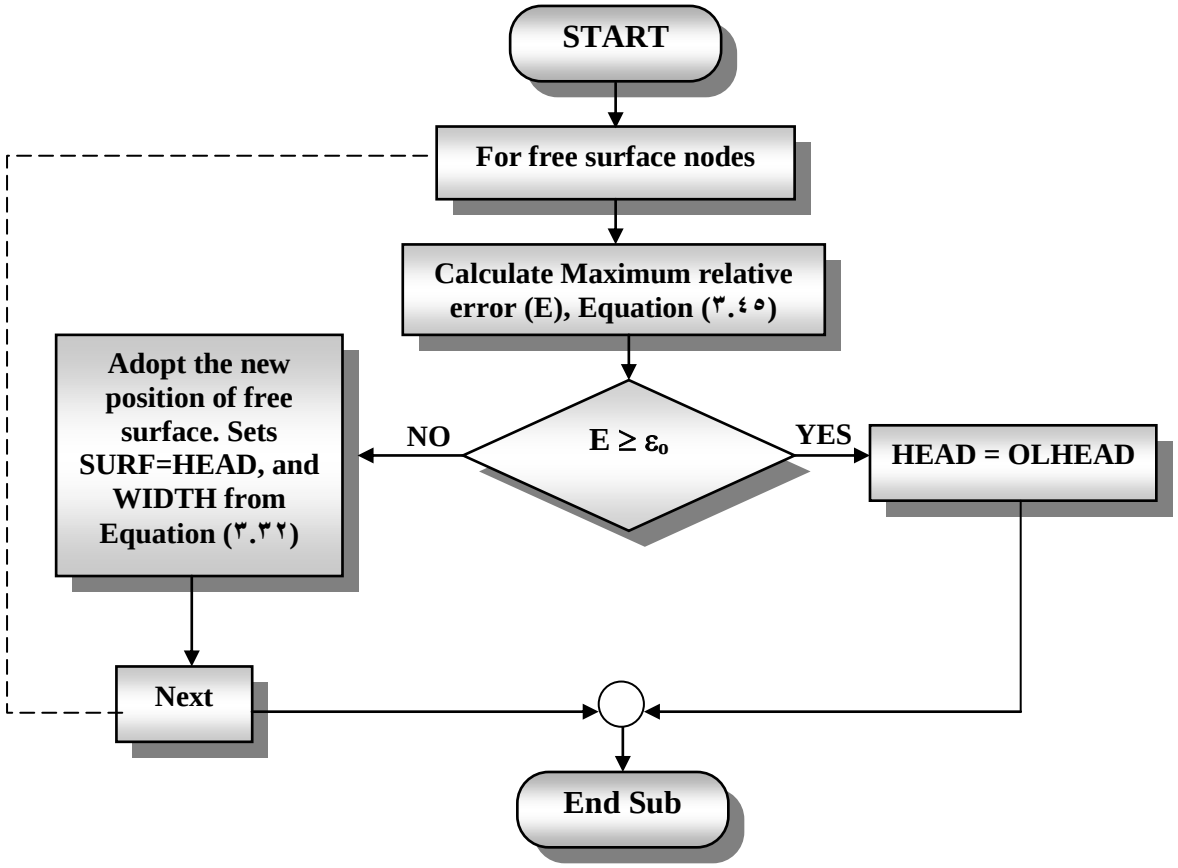

Figure (B-٥): CHECON subroutine flowchart

B-٣ Divisions of Slope Stability Program

In this program the major subroutine is MPM (Morgenstern-Price Method). This subroutine is used to perform the slope stability computation according to Mergenstern-Price Method as shown in Figure (B-٦).

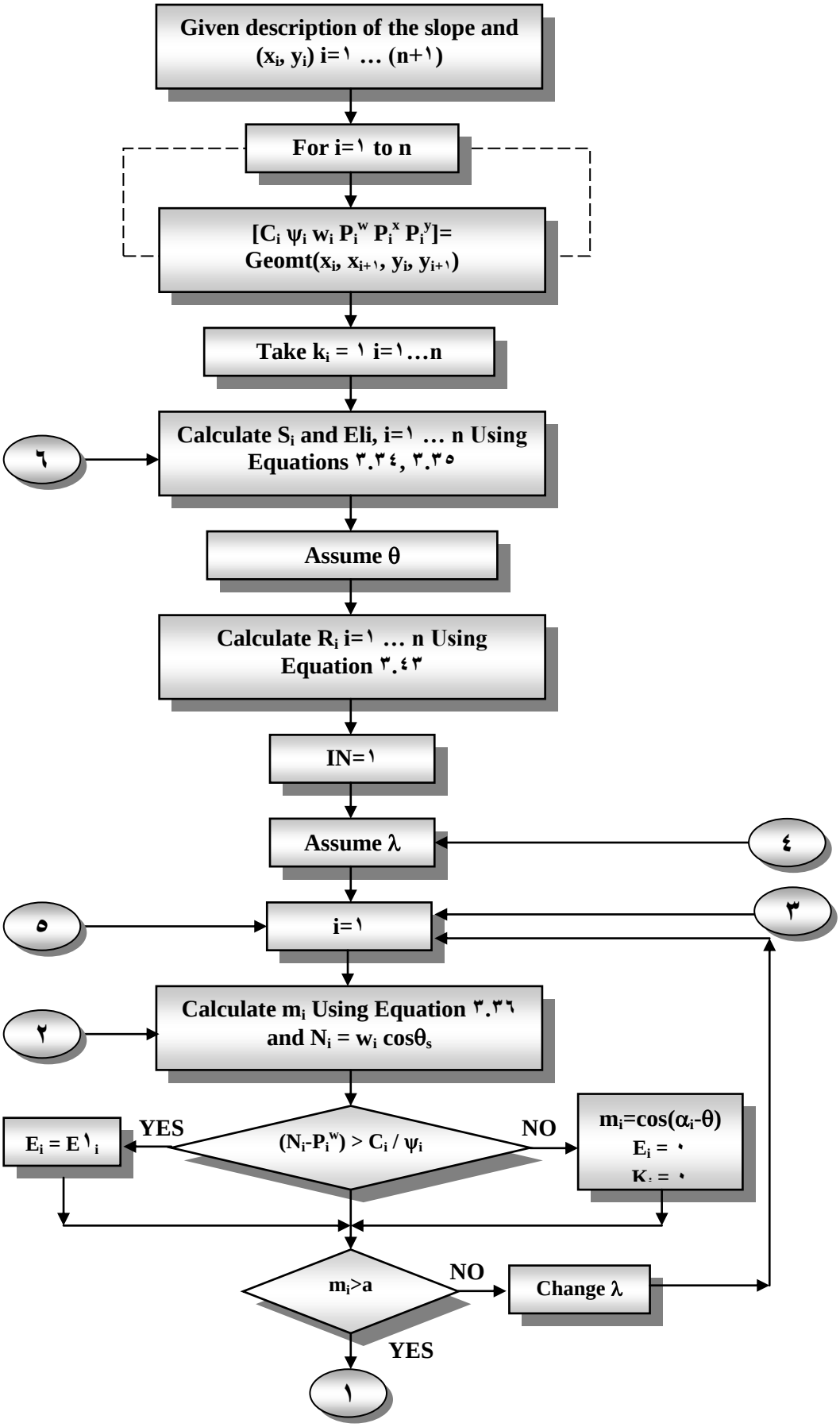
Given description of the slope and
(xi, yi) i=١ … (n+١)
For i=١ to n
[Ci ψi wi Pi^w Pi^x Pi^y]=
Geomt(xi, xi+١, yi, yi+١)
Take ki = ١ i=١…n
٦
Calculate Si and Eli, i=١ … n Using
Equations ٣.٣٤, ٣.٣٥
Assume θ
Calculate Ri i=١ … n Using
Equation ٣.٤٣
IN=١
Assume λ
٤
٥
i=١
٣
٢
Calculate mi Using Equation ٣.٣٦
and Ni = wi cosθs
Ei = E١i
YES
(Ni-Pi^w) > Ci / ψi
NO
mi=cos(αi-θ)
Ei = ٠
Ki = ٠
mi>a
NO
Change λ
YES
١

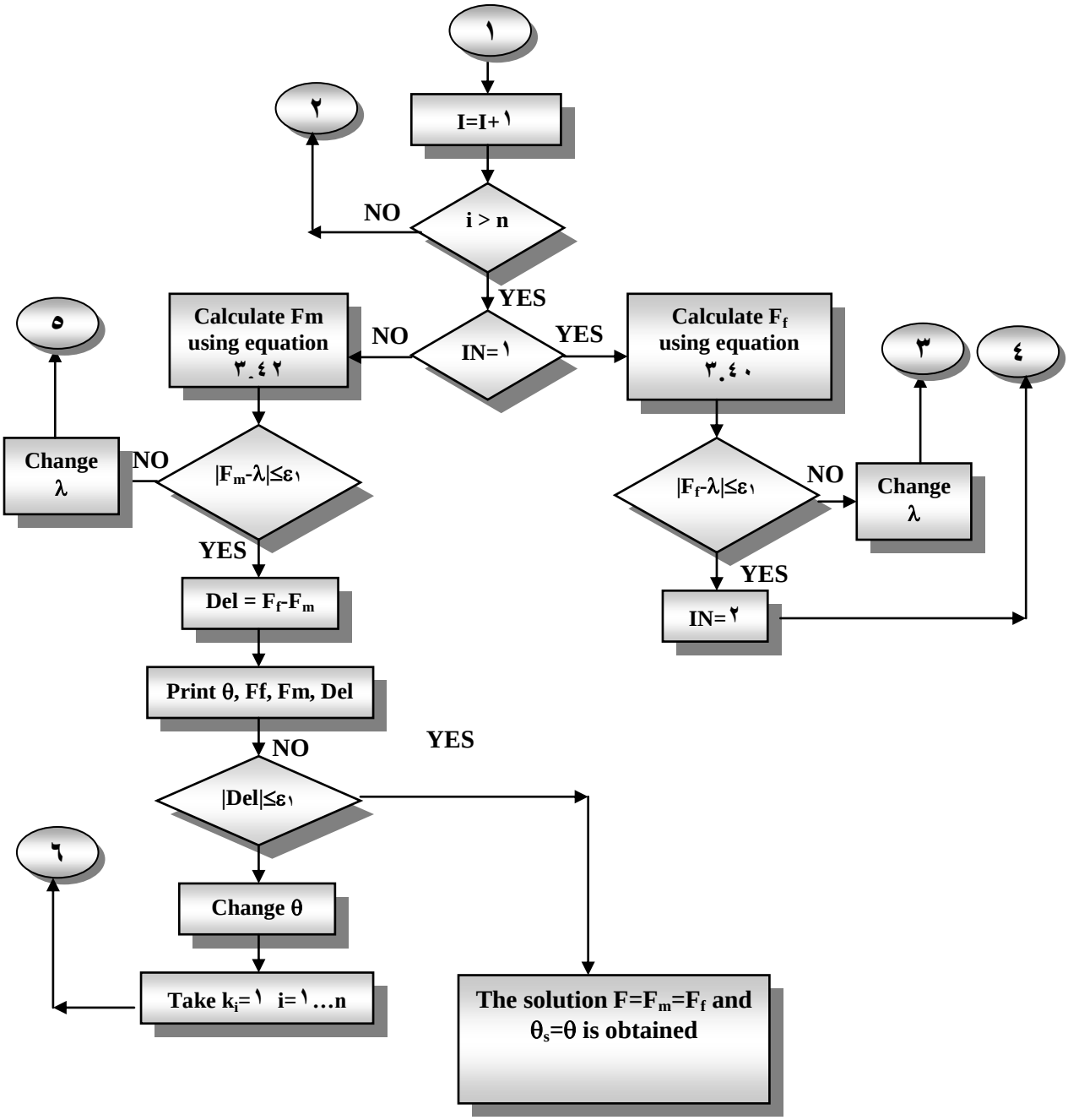

Figure (B-٦): The procedure MPM (Morgenstern-Price Method).
(Fs, θs)=MPM {(xi,yi)i=١...(n+١)}

Appendix C

INTERPOLATION OF PORE PRESSURE

The pore pressure values used in slope stability analysis are interpolated from a data file created by a finite element analysis for seepage problem. The subroutine PFIND used in slope stability program uses the coordinate positions and pore pressure values form the seepage data file, selects the three closest points to the center base of slice under consideration as shown in Figure (C-٢), and calculates the appropriate pore pressure value using the linear interpolation formula:

$$P(x_c, y_c) = \frac{\ell_2 \times \ell_3 \times P(I_1) + \ell_1 \times \ell_3 \times P(I_2) + \ell_1 \times \ell_2 \times P(I_3)}{\ell_2 \times \ell_3 + \ell_1 \times \ell_3 + \ell_1 \times \ell_2} \quad \text{.....(C-١)}$$

where:

$P(x_c, y_c)$ = interpolated pore pressure in the center base of slice (i).

$l_١$, $l_٢$, $l_٣$=the distance between the closest three points to the center base of slice (i).

$P(I_١)$, $P(I_٢)$, $P(I_٣)$ = the pore pressure values at these points.

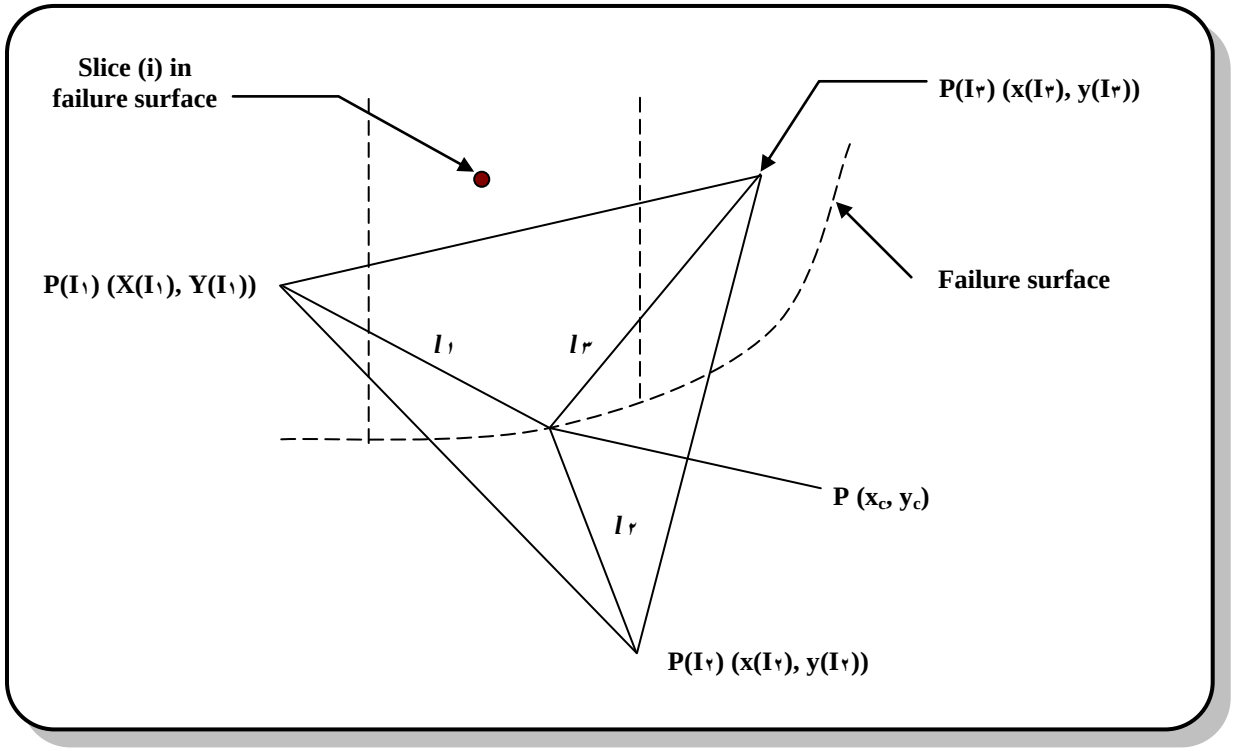

Figure (C-١): Interpolation of pore pressure from data file

Chapter One

INTRODUCTION

١.١ General Remarks

It is probably safe to say that few engineering projects have a greater ability to stir men's minds than the design and construction of a large dam. Within the engineering profession there is the excitement that a massive integrated engineering endeavor creates.

The ability of civil engineering profession to produce successful designs has promoted precedent as the most significant factor influencing the design of new dams. Dams designed on the base of precedent tend to be conservative, especially where uncertainties regarding the material properties or structural behavior exist. Performance of a new dam is estimated from previous experience and simple analysis rather than as a result of a truly fundamental understanding of the structure itself [**Al-Qaisi**, ١٩٩٩].

When the reservoir is full, the critical region is near the downstream face. If no drainage arrangement is made and the slope is also steep, the phreatic line may intersect the downstream slope creating serious conditions there. This can be avoided by provide drainage filter or drainage toe, etc. or by broadening the base of dam so that the head loss is great enough to bring the line of saturation beneath the downstream toe of the dam. For the upstream slope, the critical condition can occur, when the reservoir suddenly emptied. In such a case, the water level with the soil will remain, as it was when the soil pores were full of water. The weight of this water within the soil, now, tends to slide the upstream slope along a circular arc [**Garrg**, ١٩٩٨].

A sufficient number of failures of earth dams under draw down conditions have been recorded to demonstrate that it is important, if not critical, to investigate the stability of the structure under these conditions. These details of earth dam failures which occurred due to the draw down of the reservoir have been given by [**Sherard** ١٩٥٣, quoted from **Sherard *et al.***, ١٩٦٣].

No two dams are exactly a like, individual dams different their dimensions, design, and purpose. They differ in the nature of the site they occupy and in the size of the reservoir they impound. In the present work the role of ground water is examined in the context of large earth dams.

١.٢ Numerical Analysis and Design of Dams

A numerical analysis is of a particular significance if a new design concept is involved. The major contribution of numerical analysis in the design of dam may be divided into two aspects:

١. Ranges of solutions are possible using different values of material parameters. Variation on the geometry can also be studied with ease.

٢. The idealization of the structure and identification of the factors affecting it is behavior result in a better understanding overall the structural performance. Thus, design concepts may improved and innovations in a design can be made with confidence.

As the numerical procedures develop and improve and material properties are more closely identified, the accuracy predictions also improved. The results that will be predicted may differ form the observed measurements by only small amounts. Errors may be due, not to weakness in the analysis, but only variability of construction materials used and other associated or non-technical factors.

١.٣ Aims of the Present Work

The main targets of the present work can be summarized as follows:

١. To build a general model to study seepage problem under transient conditions and overall stability of side slopes of the earth dams.

٢. To verify the model to check the reliability of the program. The following problems are solved to investigate the aforementioned parameters:

a. Analytical solution for the previously published work by **Suresh** and **Harr** (١٩٦٢).

b. The Otter Brook dam constructed in New Hampshire, U.K.

٣. To prepare stability charts to be used as guidelines for the analysis and design of earth dams.

٤. Re-analysis the stability of side slopes of one of Iraqi zoned earth dam.

Chapter Two

A REVIEW ON SEEPAGE AND STABILITY THEORIES

٢.١ General

The aim of this chapter is to present the necessary background and theory upon which stability and seepage are based upon. Consideration must, therefore, be given to a number of different topics. First, a description of seepage theories in soil mechanics are presented . Later on, a brief description of the theories of stability are described.

٢.٢ Review on Calculation of Seepage Pressures in Embankment Dams

٢.٢.١ General

The stability of earth dams subjected to the effects of changing reservoir levels is dependent on, among other factors, the pore pressures induced within the earth mass due to seepage. The pore pressures are generally estimated from flow net analysis obtained under steady state conditions. However, a more precise determination of pore pressures is warranted for the case of a continuously moving free surface. The expected distribution of seepage pressures and the position of the free surface are required so that filters and drains can be designed and positioned correctly to give acceptable flow distribution and seepage quantities. Civil engineering has traditionally relied upon the graphical method of flow nets to determine seepage pressures for steady state conditions in the earth dams. However, the process of flow net construction requires skill and time and in many practical problems simplifying assumptions have to be made. Analytical methods are available but they are

mostly limited to simple cases. Numerical methods based on finite difference and finite elements approaches now remove the many limitations associated with anisotropy and non-homogeneity.

٢.٢.٢ Steady-State Seepage Through Earth Dams

The most critical conditions are likely to occur with the reservoir full under steady state seepage and those ensuring during and after rapid drawndown of the reservoir. In order to assess the factor of safety of a potential slip surface, the distribution of pore pressure in the dam must be known. Failures of earth or rockfill dams can be resulted from excessive leakage from piping at the toe, or from slope failures on the dam face [**Freeze** and **Cherry**, ١٩٧٩]. All the three can be analyzed with the aid of steady-state flow net. For rare situations where an earth dam is constructed on the impervious formation, the flow net can be limited to the dam itself, where the foundation materials are also permeable and the flow net must include the entire dam foundation system.

٢.٢.٣ Transient Seepage Through Earth Dams

Slope failures on the upstream face of a dam are usually the result of rapid drawdowns in the reservoir level. At full supply levels the effects of high pore pressures in the face are offset by the weight overlying reservoir water. Following rapid drawdown, the high pore pressure remain, but the support has been removed. Unless the transient dissipation of these pore pressure is rapid, that is, unless the transient drainage of the dam face is rapid, instabilities may develop on the critical slip surface and slope failures can occur.

٢.٢.٤ The Theory of Seepage in Porous Media

The principle of the flow of water in soils are outlined here and the validity of Darcy's law is discussed for saturated flow.

The equations of flow are written in terms of the total, or hydraulic heads, these being the fundamental driving potentials for both saturated and unsaturated flow. A full mathematical treatment of the whole subject is already given in numerous [**Harr**, ١٩٦٢], and [**Freeze** and Cherry, ١٩٧٩].

٢.٢.٤.١ Darcy's Law

The "Darcy's law of seepage" establishes a linear relationship between the seepage velocity and hydraulic head gradient. This law, which is a simple consequence of viscous flow neglecting inertial effects, can obviously be written in the form:

$$v = -k\,i \qquad \text{.....(٢.١)}$$

or $$v = -k\frac{d\phi}{d\,s} \qquad \text{.....(٢.٢)}$$

where:

v : seepage velocity of fluid in porous medium,

k : coefficient of permeability or hydraulic conductivity,

i : hydraulic gradient,

ϕ : total or potential head,

and s = distance between two points in flow media.

If the velocities in the direction of three orthogonal axes $\bar{x}$, $\bar{y}$ and $\bar{z}$ are designated by a vector, $\bar{v}$, or

$$\left[\bar{V}\right] = \begin{bmatrix} v_{\bar{x}} \\ v_{\bar{y}} \\ v_{\bar{z}} \end{bmatrix} \qquad \text{.....(٢.٣a)}$$

and if the head gradient is defined similarly by it's three components,

$$-\left[grad\bar{\phi}\right]=\begin{bmatrix}-\frac{\partial\phi}{\partial\bar{x}}\\-\frac{\partial\phi}{\partial\bar{y}}\\-\frac{\partial\phi}{\partial\bar{z}}\end{bmatrix} \qquad \text{.....(٢.٣b)}$$

then the most general linear relationship that can exist between the two quantities is of the form

$$\left[\bar{V}\right]=-\left[\bar{K}\right]\left[grad\bar{\phi}\right] \qquad \text{.....(٢.٣c)}$$

in which $\left[\bar{k}\right]$ is a ٣-by – ٣ matrix defined by nine numerical coefficient. It can, however, be shown that matrix $\left[\bar{k}\right]$ must be symmetrical to satisfy conservation of energy and therefore it appears that only six coefficients are necessary to define it. If direction of the axes is changed to *x*, *y*, *z*, then the velocity vector of the direction of new axes can be found as,

$$\left[V\right]=\begin{bmatrix}v_x\\v_y\\v_z\end{bmatrix}=\left[L\right]\left[\bar{V}\right] \qquad \text{.....(٢.٣d)}$$

in which [*L*] is transformation matrix of direction cosines. Similarly the vector of head gradient.

$$-\left[grad\phi\right]=\begin{bmatrix}-\frac{\partial\phi}{\partial x}\\-\frac{\partial\phi}{\partial y}\\-\frac{\partial\phi}{\partial z}\end{bmatrix}=-\left[L\right]\left[grad\bar{\phi}\right] \qquad \text{.....(٢.٣e)}$$

combining Eqs. (٢.٣c), (٢.٣d), and (٢.٣e) yields

$$\left[V\right]=-\left[k\right]\left[grad\ \phi\right] \qquad \text{.....(٢.٣f)}$$

in which the new permeability matrix is

$$[k]=[L][\bar{k}][L^{-1}] \qquad \text{.....(٢.٣g)}$$

with this type of transformation, and if *k* is symmetrical, it is always possible to find three orthogonal directions for which *k* reduces to a diagonal matrix giving

$$[V]=-\begin{bmatrix} k_x & 0 & 0 \\ 0 & k_y & 0 \\ 0 & 0 & k_z \end{bmatrix}[grad\ \phi] \qquad \text{.....(٢.٣h)}$$

these directions are known as the principal axes of the porous material and the particularly simple relationship Equation (٢.٣f), in the direction of these axes are obviously worth noting. In a stratified material such as rock or soil the behavior in a direction perpendicular to the strata is symmetrical and this axis coincides with one of principal directions. In the plane of the strata the material often has no preferential direction and axis in that plane is, therefore, a principle axis [**Zienkiewicz *et al.***, ١٩٦٦].

٢.٢.٤.٢ The Equation of Continuity

The equation of continuity states mathematically that matter can neither be created nor destroyed. The derivation is standard and applies to both saturated and unsaturated flow. The derivation is traditionally done by referring to a unit volume of porous media as shown in Figure (٢.١), such an element is usually called control volume.

The law of conservation of mass for transient flow requires that the net rate of fluid mass flow into any elemental control volume be equal to the time rate of change of fluid mass storage within the element. With reference to Figure (٢.١), The equation of continuity takes the form:

$$\frac{\partial(\rho V_x)}{\partial x}+\frac{\partial(\rho V_y)}{\partial y}+\frac{\partial(\rho V_z)}{\partial z}=-\frac{\partial(\rho n)}{\partial t} \qquad \text{.....(٢.٤)}$$

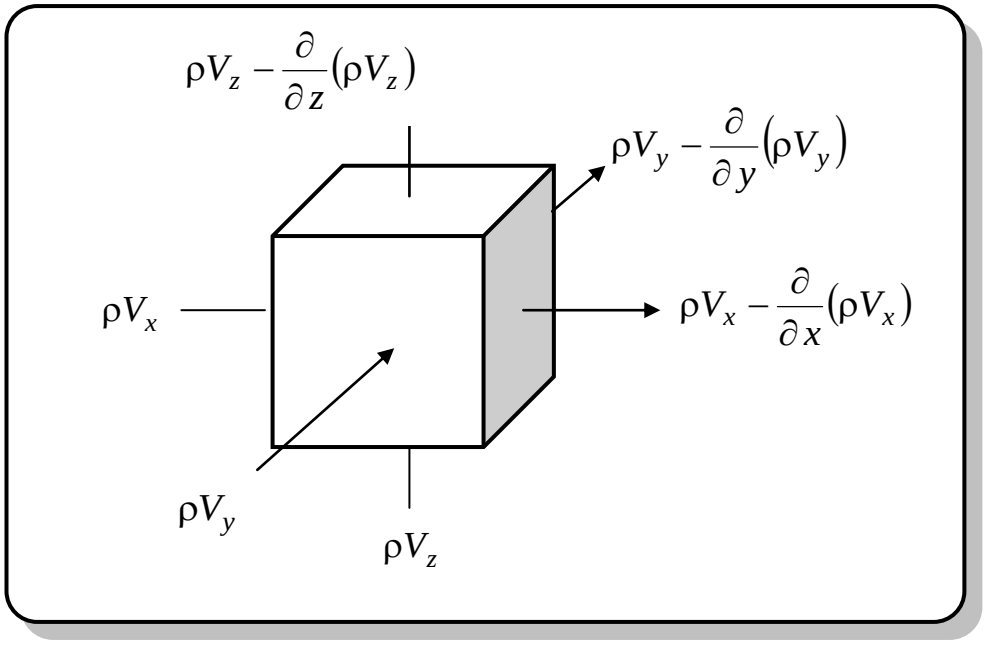

Figure (٢.١) Elemental control volume for flow through porous media. [After **Freeze** and **Cherry**, ١٩٧٩]

where (ρ) is the fluid density, (*t*) is the time, and (*n*) is the porosity of soil. The (ρ*v*) terms have the dimensions of a mass rate of flow a cross a unit cross section area of elemental control volume.

٢.٢.٤.٣ Derivation of the Governing Equation

The governing equation is derived by mathematically combining the Darcy's equations of flow with the equation of continuity. Expanding the term in right hand side of Equation (٢.٤) gives:

$$\frac{\partial(\rho V_x)}{\partial x} + \frac{\partial(\rho V_y)}{\partial y} + \frac{\partial(\rho V_z)}{\partial z} = n\frac{\partial \rho}{\partial t} + \rho\frac{\partial n}{\partial t} \qquad \text{.....(٢.٥)}$$

known that change in (ρ) and change in (*n*) are both produced by a change in hydraulic head (*h*). For a transient flow in two dimensions saturated porous media, the simplifications may be made.

The fluid under consideration is the water, i.e. ρ is constant, and $\frac{\partial V_z}{\partial z} = ٠$.

By combining the Darcy's equation for saturated porous media obtained, $V_x = k_x \frac{\partial h}{\partial x}$, *and* $V_y = k_y \frac{\partial h}{\partial y}$.

The governing equation reduces to the form.

$$\frac{\partial}{\partial x} k_x \frac{\partial h}{\partial x} + \frac{\partial}{\partial y} k_y \frac{\partial h}{\partial y} = S_s \frac{\partial h}{\partial t} \qquad \text{.....(٢.٦)}$$

where (h) is the hydraulic head at any point $P(x, y, t)$, and (S_s) is the specific storage. The governing equation for a homogeneous saturated porous media for two dimensions in linearized form [**Suresh** and, **Harr**, ١٩٦٢; **Desai** and, **Sherman**, ١٩٧١] is:

$$k_x \frac{\partial^2 h}{\partial x^2} + k_y \frac{\partial^2 h}{\partial y^2} = \lambda(t) \frac{\partial h}{\partial t} \qquad \text{.....(٢.٧)}$$

in which k_x and k_y are the horizontal and vertical permeability respectively, and $\lambda(t) = \frac{n}{h(0,0,t)}$.

This equation is often called ***Boussineq*** equation [**Bear** and **Verrvijt**, ١٩٩٠] .
For steady state flow of saturated isotropic porous media, the well known Laplace's equation is:

$$\frac{\partial^2 h}{\partial x^2} + \frac{\partial^2 h}{\partial y^2} = 0 \qquad \text{.....(٢.٨)}$$

٢.٢.٥ Methods for Solution of Seepage Equations

In order to do seepage analysis, a general model describing the phenomena of seepage must be available. Supplied with specific boundary conditions and soil properties, this model can be used to determine heads and flow distribution and seepage quantities. The Laplace's equation is a

mathematical basis for several methods have been developed to solve exactly or approximately Laplace's equation for various cases of seepage, Figure (٢.٢) [**U.S**. **Army Crops. of Engineers**, ١٩٨٦]. One of most widely used methods.

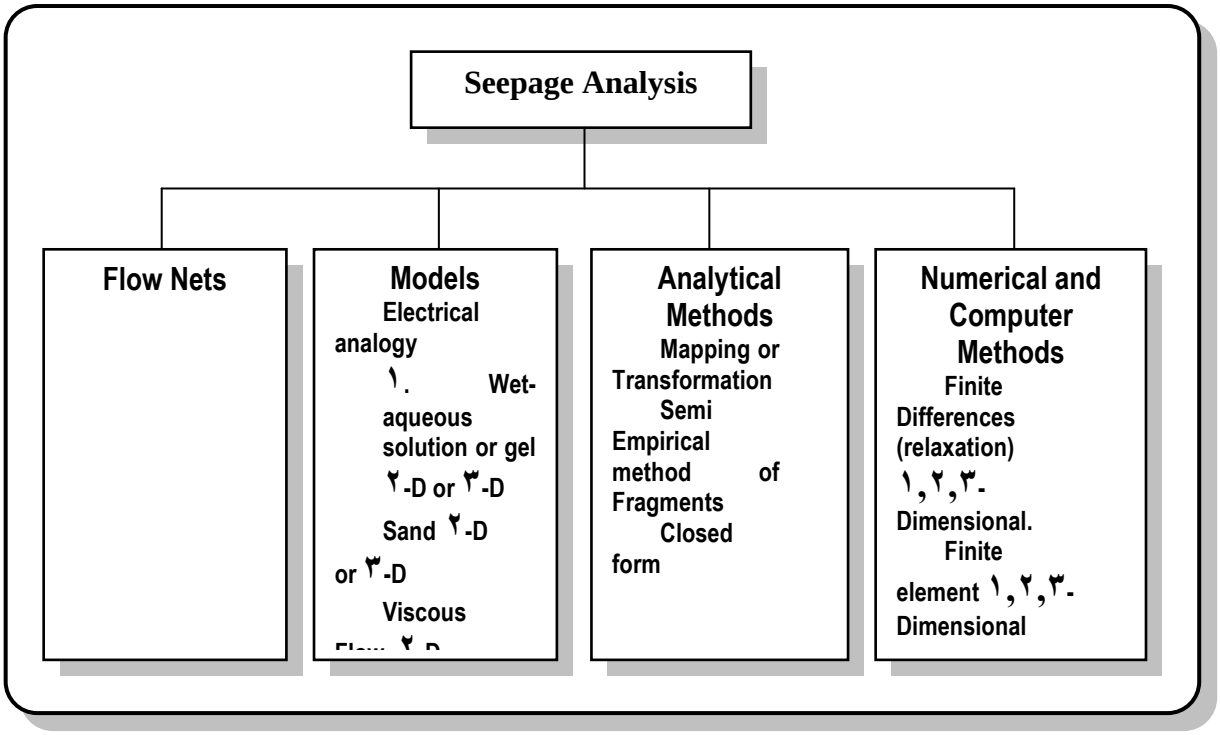

Figure (٢.٢) Seepage analysis methods. [After **U.S. Army Crops. of Engineers**, ١٩٨٦]

٢.٢.٥.١ Graphical Method-The Flow Net

Flow nets are one of the most useful and accepted methods for solution of seepage equation (e.g., Laplace's equation) [**Cedergren**, ١٩٦٧]. The solution of seepage equation (٢.٧) or (٢.٨) in two dimensions may be presented by two families of curves intersecting one another orthogonally and forming a pattern of curvilinear squares. The two families of lines are known as equipotential lines, or lines joining points of equal total head, and streamlines. A streamline is the locus of the path of flow of an individual particle of water. The mesh formed by the intersection of these two sets of curves is known as a flow net.

A unique solution of Laplace's equation may therefore be obtained graphically by trail-and-error sketching of a flow net, which satisfies the boundary conditions, preserve right angle intersections and consists of

curvilinear squares. The method may be extended to include simple anisotropic conditions by transforming the section before the flow net is constructed so that the dimensions of the cross section are shurk in the direction of greater permeability [**Lambe** and **Whitman**, ١٩٦٩ and **Garrg**, ١٩٩٨]. If a section consists of two materials having different permeabilities, the net may be drawn so that the length to width ratio of the squares is equal to the ratio of permeabilities. Confined and unconfined flow solutions to transient advance problems are also possible. **Cedergren** (١٩٦٧) comprehensively describes the method and many examples on the flow nets are given.

The undesirable feature of the flow net methods lies in the difficulty of sketching the net. An accurate net for even a simple two-dimensional flow situation can require many hours of skilful and experienced laborer.

However, the solution of two dimensional problem is relatively insensitive to the quality of flow net and even a poor attempt may yield suitably accurate results for the pore pressure, seepage quantities and gradients. Nevertheless, a solution by the flow net method is scarcely possible for the case of heterogeneous section or one in which the directions of the principal axes of anisotropy do not coincide throughout the flow domain. Non-linear problems in which the permeability is a function of pressure head are also excluded whether these are concerned with non-Darcian or unsaturated flow.

٢.٢.٥.٢ Analytical Method

Harr (١٩٦٢) explained the use of transformations and mapping to transfer the geometry of seepage problem from one complex plane to another. In this manner, the geometry of a problem may be taken from a plane where the solution is unknown to a plane where the solution is known. While this method has been used to obtain solution to general problems it is not frequently used for solutions to site-specific seepage problems since it requires the use of complex variable theory and proper choice of transformation functions.

Unconfined flow in dams was also studied by **Numerov** [reported by **Harr** ١٩٦٢] who obtained solution in graphical form but, unfortunately, its application is still not straight forward.

Suresh and **Harr** (١٩٦٢) has derived a general solution for a free surface response to the history of the reservoir fluctuations. Detailed solutions are obtained for reservoirs with constant head-water levels and with linear variations of head-water levels for various inclinations of upstream slope. The results are reduced into graphical form. Comparison between analytical results and experimental results obtained from a Hele-show viscous flow model were done. Comparisons with model studies strongly indicated that given the history of the reservoir fluctuations the developed solution can predict with some reliability the response of the free surface within homogenous earth dams, founded on impervious base with any orientation of upstream slope.

Al-Assaf (١٩٩٨) has derived analytical solution for aquifer response to the stage variation in a surface-water such as a stream. The effect of the stream fluctuation on aquifer or aquiolude that is bounded laterally by a medium of different hydraulic properties have been investigated. Analytical expressions for the change in ground water flow rate of ground-water flow, and volume of accumulated water in response to stream fluctuation have been derived. Two different approaches of approximating the stream hydrograph i.e. the sudden changes and the linear variations were investigated and given nearly the same result.

٢.٢.٥.٣ Numerical and Computer Methods

Numerical method are used for problems involving regional studies where the simplified analytical models can no longer describe the hydraulic behavior accurately [**Wang** and **Anderson**, ١٩٨٢]. Moreover, even complex numerical solutions, can be handled now-a-days with presence of a very high-speed

computer. There are many methods of numerical solutions that are used in seepage modeling. As stated in [**Bear** and **Verruijt**, ١٩٩٠], these methods are: finite difference; finite elements; integrated finite difference; boundary elements and analytical elements method. Each method has special features which may be desirable for a particular application.

١- Finite – Difference Method

The finite difference method solves the flow equations by approximating them with a set of linear algebraic equations. The flow region is divided into a discrete rectangular grid with nodal points, which are assigned values of head. Using Darcy's law and the assumption that the head at a given node is the average of the surrounding nodes, a set of *N* linear algebraic equation with *N* unknown values of head are developed [**U.S. Army Crops. of Engineers**, ١٩٨٦]. A numerical finite difference solution to steady state flow situations was first presented by **Show** and **South well** in ١٩٤١ but the development of the method accelerated with advance of digital computers [**Al-Qaisi**, ١٩٩٩].

Pinder and **Bredehoeft** (١٩٦٨) presented a numerical solution to a mathematical problem of unsteady state condition, using finite difference approximation. The results of this model were compared with those obtained from the analytical approach for problems in homogenous media of simple geometry and with electric analogue results for realistic aquifer. The results of this comparison indicated that the numerical solution gives good results.

Verma and **Brutsaert** (١٩٧١) presented a finite difference solution of unsteady free surface ground water seepage problem. They obtained by using a successive overrelaxation iterative scheme the fall of water table and the rate of outflow into adjoining stream from two-dimensional unconfined aquifer of rectangular cross section. The results and conclusions reached are summarized by:

i. In numerical solution the position of a moving free surface can be accurately predicted by means of forward finite difference technique. However, the finite difference approximations of the hydraulic gradients at free surface must be determined very accurately to obtain adequate results.

ii. A Hele-Shaw model can be used to investigate a two-dimensional saturated flow problem for predicting the position of the moving free surface especially when mathematical formulation might be difficult due to irregular geometry of the flow domain.

Freeze (١٩٧١a) has been developed a mathematical model by using finite difference method which may be applied to a two or three-dimensional transient or steady state problem. The unsaturated region is also included. Unconfined flow in earth dams has been studied by a simplified model in a later paper [**Freeze** ١٩٧١b] particularly with regard to the influence of the unsaturated flow domain above the free surface. Steady state and transient conditions are considered and the conclusions reached are that the unsaturated flow components take on a greater importance in small dams than in large, in dams with sloping cores and downstream filter blankets than in dams with more homogeneous sections, and in fine-grained, well graded soils common to internal cores than in more permeable and more uniform soils of the external sections. A simulation of the transient initial advance problem showed that the rate of growth of the saturated zone is highly dependent on the unsaturated properties of the soils and on the initial moisture contents.

Desai and **Sherman** (١٩٧١) presented a numerical solution for the problem of unconfined transient flow with a free surface in heterogeneous soils involving both rise and fall (draw down) of external water levels for river banks and embankments by finite difference technique. Both non-linear form and

linearized form of flow equation (**Bousseinesq** equation) were solved by employing a numerical method.

Special iterative schemes are employed for locating the free surface and the surface of seepage. The results of this scheme were compared with a number of experiments which were conducted by the U.S. Army Engineers Water-Ways Experiment Station with a viscous flow model. The results reached indicted a satisfactory correlation between the numerical and experimental results .

A non-linear form of the flow equation showed promise of excellent agreement with refinement of the time-wise subdivision. It is further showed that the nonlinear equation proposed in this study gives better results than the linearized equation. It is believed that the numerical method adopted by such study can be conveniently adopted for field-design applications.

Amar (١٩٧٥) investigated two dimensional hydrodynamic behavior of recharge of an unconfined aquifer based on the potential theory of flow through porous media. Laplace's equation in combination with time-dependent non-linear boundary conditions on the curvilinear moving free surface solved by finite difference technique. A computational algorithm to determine the numerical solution and the location of moving free surface at any time stage was proposed. The results of this model were compared with the pertinent experimental data obtained from sand-model studies. The results of the comparison between the theoretical solution curves with the pertinent experimental data, have clearly demonstrated that, in general, may well provide the answer for a correct description of the problem over a wide range of significant parameters relating to the hydrodynamics of recharge into unconfined aquifer phenomenon.

Stephenson (١٩٧٨) studied the recession of the free surface in an embankment following sudden drawdown of a reservoir. The non-equilibrium equation for flow in porous media was adopted and solved by using finite

difference indicating the variation of water surface with time, for both battered cut and triangular embankments. The location of point of emergence of the phreatic line was investigated and the relationship between the storage coefficient and coefficient of consolidation was explained.

٢. Finite–Elements Method

The finite elements method is a second way of numerical solution .This method is also based on grid pattern (not necessarily rectangular) which divides the flow region into discrete elements and provides N equations with N unknowns. Material properties, such as permeability, are specified for each element and boundary conditions (heads and flow rates) are set. A system of equations is solved to compute heads at nodes and flows in the elements. The finite element has several advantages over the finite difference method for more complex seepage problems. These include [**U.S. Army Crops. of Engineers**, ١٩٨٦].

(a) Complex geometry including sloping layers of material can be easily accommodated.

(b) By varying the size of elements, zones where seepage gradients or velocity are high can be accurately modeled.

(c) Pockets of material in a layer can be modeled.

The finite element method was first applied to boundary value field problems by **Zienkiewicz** and **Cheung** (١٩٦٥) and their method was later extended to obtain a solution for steady state seepage in an anisotropic foundation under a concrete dam (**Zienkiewics *et al.***, ١٩٦٦). Solutions for unconfined flow problems were presented by **Finn** (١٩٦٧) and **Taylor** and **Brown** (١٩٦٧) shortly after. In the unconfined case the position of the free surface in the dam is unknown at the start of the analysis and an assumption has to be made as to it's position. In both analyses the free surface is assumed to define the upper boundary of the mesh

and an iterative procedure is adopted to adjust the position of nodes on this boundary until all boundary conditions are satisfied.

Finn's solution can be described in a number of steps

i. A free surface line is assumed for the section to be analyzed.

ii. The saturated region below that line is divided into finite elements.

iii. The co-ordinate and element data are then supplied to the program with the other boundary conditions. (The pressures within the and on the free surface are assumed unknown).

iv. A solution for the Laplace's equations is obtained and the potentials printed.

v. If the boundary condition of the pressure head (ψ) being zero on the free surface is not at any node (to a reasonable degree of accuracy) the co-ordinate data is modified so that the second guess would satisfy the (ψ=٠) condition along the free surface. If the first guess was poor the mesh is also modified by adding or subtracting elements to avoid any unreasonable deformation.

vi. A second solution is obtained and iteration continues until the boundary conditions on the free surface are satisfied.

France, *et al.* (١٩٧١) presented a numerical analysis of free surface seepage problems by using finite element methods based on the principle of minimum potential energy. Essentially the transient problem was solved by considering the solution to be a series of steady state solutions at small intervals of time apart. Four examples of transient state were analyzed. The conclusions reached were despite their inherent complexity, free surface ground water flow problems could be treated by using finite elements, which has proved to be extremely versatile, and is completely general enough to solve most practical seepage problems.

Neuman and **Witherspoon** (١٩٧١) presented their solution to the analysis of non-steady flow conditions with a free surface the situation arising on drawdown is considered and the contribution of the unsaturated region is included indirectly by assuming a specific yield term for the unsaturated domain. Flow from the unsaturated region is added into the free surface. The method of adjusting the mesh to accommodate the falling position of the free surface is not fully described and they assume that drastic alteration in the geometry of mesh is necessary with the consequent loss of accuracy.

Desai (١٩٧٢) investigated the problem of unsteady unconfined seepage in porous media by using finite element procedure. The changing free surface was located by computing movements of the nodes on the free surface and by using iterative scheme. The formulation has been presented in this study was applicable also to axisymmetric idealizations. Moreover, the procedure could be conveniently extended for three-dimensional analysis. In this study isoparametric element was found to facilitate formulation and computational efforts. An important answer adopted by this study for finite representation of infinite media such as riverbanks depending upon results of numerical solutions. The results obtained by this study were compared with laboratory tests and with various boundary assumptions possible in long porous banks were examined. Attention was directed toward developing a general computer procedure for design analysis based upon such study.

Guvanasen and **Volker** (١٩٨٠) presented one finite difference and three finite element schemes for solving unsteady flow problem in unconfined aquifer. Results form various numerical schemes were compared with experimental results from a sandbox model, which simulated the problem of unsteady free surface seepage. The conclusions reached that the finite element schemes were bound to be more computationally economical for this particular problem, the particular finite element scheme preferred was one that incorporates the prescribed flux and head conditions on the free surface in an iterative solution for the new free surface at the end of each time step. The increased stability of

this scheme allows a large time increment to be used without significantly affecting accuracy, so that solutions can be obtained with minimum of computational effort.

Li and **Desai** (١٩٨٣) developed a finite elements procedure for seepage and stability analysis of dams and earth banks. The seepage analysis adopted in this study was based on a residual flow scheme involving saturated and unsaturated zones in which the original mesh remains invariant during transient flow and iterations. Application of proposed procedure for solution of typical problems involving seepage and stability analysis. The procedure has been found to provide satisfactory correlation with analytical solutions and field observations for a number of problems. It could be useful and appropriate for seepage and stability analysis of dams and earth banks.

Rank and **Werner** (١٩٨٦) adopted an adaptive finite element approach and it was applied to the two dimensional fluid flow with free surface. It was shown for a quite general class of non-linear iteration schemes, how the well-known linear a posteriori error estimates could be used and how an adaptive non-linear iteration could efficiently be carried out. As only very few iterations have to be performed a coarse meshes, the ratio of adaptive mesh construction to non-linear iterative solution on the finest mesh was much better than for linear problems. This makes the use of adaptive codes even more attractive in the non-linear case.

Al-Qaisi (١٩٩٥) made a numerical study of the elastic – inelastic finite element solutions to investigate the behavior of the core of the Main Adhain Dam. The effects of core geometry (shape and dimensions) and the relative core stiffness to shell have been investigated. He found that the upstream inclination of the core reduces the generation of pore pressure.

٢.٢.٥.٤ Models

Models which scale or simulate the flow of water in porous media can provide a good feel for what is occurring during seepage and allow a physical

feel for the reaction of the flow system to changes in head, design geometry and other assumptions. These models includes the following:

(a) Analogy Methods

Processes which involve movement of energy due to differences in energy potential operate by the same principle as movement of ground water. These processes include electricity and heat flow, which have been used as seepage analogies. Electrical analogues have proven particularly useful in the study of three-dimensional problems and in problems where geometric complexities do not allow adequate simplifying assumptions for analytical methods. [**U.S. Army Crops of Engineers**, ١٩٨٦].

(b) Sand Models

Which may use prototype materials can provide information about flow path and head at particular points in the aquifer. The sand or porous material may be placed under water to provide a homogenous condition, or layers of different sand sizes may be used to study the effect of internal boundaries or layers. If flow is unconfined and the same material is used for model and prototype in the model.

Flow can be traced by dye injection and heads determine by small piezometers. Disadvantages include effects of layering when the porous material is placed, difficulty in modeling prototype permeability and boundary effects.

(c) Viscous flow Models

These type have been used to study transient flow (e.g., sudden drawdown) and effects of drains. This method depends on the flow of a viscous fluid such as oil or glycerin between two parallel plates and is normally used to study two-dimensional flow. As with sand models, dye can be used to trace flow lines. Construction is normally complicated and operation requires care since

temperature and capillary forces affect the flow. Flow sharp changes in boundary geometry.

٢.٣ A Review on Stability Analysis

٢.٣.١ General

Reservoirs can be subjected to rapid drawdown. In this case the lateral forces provided by the water is removed and the excess pore water pressure does not have enough time to dissipate. The net effect is that the slope can fail under undrained conditions. If the water level in the reservoir remains at low levels and failure did not occur under undrained conditions, seepage of ground water would occur and the additional seepage forces can provoke failure.

The failure of a mass of soil in a downward and outward movement of a slope is called a slide or slope failure. The surface a long which slide takes place has a variety of shapes and represents the surface of minimum resistance. The slope stability analysis is the matter of assigning the degree of safety of a certain slope profile or to decide whether a slope of given geometry and material meets the safety requirements.

A stability analysis of earth dams and banks requires consideration of the coupled effects of:

١. External loads such as body weight, surcharge, and forces caused by sequential construction.

٢. Seepage forces due to steady or transient flow of water. Often, for simplicity, the effects of external and seepage forces are uncoupled and superimposed [**Li** and, **Desai**, ١٩٨٣].

٢.٣.٢ Two Dimensional Slope Stability Analysis

Slope Stability can be analyzed by using one or more of the following: the limit equilibrium method, limit analysis, finite difference method and finite element method. Several failure mechanics must be investigated and the minimum load required for collapse is taken as the collapse load. The limit equilibrium method gives an upper bound solution because a more efficient mechanism of collapse is possible than those postulated. The limit analysis makes use of stress-strain characteristics and a failure criterion for the soil. The solution for a limit analysis is a lower bound. The finite element method requires discretization of the soil and a failure criterion to identify soil regions that have reached the failure Stress State. The finite element method does not require speculation on a possible failure surface [Muni, ٢٠٠٠].

Most of the methods currently utilized in slope stability analysis are based on the limit equilibrium approach. The essential assumption of this approach is the validity of well known Moher-Coulomb failure criterion which defines the shear strength of soil as follows:

$$S = c + \sigma \tan \phi \qquad \text{.....} (٢.٩)$$

where (c) and (ϕ) are cohesion intercept and effective angle of internal friction, respectively and (σ) is the normal effective stress. The methods of limit equilibrium assume that the shear strength of the soil is partially mobilized a long an assumed failure surface which my be a straight line, circular arc, logarithmic spiral curve or any other irregular surface. The methods however, defines the factor of safety (F) as the ratio of available shear strength the developed shear stress, (τ):

$$F = \frac{S}{\tau} \qquad \text{.....} (٢.١٠)$$

Equation (٢.١٠) is form of definition introduced by **Bishop** (١٩٥٥) which has gained fairly wide acceptance, the factor of safety (F) is taken as the ratio of the total shear strength available on the slip surface to total shear strength mobilized

(τ) in order to maintain equilibrium [**Spencer**, ١٩٦٧]. Our interest lies in materials that are saturated with ground water, in such case equation (٢.٩) takes the form:

$$S = c + (\sigma - u)\tan\phi \qquad \text{..... (٢.١١)}$$

in which (u) is the pore water pressure. For the present, the method of slices appears to affair the good approach for obtaining an accurate solution for any shape of failure [**Whitman**, and **Bailey**, ١٩٦٧]. There are many methods using this general approach, from these methods :

٢.٣.٢.١ Ordinary Method

The ordinary method of slices is considered as the simplest method, since it is the only procedure that results into a linear factor of safety equation. The basic assumption of this method is that the resultant of interstice forces acting on each slice has a line of action parallel to the base of that slice. This assumption in fact violates Newton's principle of "action equal reaction" at the interface between any two adjacent slices [**Al-Jorany**, ١٩٩٦]. Since forces equilibrium is not satisfied at some slices. However, the factor of safety computed by this method will be in error. In some problems, (F) from this method may be only ١٠٪ to ١٥٪ below the range of equally correct answer, but in other problems the error may be as much as ٦٠٪ [**Whitman,** and **Bailey**, ١٩٦٧].

٢.٣.٢.٢ Simplified Bishop Method

This method was first described by **Bishop** (١٩٥٥); simplified version of method was developed further by **Janbu *et al.*** (١٩٥٦) [**Lambe**, and **Whitman**, ١٩٦٩]. In this method it is assumed that the forces acting on the sides of any slice have zero resultant in the vertical direction. According to [**Whitman**, and **Bailey**, ١٩٦٧], the simplified Bishop method is recommended to be used for routine calculations involving circular failure surfaces. Using this method, a solution was obtained by successive approximation, an initial value for (F) being obtained by using an expression which had been simplified by assuming that the

inter-slice forces were horizontal. This simplified expression satisfies the conditions of equilibrium in respect to moment but not in respect of forces [**Spencer**, ١٩٦٧].

٢.٣.٢.٣ Morgenstern-Price Method

In this method [**Morgenstern**, and **Price**, ١٩٦٧] an admissible mathematical function is assumed to describe the direction of interstice forces:

$$\frac{x}{E} = \lambda\, f(x) \qquad \text{..... (٢.١٦)}$$

where (x) and (E) are the shear and normal components of the interstice respectively, (λ) is the constant to be evaluated by solving for the factor of safety, and $f(x)$ is a function variation with respect to x. f(x) may be constant, half sine, clipped sine or any other admissible function.

The value of the factor of safety is calculated by using two different equations. The first is based on the forces equilibrium which gives the factor of safety with respect to forces (F_s) while the other concerns the moment equilibrium giving factor of safety with respect to moments (F_m). Both of (F_f) and (F_m) are depend on the value of (λ). The solution is obtained as these two factors of safety converge to a unique value.

This method of slope stability analysis which is valid for slip surfaces of any arbitrary shape, is considered as the more general rigorous method [**Baker**, ١٩٨٠]. It stems its generality from the fact that no stringent restriction is imposed neither on the direction or location of the interslice forces nor on the shape of the slip surface analyzed [**Al-Jorany**, ١٩٩٦].

For these reasons, the Morgenstern – Price method is chosen among all the other methods to be used in the limit equilibrium computation procedure presented in this work. More details about this method will be introduced in the following chapter.

From the preceding literature review on the available theoretical investigations, no detailed work is found to study the stability of zoned earth

dam under unsteady drawdown conditions. Such problem will be attempted to studied well in the present work .

Chapter Three

FUNDAMENTALS AND THEORIES OF THE PRESENT WORK

٣.١ General

In this chapter, at first the governing equation for transient unconfined seepage in porous media is formulated with aid of finite element technique. A special procedure for locating the upper boundary (phreatic line) of flow domain is adopted. The field variable (piezometric head in this work) is obtained.

The second part of the present work therefore includes the construction of a complete computation procedure based on the Morgenstern – price method. The most critical slip surface and the relevant minimum factor of safety of any slope profile under different drawdown conditions can be obtained by this procedure.

A computer program is then built. This program contains an algorithm to solve the governing equation numerically. The solution of ground water flow equation is used as input data to the stability program to examine the stability of the slopes of earth dam undergoing seepage.

٣.٢ Fundamental concept of the finite element method

The finite element method is a very powerful numerical method [**Zienkiewicz**, ١٩٧٧]. It requires the use of digital computer because of the large number of computations involved.

In ground water flow problems, one could imagine that a region is subdivided into small elements, these elements may be two, or three dimensional and joined to each other by nodes existing on the element

boundaries. Such that for each element the flow is described in terms of the head in the nodal points, and that then a system of equations is obtained from the conditions that the flow must be continuous at each node [**Bear**, and **Verruijt**, ١٩٩٠].

The field variable model describing an approximate variation of piezometric head (H^e) within the element is

$$H^e(x,y)=\sum_{i=1}^{n} N_i(x,y)H_i \qquad \text{.....(٣.١)}$$

where:

x and y = The coordinates of element.

H_i = Nodal value of head, H, of element.

n = Number of nodes per element.

N_i = Shape function of the element.

and in matrix form

$$H^e=[N_i]\{H_i\} \qquad \text{.....(٣.٢)}$$

where:

$\{H_i\}$ = is the vector of nodal heads.

$[N_i]$ = is the matrix of shape functions.

The approximate solution of head distribution, H, throughout the flow domain is:

$$H=\sum_{e=1}^{m}[N_i]\{H_i\} \qquad \text{.....(٣.٣)}$$

where:

m = is the total number of elements in the flow domain.

٣.٢.١ Methods of approximate solution

The approximate solution techniques that are useful for a through understanding of how finite element method work, are the following:

١. Ritz Method
٢. Vartiational or Rayleigh-Ritz Method.
٣. Weighted residual method.

Of these, weighted residual method is the most widely used in finite element work [**Smith,** ١٩٩٨].

٣.٢.١.١ Weighted residual Method

The weighted residual method is a technique, which can be used to obtain approximate solutions to linear and non-linear differential equations. In such method the finite element equations can be derived directly from governing differential equation of the problem [**Zienkiewicz**, ١٩٧٧]. Considering a problem for which the governing equation in the domain (D) involves one dependent variable (h) and its derivatives, and several independent variables $x_1, x_2, \ldots, x_n$ collectively denoted by x_i. The governing equation can be written in the general form

$$f_D(h; x_i) = 0 \qquad \text{.....(٣.٤)}$$

substitution of an approximate solution (H) as given in Equation (٣.٣) into Equation (٣.٤) will not in general result in

$$f_D(H; x_i) = 0 \qquad \text{.....(٣.٥)}$$

and an equation error or residual (R) can be formed as:

$$R = f_D(h; x_i) - f_D(H; x_i) \qquad \text{.....(٣.٦)}$$

The closer the approximate solution (*H*) approaches the exact solution (*h*), the nearer will the residual (*R*) approach toward zero. Substitution of Equation(٣.٤) into Equation (٣.٦) allows the simplified residual form

$$R = -f_D\left(H; x_i\right) \qquad \text{.....(٣.٧)}$$

to be obtained.

In residual trail function methods, the residual (*R*) is required to satisfy some conditions that force it to be small. For residual finite element method it is the weighted integral over the domain as:

$$\int_D W\ f\left(R\right) d\,D \qquad \text{.....(٣.٨)}$$

which is required to satisfy the smallness criterion, where (*W*) is a weighting function, thus [**Norrie,** and **DeVries**, ١٩٧٨]

Galerkin $\int_D W_j\, R\, dD$ .....(٣.٩)

or $\sum_{e=1}^{m} \int_D W_j\, R^e\, dD = 0;\ j = 1, 2, ..., m$ .....(٣.١٠)

where:

m = total number of elements.

R^e = element residual.

The method consists of multiplying or "weighting" the residual (*R*) by each shape function (i.e., $W_j = N_j$) in turn, integrating over the element and equating to zero [**Smith**, ١٩٩٨].

٣.٣ Finite Element Formulation

The finite element method will be applied to Equation (٢.٧) in terms of piezometric head. The field variable model describing an approximate variation of (H^e) within the element is as indicated in Equation (٣.١).

$$H^e = \sum_{i=1}^{n} N_i H_i$$

The shape function (N_i) is assumed to be function of (x,y) i.e.:

$$\frac{\partial H^e}{\partial x} = \frac{\partial}{\partial x}\sum_{i=1}^{n} N_i H_i \qquad \text{..... (٣.١١)}$$

$$\frac{\partial H^e}{\partial y} = \frac{\partial}{\partial y}\sum_{i=1}^{n} N_i H_i \qquad \text{..... (٣.١٢)}$$

The finite element approximation is now applied to Equation (٢.٧).

$$\left(k_x \frac{\partial^2}{\partial x^2}\sum_{i=1}^{n} N_i H_i + k_y \frac{\partial^2}{\partial y^2}\sum_{i=1}^{n} N_i H_i \right) - \lambda\,(t)\frac{\partial}{\partial t}\sum_{i=1}^{n} N_i H_i = R \qquad \text{..... (٣.١٣)}$$

By applying Galerkin Method and substituting Equation (٣.١٣) into the Equation (٣.١٠) the result is:

$$\sum_{e=1}^{m}\int_D N_j \left[k_x \frac{\partial^2}{\partial x^2}\sum_{i=1}^{n} N_i H_i + k_y \frac{\partial^2}{\partial y^2}\sum_{i=1}^{n} N_i H_i - \lambda(t)\frac{\partial}{\partial t}\sum_{i=1}^{n} N_i H_i \right] dD = 0 \qquad \text{.. (٣.١٤)}$$

where, $dD = dx \times dy$; $i, j =$ ١, ٢, …, n and $\lambda(t) = \dfrac{n}{\bar{h}(0,0,t)}$.

In Equation (٣.١٤) the appearance of second derivatives for (H) necessitates a smooth distribution in space due to the integration of this variable. In order to overcome this limitation, by mean of Green's theorem, which proves that [**Zienkiewicz**, ١٩٧٧].

$$\int_D \phi \frac{\partial \psi}{\partial x} dD = -\int_D \frac{\partial \phi}{\partial x}\psi\, dD + \int_s \phi \psi\, n_x\, d_s \qquad \text{..... (٣.١٥)}$$

where (s) is the boundary portion over which integration takes place, and (n_x) is the direction cosine between the normal and (x) direction.

By applying Green's theorem, Equation (٣.١٤) can be modified to:

$$\sum_{e=1}^{m}\left[-\int_{D^e}\left[\frac{\partial N_j}{\partial x}k_x\frac{\partial}{\partial x}\sum_{i=1}^{n}N_i H_i+\frac{\partial N_j}{\partial y}k_y\frac{\partial}{\partial y}\sum_{i=1}^{n}N_i H_i-\lambda(t)\frac{\partial}{\partial t}\sum_{i=1}^{n}N_i H_i\right]dD+\int_s N_j k_n\frac{\partial}{\partial n}\sum_{i=1}^{n}N_i H_i\, d_s\right]=\mathbf{0}$$

..... (٣.١٦)

Re-arrange Equation (٣.١٦), yields

$$\sum_{e=1}^{m}\left[-\int_{D^e}\left(\frac{\partial N_j}{\partial x}k_x\frac{\partial}{\partial x}\sum_{i=1}^{n}N_i H_i+\frac{\partial N_j}{\partial y}k_y\frac{\partial}{\partial y}\sum_{i=1}^{n}N_i H_i\right)dD+\right.$$

$$\left.\int_{D^e}\lambda(t)N_j\frac{\partial}{\partial t}\sum_{i=1}^{n}N_i H_i\,dD+\int_s N_j k_n\frac{\partial}{\partial n}\sum_{i=1}^{n}N_i H_i\,ds\right]=0 \qquad \text{..... (٣.١٧)}$$

or, in matrices form

$$[D]\{H\}+[M]\left\{\frac{\partial H}{\partial t}\right\}=\{F\} \qquad \text{..... (٣.١٨)}$$

in which

$$D=\sum_{e=1}^{m}\int_{D^e}\left(\frac{\partial N_j}{\partial x}k_x\sum_{i=1}^{n}N_i H_i+\frac{\partial N_j}{\partial y}k_y\sum_{i=1}^{n}N_i H_i\right)dD \qquad \text{..... (٣.١٨a)}$$

$$M=\sum_{e=1}^{m}\int_{D^e}\lambda(t)N_j N_i\,dD \qquad \text{..... (٣.١٨b)}$$

$$F=-\sum_{e=1}^{m}\int_{D^e}N_j k_n\frac{\partial N_i}{\partial n}H_i\,ds \qquad \text{..... (٣.١٨c)}$$

where, $[D^e]$ represents the element matrix

$$\left[D^e\right]=\int_{D^e}\left[T^e\right]^T\left[k^e\right]\left[T^e\right]dx\,dy \qquad \text{..... (٣.١٩)}$$

where:

$$[T]=\begin{bmatrix}\frac{\partial N_1^e}{\partial x} & \cdots & \frac{\partial N_n^e}{\partial x}\\ \frac{\partial N_1^e}{\partial y} & \cdots & \frac{\partial N_n^e}{\partial x}\end{bmatrix},\quad [k]=\begin{bmatrix}k_x & 0\\ 0 & k_y\end{bmatrix}$$

and from assemblage:

$$[D]=\sum_{e=1}^{m}[D^e] \qquad \text{..... (٣.١٩a)}$$

$[M^e]$ represents mass matrix.

$$[M^e]=\lambda(t)\int_{D^e}[N^e]^T[N^e]dx\,dy \qquad \text{..... (٣.٢٠)}$$

where:

$$[N]=\begin{bmatrix} N_1 N_1 & \cdots & N_1 N_n \\ N_n N_1 & \cdots & N_n N_n \end{bmatrix}$$

from assemblage:

$$[M]=\sum_{e=1}^{m}[M^e] \qquad \text{..... (٣.٢٠a)}$$

and $[F^e]$ represents forcing parameter vector. The assembled Equation (٣.١٨) is solved by using explicit finite difference approximation for time derivative.

٣.٤ Isoparametric Representation

The isoparameteric concept allows any arbitrary geometry to be closely approximated, thereby minimizing any errors associated with modeling the geometry and without resorting to those of fine mesh along the boundaries. The main advantages of this element are that it can follow curved boundaries and that it predicts linear "stress" distributions over each element [**Zienkiewicz**, ١٩٧٧].

The basic idea behind the isoparametric element is to use of the same shape function or geometry as well as the field variable (piezometric head in this work) within the element i.e., under special circumstances the same shape functions can also be used to specify the relation between the global (x,y) and

local (ζ, η) coordinates systems. If this is so the element is of type called "isoparametric" [**Smith**, ١٩٩٨].

٣.٤.١ Element Used

From previous discussion, apparently, there is appreciate agreement for using isoparametric element especially for the solution of field equations that govern such problems as flow through an aquifer **Desai** (١٩٧٢) introduced the four noded isoparametric quadrilateral element which was found to facilitate formulation and computational efforts. **Al-Assedy** (١٩٩٨) used two types of elements to investigate the suitable schemes required to model soil consolidation. First, was an isoparametric four nodded element used (See Figure ٣.١). He found that displacement and pore fluid pressure vary linearly. Second, was an isoparametric eight-nodded element, in this type of element the displacement and pore fluid pressure vary quadratically over the element. In the present work the four nodded isoparametric element a two point Gauss rule for each dimension is considered the optimum to be used. The shape function of four noded isoparametric element with respect to local coordinate (ζ) and (η) as given in [**Segerlind**, ١٩٨٤] is shown in Appendix A.

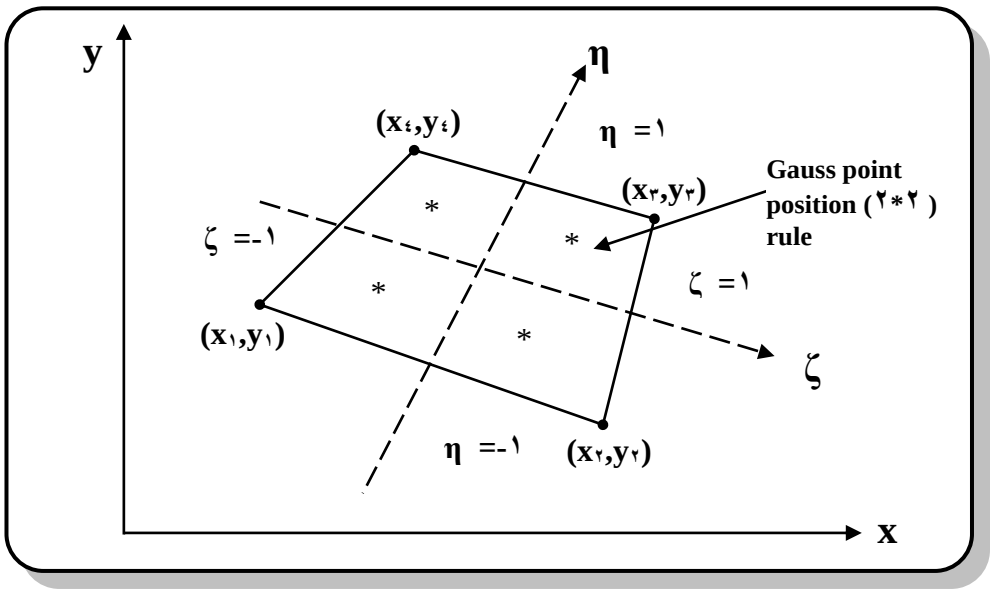

Figure(٣.١) Four Nodded Quadrilateral Finite Element [After **Segerlind**,١٩٨٤]

The coordinates transformation according to [**Smith**, ١٩٩٨] are as follows:

$$x = \sum_{i=1}^{n} N_i \, x_i = x(\zeta, \eta) \qquad \text{..... (٣.٢١)}$$

$$y = \sum_{i=2}^{n} N_i \, y_i = y(\zeta, \eta) \qquad \text{..... (٣.٢٢)}$$

where:

n = total number of nodes per element.

x_i , y_i = are the coordinates of nodes.

when developing element matrix equations, using isoparametric elements it is necessary to calculate derivatives of shape functions with respect to local coordinate system from corresponding derivatives in the global coordinate system. These sets of derivatives can conveniently be related through the Jacobian matrix transformation [**Norrie**, and **DeVries**, ١٩٧٨].

$$\begin{bmatrix} \frac{\partial N_i}{\partial \zeta} \\ \frac{\partial N_i}{\partial \eta} \end{bmatrix} = \begin{bmatrix} \frac{\partial x}{\partial \zeta} & \frac{\partial y}{\partial \zeta} \\ \frac{\partial x}{\partial \eta} & \frac{\partial y}{\partial \eta} \end{bmatrix} \begin{Bmatrix} \frac{\partial N_i}{\partial x} \\ \frac{\partial N_i}{\partial y} \end{Bmatrix} = [J] \begin{Bmatrix} \frac{\partial N_i}{\partial x} \\ \frac{\partial N_i}{\partial y} \end{Bmatrix} \qquad \text{..... (٣.٢٣)}$$

where, [J] is Jacobian matrix, or

$$\begin{bmatrix} \frac{\partial N_i}{\partial x} \\ \frac{\partial N_i}{\partial y} \end{bmatrix} = [J]^{-1} \begin{Bmatrix} \frac{\partial N_i}{\partial \zeta} \\ \frac{\partial N_i}{\partial \eta} \end{Bmatrix}$$

where, $[J]^{-١}$ is the inverse of Jacobian matrix.

Substitution of Equation (٣.٢١) and (٣.٢٢) into [J] yields

$$[J] = \begin{bmatrix} \frac{\partial \sum N_i \, x_i}{\partial \zeta} & \frac{\partial \sum N_i \, y_i}{\partial \zeta} \\ \frac{\partial \sum N_i \, x_i}{\partial \eta} & \frac{\partial \sum N_i \, y_i}{\partial \eta} \end{bmatrix} \qquad \text{..... (٣.٢٤)}$$

The infinitesimal area element ($dx\ dy$) is related to an infantilism at area element in the (ζ, η) coordinate system by:

$$dx\ dy = \det[J]d\zeta\ d\eta \quad \text{..... (٣.٢٥)}$$

where, det [J] is the determinant of Jacobian matrix.

Substituting in Equation (٣.١٨ a& b) yields

$$[D] = \int_{D^e} [T^e]^T [k^e][T^e] \det[J] d\zeta\, d\eta \quad \text{..... (٣.٢٦)}$$

$$[M] = \lambda(t) \int_{D^e} [N^e]^T [N^e] \det[J]\, d\zeta\, d\eta \quad \text{..... (٣.٢٧)}$$

٣.٤.٢ The Initial Conditions

The initial conditions refer to head distribution every where in the system at the beginning of the simulation and thus are boundary conditions in time. It is standard practice to select as the initial condition a steady state head solution.

In selecting a starting head distribution for a transient simulation, an arbitrarily define heads distribution is used and then run the transient model until it matches field-measured heads. Then these heads are used as starting condition in predictive simulation. The rational behind this selection of initial conditions is that the influence of the initial conditions diminishes as the simulation progresses, so errors associated with selecting possibly erroneous initial conditions will be small provided sufficient simulated time has elapsed.

٣.٤.٣ The Boundary Conditions

The saturated soil which is considered for analysis must be defend by boundaries, permeability of the soil, and heads imposed upon the water. Here in defining the types of boundaries which may define a particular porous soil mass considered for analysis, the nature and location of these boundaries are

determined by a soil exploration program, assumptions based on engineering judgment and conditions imposed by the proposed design. Normally, simplifying assumptions are required in order to establish boundaries which will make analysis feasible [**U.S. Army Crops. of Engineers**, ١٩٨٦].

Considering the typical problem of flow through a dam with toe drain [see Figure ٣.٢]. If the water level in the reservoir drops instantaneously or at some prescribed rate, the free surface will start falling until a new state of equilibrium is established. In general the following four kinds of boundaries are considers [**Neuman,** and **Witherspan**, ١٩٧١].

١. Prescribed head boundaries.
٢. Prescribed flux boundaries
٣. A free surface.
٤. Seepage face.

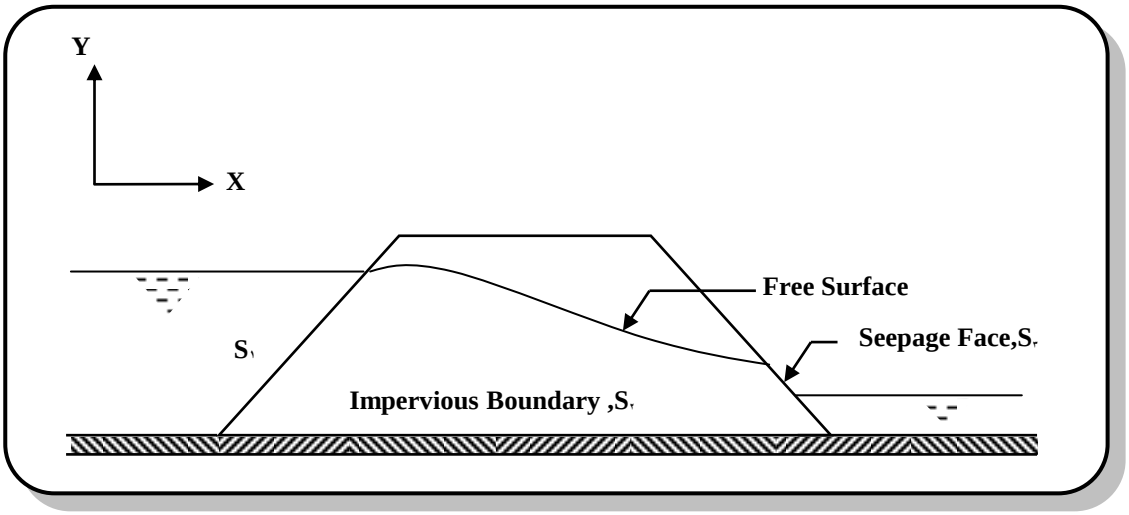

Figure(٣.٢) Schematic Representation Of Flow Region.

This boundary value problem can be described by the following set of equations:

$$h(x,y,t)=H(t) \qquad on \;\; S_1 \qquad \text{..... } (٣.٢٨)$$

$$q_n = k_n \frac{\partial h}{\partial n} l_i \qquad on \;\; S_2 \qquad \text{..... } (٣.٢٩)$$

where (q_n) is the flux normal to the boundary, and (l_i) the component of unit normal to the boundary.

$h(x,y,t)=Y(x,t)$ on the free surface, and on the seepage face (S_3) [**Desai,** ١٩٧٢].

٣.٤.٤ Integration with Respect Time

Note that Equation (٣.١٨) is a set of partial differential equations that must be integrated with respect to time. In performing this integration, it is convenient to divide the time domain into a discrete number of time steps (Δt), the approach is to replace the time derivatives in Equation (٣.١٨) with finite difference.

In so called forward difference scheme, Equation (٣.١٨) is expressed at the old time level (t) as

$$[D]\{H\}^t+\left[\frac{M}{\Delta t}\right]\left(\{H\}^{t+\Delta t}-\{H\}^t\right)=\{F\}^t \qquad \text{..... (٣.٣٠)}$$

where (t) represents a time level at which the position of the free surface is known. Equation (٣.٣٠) can be solved explicitly for $\{H\}^{t+\Delta t}$. The method described above for the time discrtization may regarded as explicit finite difference approximation [**Guvanasen**, and **Volker**, ١٩٨٠].

٣.٤.٤.١ Size of Time Step

Selection of time step (Δt) is a critical step in model design because the values of time discretization strongly influence the numerical results. Ideally, it is desirable to use small time steps so that the numerical representation better approximates the partial differential equation. **Neuman** and **Witherspoon** (١٩٧١) reported that this scheme becomes unstable unless (Δt) is kept sufficiently small, and therefore an extremely large number of time steps may often be required to obtain a satisfactory solution. It is good modeling practice to make several trail

runs of model using different (Δt)'s. Then, the largest possible (Δt) that does not significantly change the solution can be used in production runs [**Anderson**, and **Woessner**, ١٩٩٢]. For instantaneous change in the reservoir level (constant head) gradually increasing time – steps can be used. In actual analysis, therefore, a few changes in time step size a long with the use of several steps of equal size at each stage is the most economical. Obviously where the head is changing as a function of time, small time-steps may be necessary throughout.

٣.٥ Determination of Changing Free Surface

The location of the free surface is a vexing problem in many areas of fluid mechanics. Since part of the boundary values must be applied at surface, the problem can not be solved without the knowledge of the location of the surface [**Liggett**, ١٩٧٧].

Under small change in external head, (see Figure ٣.٣) the free surface experiences corresponding movements. For a transient problem, the conditions of null normal flow and velocity across the free surface are not satisfied. The actual particle velocities need to be computed from the following.

$$\{v_p\} = \frac{-1}{n}\{v\} \qquad \text{..... (٣.٣١)}$$

where $\{v\}$ is the velocity vector computed by Darcy's law, and (n) is the soil porosity. The procedure adopted here can permit modification of coordinates of a portion of the mesh in the neighborhood of the free surface. The following equations summarize the process of modification of mesh [**Desai**, ١٩٧٢]:

$$\left.\begin{aligned} \overline{V}_x &= \frac{V_x^m + V_x^{m+1}}{2} \\ \overline{V}_y &= \frac{V_y^m + V_y^{m+1}}{2} \end{aligned}\right\} \qquad \text{..... (٣.٣١a)}$$

for all free surface nodes except at entrance and end faces.

$$\bar{V}_x = v_x^m \quad and \quad \bar{V}_y = v_y^m \qquad \text{..... (٣.٣١b)}$$

at entrance and end faces.

$$V_n = \frac{\bar{V}_x \sin\theta + \bar{V}_y \sin\theta}{n} \qquad \text{..... (٣.٣١c)}$$

$$U_n = V_n . \Delta t \qquad \text{..... (٣.٣١d)}$$

$$U_r = \frac{U_n}{\cos\beta} \ , \ \beta = \frac{\pi}{2} - \alpha + \theta \qquad \text{..... (٣.٣١e)}$$

$$U_x = U_r \cos\alpha \qquad \text{.....(٣.٣١f)}$$

$$U_y = U_r \sin\alpha \qquad \text{..... (٣.٣١g)}$$

$$\left.\begin{aligned} x_i^{t+\Delta t} &= x_i^t + u_x \\ y_i^{t+\Delta t} &= x_i^t + u_y \end{aligned}\right\} \qquad \text{..... (٣.٣٢)}$$

where, (*i*) denotes a nodal point, (*t*) denotes a time level. Other symbols are explained in Figure (٣.٣). As the field variable model yields discontinuous velocities at a node between tow elements, an average of the velocities at that node is adopted for computing the forgoing movements (first two equations of Eq.٣.٣١). A number of iterations may be performed at each time increment in order to improve satisfaction of the conditions at free surface. Various investigations, including **France, *et al***. (١٩٧١), and **Guvanasen** and **Volker** (١٩٨٠), employed the equations above for steady unconfined and unsteady flow analysis.

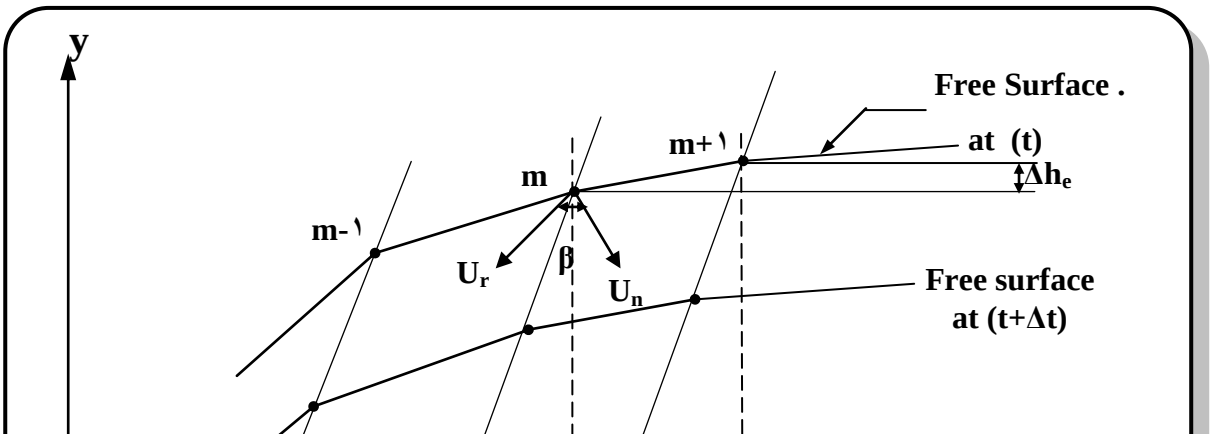

Figure(٣.٣): Movement Of Free Surface .

٣.٦ The Safety Functional for Morgenstern – Price Method

Considering a general slip surface that is shown in Figure (٣.٤a), the continuos slip surface $y(x)$ is approximated by a sequence of coordinates (x_i,y_i), i = ١, ٢, …, (n+١) defining (n) slices. The analysis is performed in term of unit weight and boundary water pressure.

Considering the forces acting on slice shown in Figure (٣.٤b):

Summation of forces in the direction parallel and perpendicular to the base of slice and then the solving for dQ_i yields:

$$dQ_i = \frac{F.S_i - E_i}{F.m_i} \qquad \text{..... (٣.٣٣)}$$

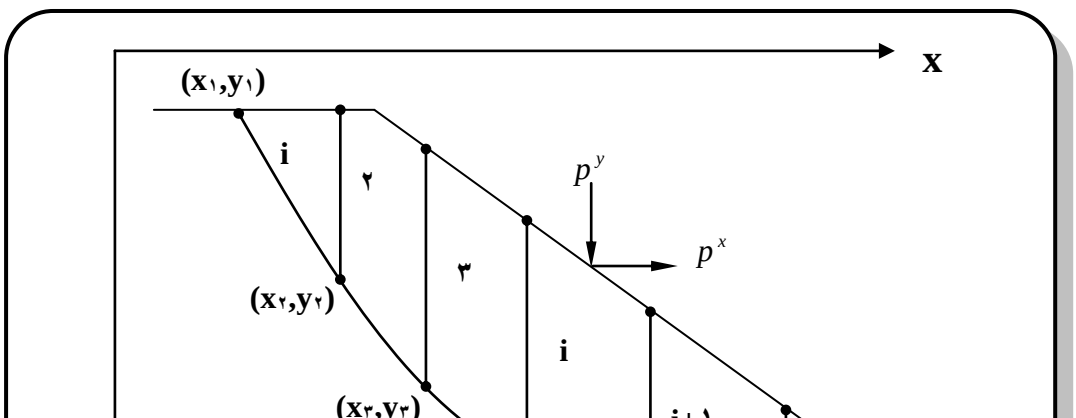

Figure(٣. ٤) Definition Of Variables .

where:

$$S_i = P_i^x \cos\alpha_i + \left(w_i + P_i^y\right)\sin\alpha_i \qquad \text{..... (٣.٣٤)}$$

$$E_i = C_i + \psi_i \left[\left(P_i^y + w_i \right) \cos \alpha_i - P_i^x \sin \alpha_i - P_i^w \right] \quad \text{..... (٣.٣٥)}$$

$$m_i = \cos\left(\alpha_i - \theta_i\right)\left[1 + \left(\psi_i / F\right) \sin\left(\alpha_i - \theta_i\right)\right] \quad \text{..... (٣.٣٦)}$$

in which:

P_i^x , P_i^y = forces in *x* and *y* directions per slice, respectively.

w_i = slice weight.

α_i = angle of inclination of slice base.

P_i^w = forces due to pore water pressure on base of slice.

C_i = the forces due to effective cohesion.

ψ_i = tanϕ, ϕ is the effective angle of internal friction.

F_i = a factor of safety.

θ_i = angle of inclination of interslice force.

Now if the external forces on the embankment are in equilibrium, the vertical sum of the interslice forces must be equal to zero. In other word, the sum of horizontal components of the interslice forces must be zero and the sum of vertical components must also be zero, i.e.

$$\left.\begin{aligned} \sum \left(d Q_i \cos\theta_i \right) = 0 \\ \sum \left(d Q_i \sin\theta_i \right) = 0 \end{aligned}\right\} \quad \text{..... (٣.٣٧)}$$

Furthermore, if the sum of moments of the external forces about any point is zero, the sum of moments of the interslice forces about that point must also be zero:

$$\sum d Q_i \, R_i = 0 \quad \text{..... (٣.٣٨)}$$

where, R_i is the distance between the force (dQ_i) and any point about which the moment are summed.

The summation of forces in the horizontal direction yields:

$$\sum \frac{S_i}{m_i}\cos\theta_i - \frac{1}{F}\sum \frac{E_i}{m_i}\cos\theta_i = 0 \qquad \text{..... (٣.٣٩)}$$

or:

$$F = F_f = \frac{\sum (E_i \cos\theta_i)/m_i}{\sum (S_i \cos\theta_i)/m_i} \qquad \text{..... (٣.٤٠)}$$

Equation (٤.٣٠) represents the safety functional with respect to forces equilibrium. The moments equilibrium Equation (٣.٣٨) can be written as follows:

$$\sum \frac{S_i}{m_i} R_i - \frac{1}{F}\sum \frac{E_i}{m_i} R_i + \sum P_i^x H_i = 0 \qquad \text{..... (٣.٤١)}$$

or:

$$F = F_m = \frac{\sum (E_i / m_i) R_i}{\sum (S_i / m_i) R_i + \sum P_i^x H_i} \qquad \text{..... (٣.٤٢)}$$

where:

$$R_i = (y_i - y_c)\cos\theta_i - (x_i - x_c)\sin\theta_i \qquad \text{..... (٣.٤٣)}$$

and:

(x_i, y_i) = coordinates of the slice center.

(x_c, y_c) = coordinates of point about which moments are sumed.

H_i = height of slice (i).

In this derivation the following remarks should be considered [**Al-Jorany**, ١٩٩٦].

١. The force (dQ_i) represents the resultant of all forces that act on the slice (i). This force is assumed to act along a line that passes through the center of the slice base. This assumption can be easily achieved by replacing each of

the forces that does not pass through the center, by a force and a moment. This treatment explain the appearance of the term ($\sum P_i^x H_i$) in Equation (٣.٤٢).

٢. The inclination of the force (dQ_i) with the horizontal is represented by the angle (θ_i) which varies from the one slice to another. This variation of (θ_i) with respect to (i) assumed as the follows:

$$\tan\theta_i = \tan\theta_o \times f(i) \qquad \text{..... (٣.٤٤)}$$

where:

θ_o = an unknown to be determined during the solution.

$f(i)$ = a certain presumed function of (i), it should be selected reasonably to describe the variation of the inclination of interslice forces.

A brief description of the Morgenstern-Price method is presented above which adopted from [**Al-Jorany**, ١٩٩٦]. A detail discursion of the whole subject is given in numerous [**Morgenstern** and, **Price**, ١٩٦٥] and [**Whitman** and, **Bailey**, ١٩٦٧].

٣.٧ Outline of Computer Program

The computer program is coded in QUICK BASIC language. The Microsoft QUICK BASIC ٤.٥ compiler, produced by Microsoft corporation is used to create the program under PC PENTIUM III at ٦٥٠ MHz Intel Compatible computer with ١٢٨ MB RAM.

٣.٧.١ Plane Free – Surface Flow Program

In this program considering a boundary condition frequently met in geomechanics in relation to flow of water through dam. Time depended free surface problems involve an upper boundary, the location of which is not known priori. This boundary can be located by using the procedure detailed in Section (٣.٥). The main function of the program is to determine the fluid potential (head)

and pore pressure within dam body and foundations. The initial part of the program includes the discretization process to region through dam. The region is subdivided into four noded elements by using automatic mesh generation in order to avoid the error which is involved in preparing the element data. After generation of the mesh, a formation and reduction of the element and mass matrices of the whole structure is performed element by element, integrations have to be performed numerically using Gauss-Quadrature method. The main loop concerns the different values of fluid head at each time step. The analysis is starts by assuming an initial position for the free surface. Solution of flow equation gives values of the fluid potential at each time level which will not in general equal the elevation of the free surface. To determine whether these new values are acceptable defining the maximum relative error on free surface as

$$E = Max\left|\frac{h_i^{j+1} - h_i^{j}}{h_i^{j+1} - h_i}\right| \qquad \text{..... (٣.٤٥)}$$

where:

E = maximum relative error on free surface.

h_i^{j+1} = fluid potential at nodal point (i) for iteration (j+١).

h_i^{j} = fluid potential at nodal point (i) for iteration (j).

h_i = fluid potential at nodal point (i) at the beginning of process.

If E is found to be sufficiently small, the iteration is completed, and one can proceed to the next time step. If E is larger than a prescribed error tolerance (ε_o), the final step of the iteration is to shift the position of free surface. The program is based on algorithm for explicit time integration from smith, (١٩٨٨), and procedure of solution reported by **Neuman** and **Witherspoon**, (١٩٧١). Figure (٣-٥) displays the overall structure chart of the program, an explanation of the different parts of the program is indicated in Appendix (B).

Given;description of the dam geometry and input data defining boundary conditions and material properties

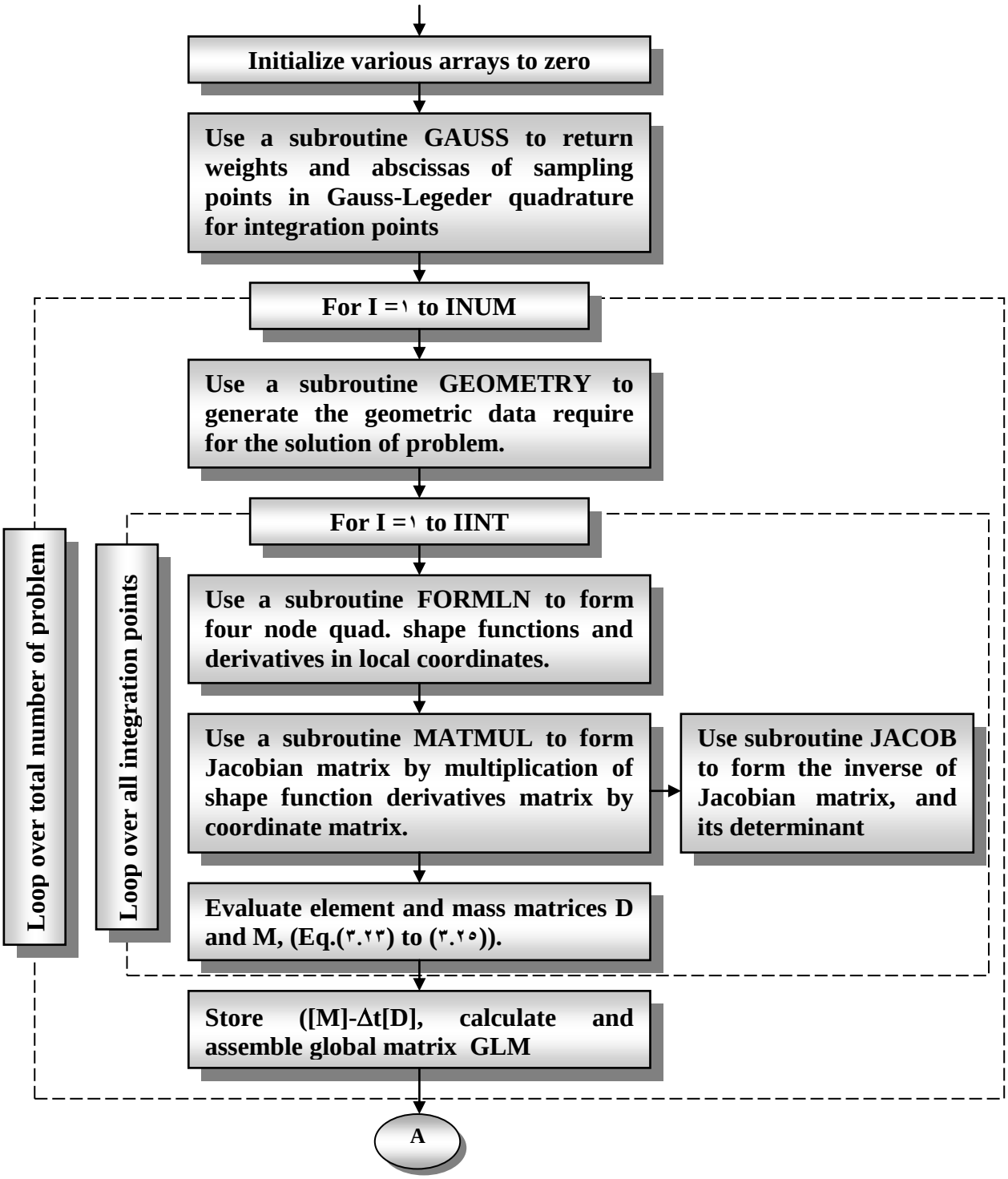

Figure (٣.٥) Overall structure chart of plan free surface flow program.

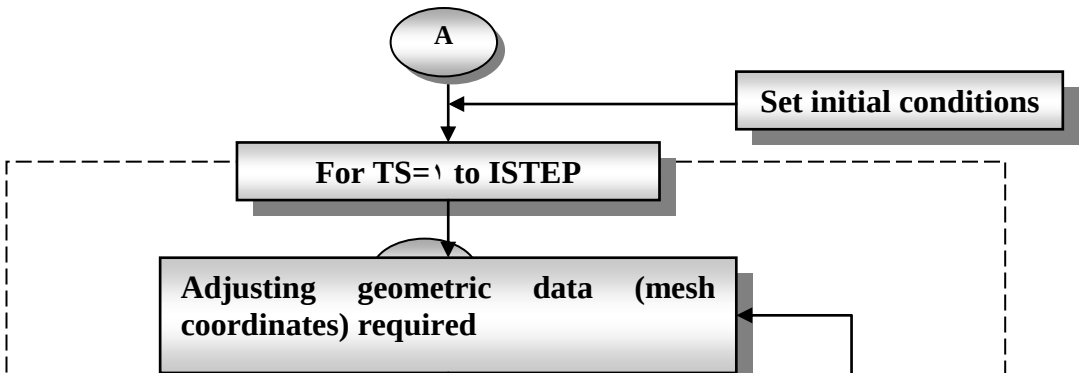

NO

Figure (٣.٥) Continued.

٣.٧.٢ Slope Stability Program

Figure (٣.٦) displays the overall structure chart of slope stability program. The main input information includes slope geometry, soil stratification, soil properties, discretization pattern, and the pore water condition. The pore water pressure values used in the analysis are interpolated from data file created by a finite element analysis of seepage problem which was described previously. The interpolation process is detailed in Appendix C.

The computation procedure starts by assuming a certain reasonable value for the factor of safety (F) and a value for the angle of inclination of the interslice forces (θ_o). After assigning the function $f(i)$ which described the variation of the angle (θ) with the slice number (i), each of angles (θi) can be easily determined by using Equation (٣.٤٤) [**Al-Jorany**, ١٩٩٦]. Search procedure is then performed by the subroutine (SEARCH), the searching for line of minimum resistance carried out. A tentative solution (y_i; i=١, ٢, …, n+١) is then obtained as an output of this subroutine. The calculating of the precise values of the factor of safety and angle (θ_o) corresponding to this tentative slip surface is achieved by subroutine MPM (Morgenstern-Price Method). The factor of safety value is obtained iteratively since for each trial value for the angle (θ_o) two values for factor of safety are obtained. The first is determined according to the equation of moment equilibrium (F_m) and the other is based on the equation of force equilibrium (F_f). The convergence is reached as the value of (F_m) approaches to the value of (F_f) to a certain tolerance (ε_1). The value of the angle (θ) at which convergence takes place and the corresponding factor of safety are considered as the output of this subroutine.

Before starting another cycle of computations, the obtained values of (F) and (θ) are to be compared with those assumed in the beginning of the computation procedure. When the difference between each corresponding pair is greater than a certain tolerance, the process is repeated from the beginning to determine anothetentative slip surface and so on until the required convergence is reached [**Baker**, ١٩٨٠]. An explanation of different parts of program are indicated in Appendix B.

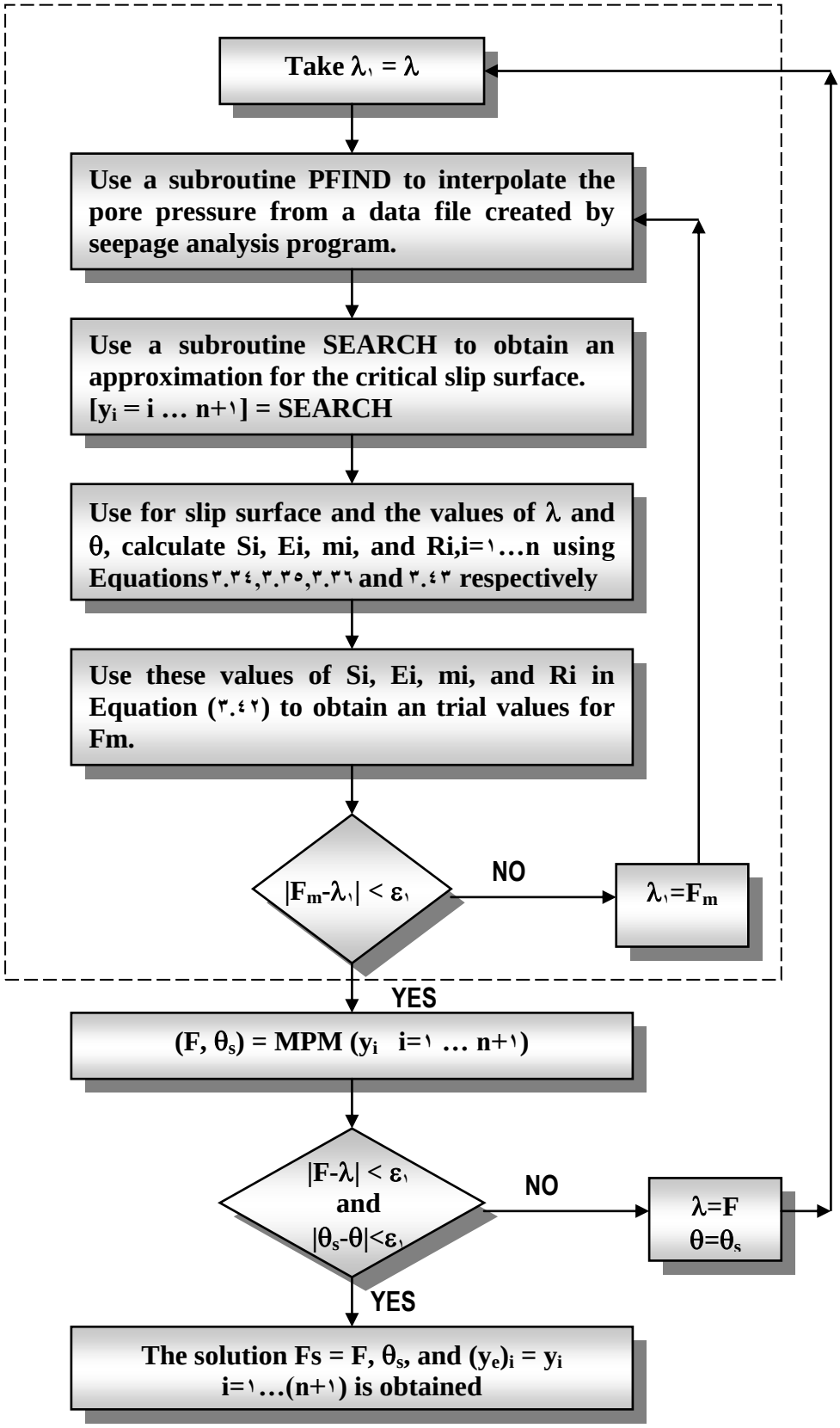

Figure (٣.٦) Overall structure chart of slope stability analysis.

Chapter Four

VERIFICATION AND APPLICATION

٤.١ General

The computation procedure for both seepage of water through earth dam and slope stability analysis have been presented in the preceding chapter. It is thought that the verification of these procedures is very important, thus it should be done before applying the present approaches to any practical problem. The main aims of the verification are; to check the reliability of the theoretical aspects utilized in the derivation of the present approaches, and then examine the proper working of the computer program that have been prepared to execute the computations in the approach.

The verification is performed by applying the developed computation procedure to some problems that had been analyzed previously by other researchers. In this respect, two different problems are considered; the first is an analytical solution presented by **Suresh** and **Harr** (١٩٦٢), while the second is the analysis of Otter Brook dam which was done by **Li** and **Desai** (١٩٨٣). Finally, a stability charts are presented to facilitate the computation of the factor of safety of earth slopes and dams during rapid drawdown.

٤.٢ Analytical Solution

Analytical study had been made by **Suresh** and **Harr** (١٩٦٢) for investigating the total head distribution in the porous body and determination of the response of the free surface in an incompressible homogenous earth mass, with an inclined up stream slopes (α) (Figure ٤.١), given the history of head water fluctuations, $h = f(t)$. The structure is assumed to be found on a horizontal impervious base.

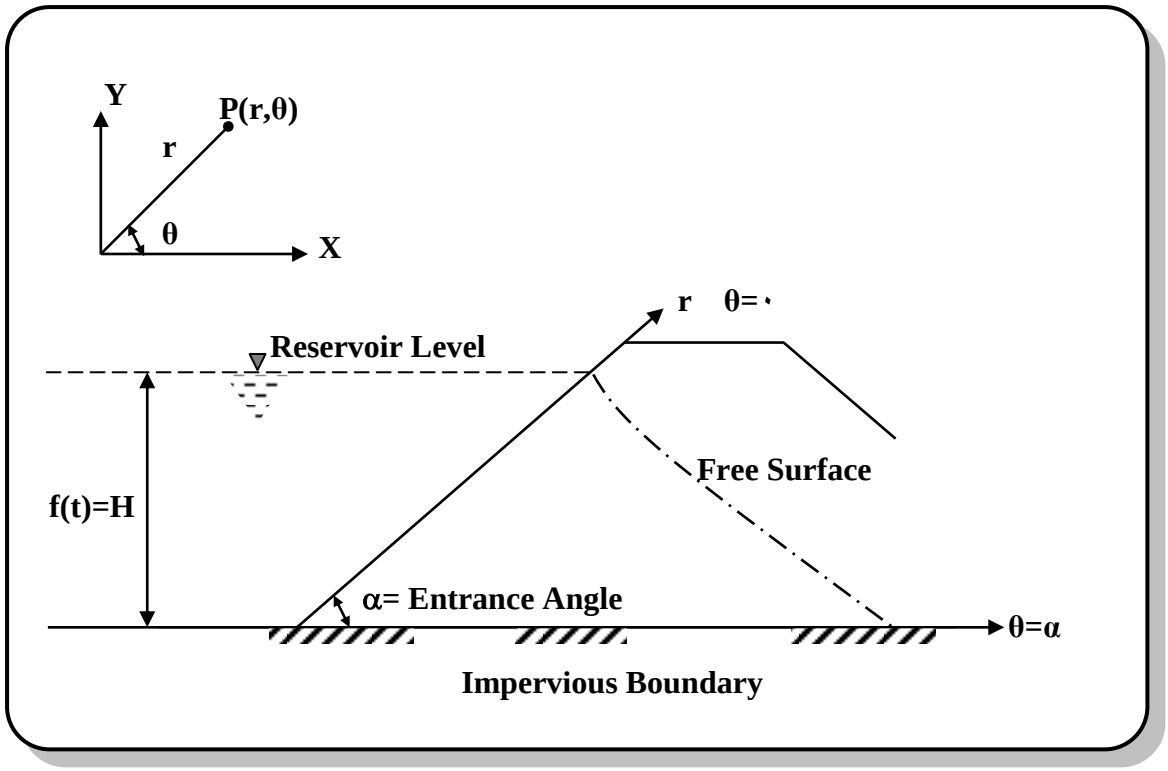

Figure (٤.١) Section Through Porous Body on an Impervious Boundary [After **Suresh** and **Harr**,١٩٦٢].

The problem is reduced to find a solution of **Boussinesq** equation that satisfies the following water case which represents an instantaneous change in reservoir level (or reservoir held at constant level H), for this case,

$$f(t) = H \qquad \text{.....} (٤.١)$$

where H is the constant level.

The solution for this particular case of $f(t)$ is derived analytically using Laplace transformations

$$\frac{h(r,\theta,t)}{H} = 1 - \frac{2}{\alpha}\sum_{n=0}^{\infty} \sin s\theta \int_0^{\infty} e^{-\tau u^2} \frac{J_s(u)}{u} du \qquad \text{.....} (٤.٢)$$

where,

h = total head at point $P(r, \theta)$ at time t.

$$\tau = \frac{k\,t}{r^2} \qquad \text{with units}(\ ^1/_T\ )$$

$$s = \left(\frac{2n+1}{2}\right)\frac{\pi}{\alpha}, \text{ and}$$

$J_s(u)$ = is the **Bessel** function of first kind of order *s*, or

$$\frac{h(r,\theta,t)}{H} = 1 - \frac{2}{\alpha}\sum_{n=0}^{\infty}\sin s\theta\left[\frac{\sqrt{\pi}}{4s\sqrt{\tau}}\left\{I_{\frac{s-1}{2}}\left(\frac{1}{8\tau}\right) + I_{\frac{s+1}{2}}\left(\frac{1}{8\tau}\right)\right\}\exp\left(\frac{1}{8\tau}\right)\right] \quad ....(٤.٣)$$

in which *I* represents the modified **Bessel** function.

Table (٤.١) indicates the percentage of absolute difference in the results of finite element method from the analytical solution at different points within dam body, that is computed from

$$Difference = \left|H_m - H_a\right| \quad .....(٤.٤)$$

where:

Difference = Difference between finite element head and analytical head. Usually recorded as (%).

H_m = Model head.

H_a = Head predicated analytically.

Table (٤.١) Comparison of Finite Element and Analytical Results for Various Entrance Angles (α) with Different θ's.

$\tau(^1/_T)$	**Entrance Angle (α) = ٣٠°**			**Entrance Angle (α) = ٦٠°**			**Entrance Angle (α) = ٩٠°**		
	F.E.M (θ=١٥°)	**Analytic (θ=١٥°)**	**% Diff. of F.E.M**	**F.E.M (θ=٣٠°)**	**Analytic (θ=٣٠°)**	**% Diff. of F.E.M**	**F.E.M (θ=٤٥°)**	**Analytic (θ=٤٥°)**	**% Diff. of F.E.M**
٠.٢	٠.٧٩١٨	٠.٨١١١	١.٩٣	٠.٤٧٦٤	٠.٤٩٧٤	٢.١٠	٠.٣١٧٤	٠.٣٣٧١	١.٩٧
٠.٤	٠.٩٠٩٤	٠.٩٢٢١	١.٢٧	٠.٦٤٩٦	٠.٦٦٠٤	١.٠٨	٠.٤٥٠٩	٠.٤٦٢٣	١.١٤
٠.٦	٠.٩٤٦٩	٠.٩٥٤٤	٠.٧٥	٠.٧٣٠٠	٠.٧٣٧٦	٠.٧٦	٠.٥٣٠٩	٠.٥٣٩٢	٠.٨٣
٠.٨	٠.٩٦٤٢	٠.٩٦٩٢	٠.٥٠	٠.٧٧٧٤	٠.٧٨٣٤	٠.٦٠	٠.٥٨٤٢	٠.٥٩٠٩	٠.٦٧
١.٠	٠.٩٧٣٨	٠.٩٧٧٥	٠.٣٧	٠.٨٠٩٠	٠.٨١٤٠	٠.٥٠	٠.٦٢٢٨	٠.٦٢٨٥	٠.٥٧

From this table, it can be seen that maximum percentage difference is (١.٩٧). In view of the number of assumptions in the finite element procedure, and as in all transient solutions, the magnitude of time step deserves some difficult to choose, it can be expected that this difference be due to these reasons. It can also be noted that the differences are decreased as time increases, which indicates the stability of the solution. Beside the numeric comparison between the finite element and analytical results, a graphical comparison of the trend of variation of heads distribution for typical points within dam body is always useful. This could be viewed through Figures (٤.٢) to (٤.٥) which shows a good agreement.

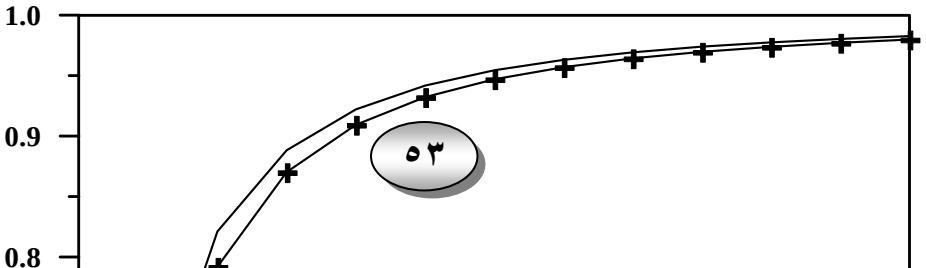

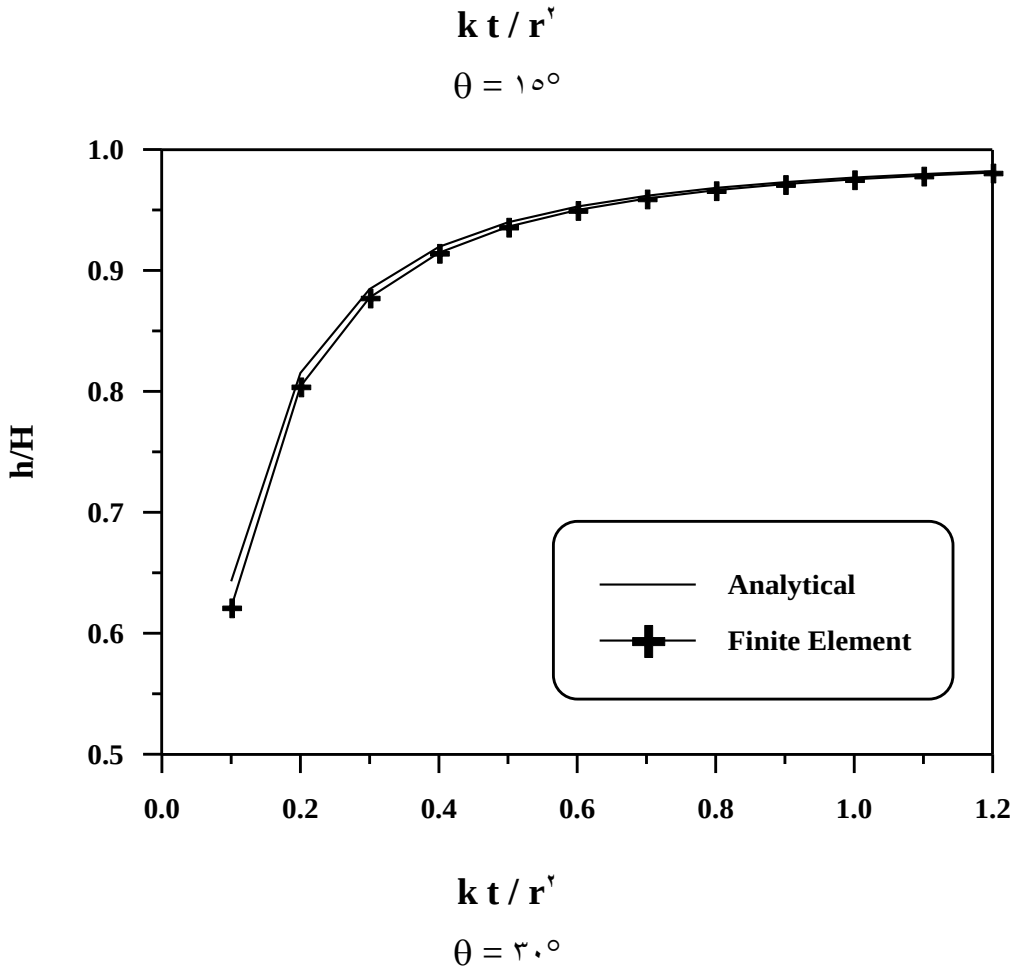

Figure (٤.٢) Comparison of Analytical and Finite Element Results for Different θ's with α = ٣٠°.

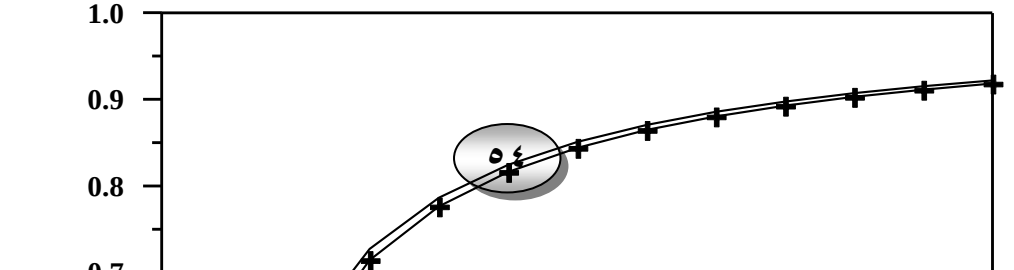

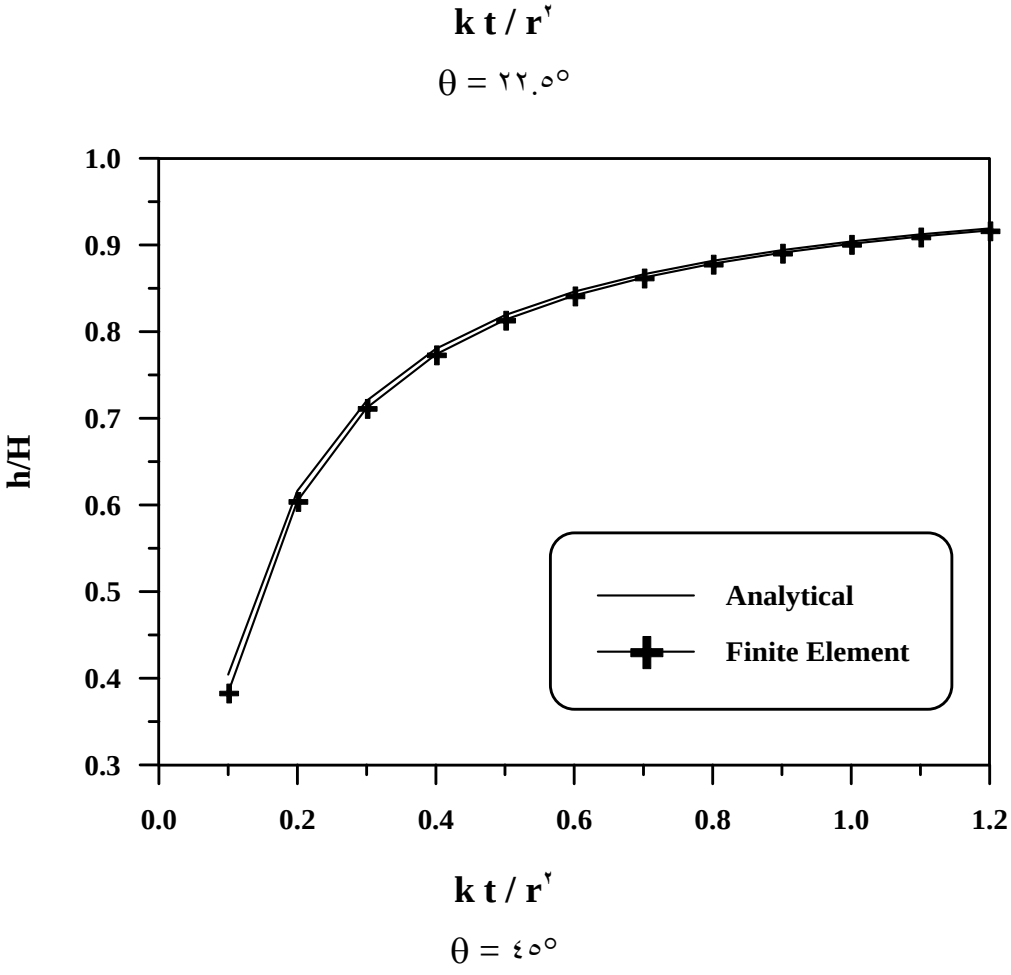

Figure (٤.٣) Comparison of Analytical and Finite Element Results for Different θ's with α = ٤٥°.

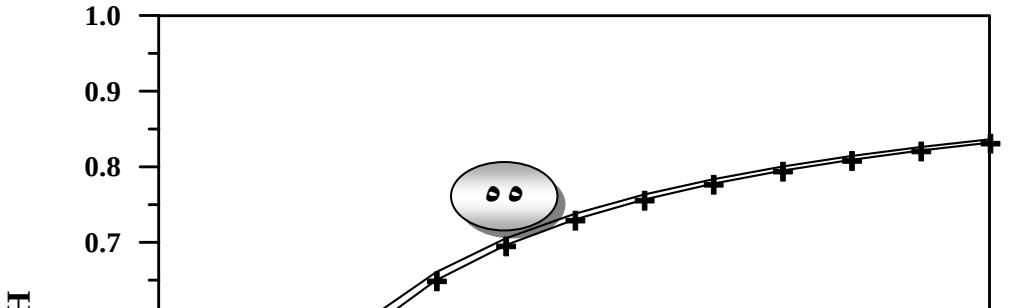

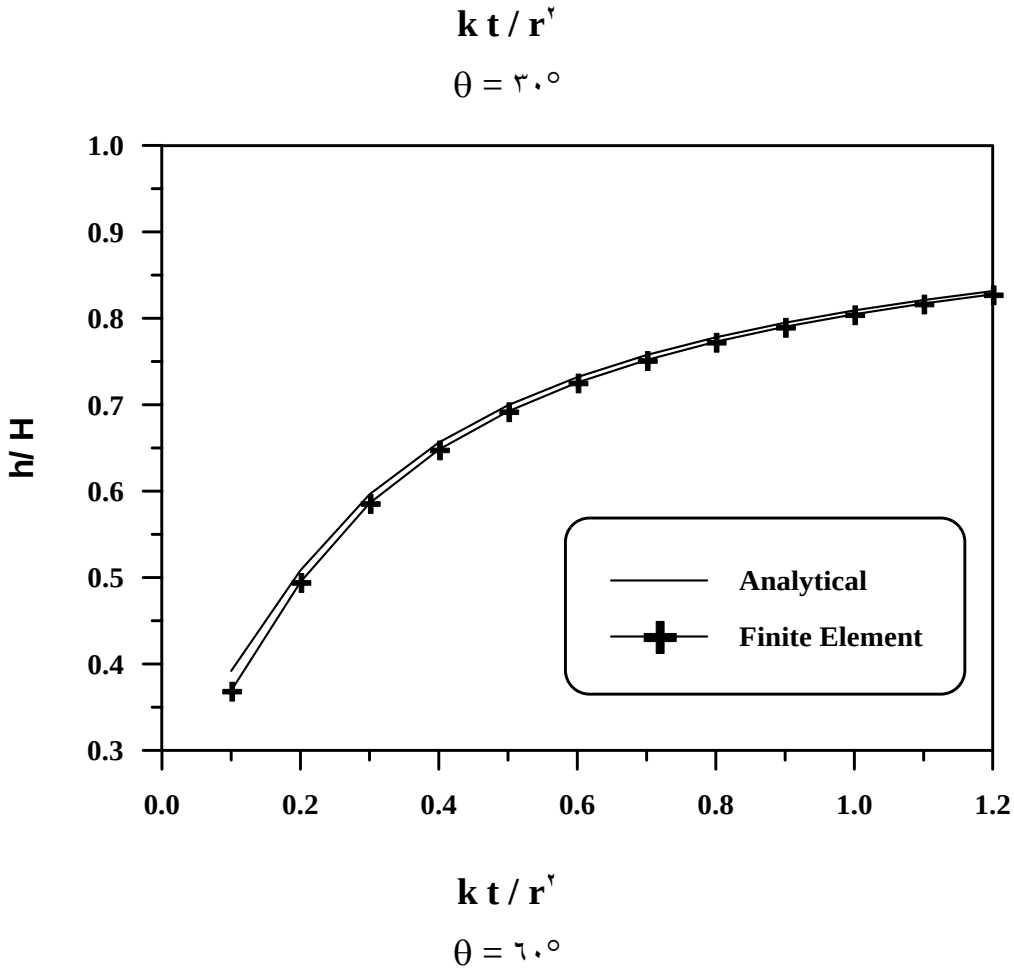

Figure (٤.٤) Comparison of Analytical and Finite Element Results for Different θ's with α = ٦٠°.

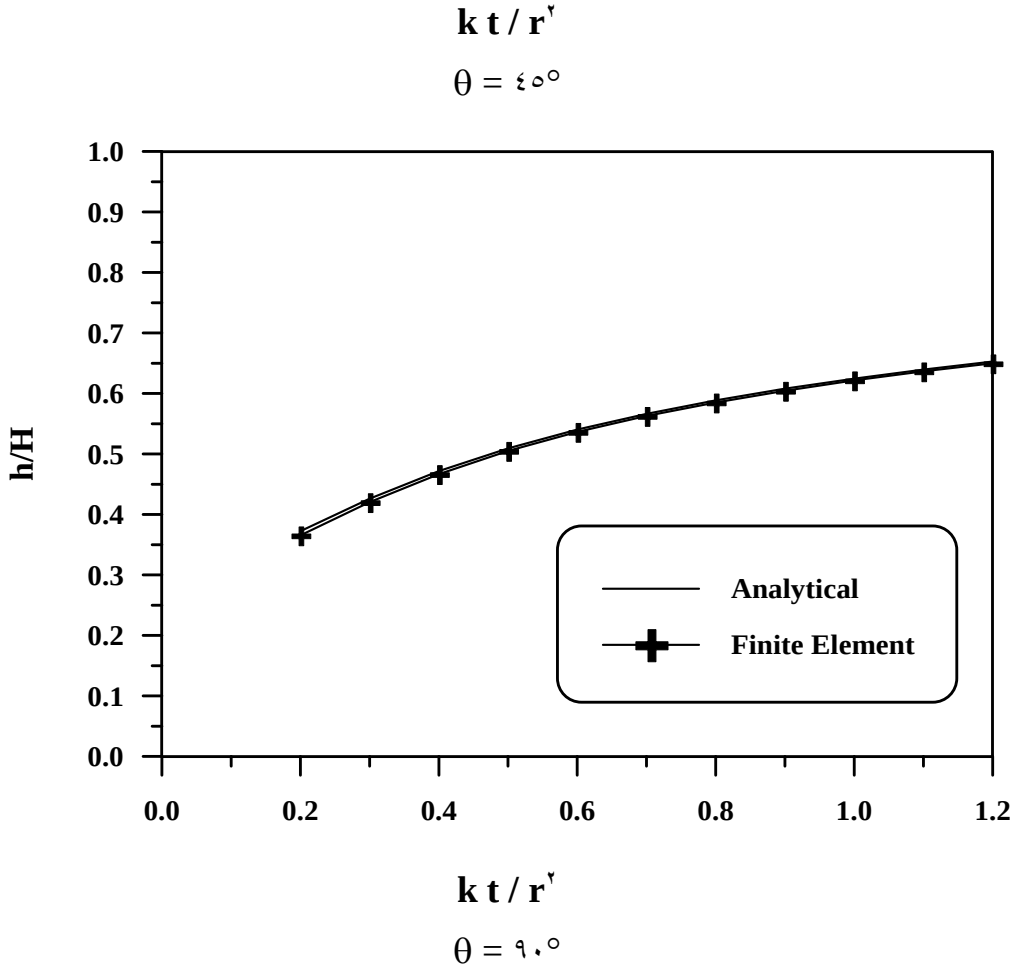

Figure (٤.٥) Comparison of Analytical and Finite Element Results for Different θ's with α = ٩٠°.

٤.٣ Analysis of Otter Brook Dam

The Otter Brook dam as described by **Li** and **Desai** (١٩٨٣) was constructed in New Hampshaire in U.K. in ١٩٥٧ with a height of ٤٠m (١٣٠ft), a base width of ٢١٠.٥m (٦٩٠ ft) and crest width of ٧.٦m (٢٥ft). The upstream and downstream slopes have roughly the same angels and the geometry is somewhat symmetrical except for chimney drain on the downstream side. Part of final design cross section of the dam which adopted from **Desai** and **Abel** (١٩٧٢) is shown in Figure (٤.٦), two material types were used in the analysis of Otter Brook dam. The material properties for each material type, as shown in Table (٤.٢) and Table (٤.٣), are adopted from **Clough** and **Woodward** (١٩٦٧).

The finite element mesh used in this analysis is drawn in Figure (٤.٧), in the past, most finite elements procedures for free surfaces seepage involved discretization of flow domain below free surface, this referred to as the variable mesh procedure. The variable mesh procedure can cause computational difficulties in cases of layered soil, particularly those with nearly horizontal interfaces, and for soils involving pockets of nonhomogenties of a very low or high permeability. It is also difficult to assign appropriate material properties when the free surface crosses the interfaces. These difficulties are significantly reduced in the case of the invariant mesh procedure based on weighted residual method used here.

An idealized dam section [see Figure ٤.٧] is analyzed by using a mesh contains (٢٨٠) finite elements and (٣١٥) nodal points which arrange carefully to consider the slope geometry and soil layering.

Figure (٤.٨) shows three different rates of drawdown (٠.٣ m/day, ٣ m/day, ٣٠ m/day), the drawdown involved a drop of water level from a height (٤٠ m) measured from the bottom of foundation to a height of (١٠m). This is a high rate of drawdown corresponding to sudden drawdown [**Li** and **Desai**, ١٩٨٣].

Table (٤.٢) Material Properties Used for Analysis of Otter Brook dam; Seepage Analysis [Collected from **Clough** and **Wood Ward** ١٩٦٧, and **Li** and **Desai**, ١٩٨٣].

Parameter	Magnitude for Different Material		
	Dam	Foundation	Drain
Horizontal permeability, k_x (cm/sec)	٦×١٠^{-٧}	٦×١٠^{-٧}	١×١٠^{-٣}
Vertical permeability, k_y (cm/sec)	٦×١٠^{-٧}	٦×١٠^{-٧}	١×١٠^{-٣}
Specific storage, $m^{-١}$	١.٥×١٠^{-٨}	١.٥×١٠^{-٨}	١.٥×١٠^{-٦}
Dry Soil			
Cohesion, C, $kN/m^{٢}$	١٠٣.٥	٩٥.٧٠	٩.٦٠
Angle of internal friction, ϕ, deg.	١٤.٠	٢٤.٠	١٤.٠
Unit weight, γ, $Ton/m^{٣}$	١.٥٩٦	١.٥٩٦	١.٥٩٦
Wet Soil			
Cohesion, C, $kN/m^{٢}$	٩٣.٠٠	٨٦.١٣	٨.٦٠
Angle of internal friction, ϕ, deg.	١٥.٤	٢٦.٤	١٥.٤
Unit weight, γ, $Ton/m^{٣}$	٢.١٧١	٢.٢٣٤	٢.١٧١

Table (٤.٣) Material Properties Used for Analysis of Otter Brook Dam; Stability Analysis.

Parameter	Symbol	Magnitude
Unit weight, $Ton/m^{٣}$	γ	٢.٢٣٥
Cohesion, $kN/m^{٣}$	C	١٠٣.٥
Angle of internal friction	ϕ	١٤٥
Modulus number	ν	٠.٤٨
Failure ratio	R_f	٠.٦٨
Poisson's ratio parameters	G_r	٠.٤٣
	F_r	-٠.٠٥
	D_r	٠.٦٠

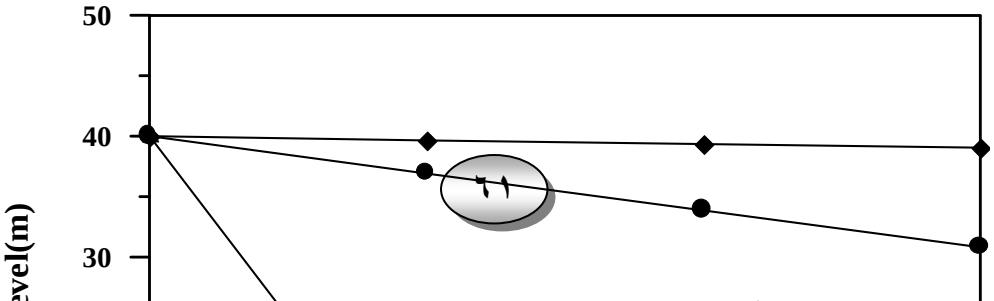
50
40
30
evel(m)

Figure (٤.٨) Typical History of Variations of Water Level Versus Time for Otter Brook Dam [After **Li** and **Desai**, ١٩٨٣].

٤.٣.١ Results and Comparison

Figure (٤.٩) shows computed successive movement of free surface due to drawdown of upstream water level. Figure (٤.١٠) revealed the distribution of pressure head within dam body corresponding steady state conditions.

A case of sudden drawdown is considered to be exist with a rate of drawdown (٣٠m/day). Figure (٤.١١) show contour map pressure head distribution after (٠.٥ day) of drawdown beginning, the head and pressure on the upstream side are decrease at a much slower rate than the sudden drawdown rate. A case of linear drawdown is considered to be exist with the rate of (٣ m/day). Figure (٤.١٢a) to (٤.١٢c) show contour maps of pressure head distribution at typical time levels (٠.٥, ١, ٣ days) during drawdown, the head and pressure are decreased in a rate similar to the drawdown rate of reservoir.

٤.٣.١.١ Analysis of Factors Effecting Solution

١. Improvement of accuracy

A four node isoparametric quadrilateral element, with linear field variable model was used. this model did not affect the numerical solution to any significant extent. High order model such as a cubic model includes the gradient of the heads at the nodes as unknowns in addition to the nodal heads, so that, there are four unknowns per element. Such element improve the solution only slightly. Also, because of the compatibility of the gradients at interelement nodes, a cubic model may not be suitable for nonhomogeneous media. It seems that due to such factors as linearization and the Dupuit assumption, increasing the order of the field variable model does not improve the solution significantly.

٢. Spatial and Temporal Discretizations

The time integration scheme used in the present work is essentially similar to the forward difference procedure, and is subjected to numerical instability beyond a certain range of discretization. A number of factors such as spatial and time wise subdivision can influence the stability behavior. Within the range of spatial and temporal discretization, the user may adopt irrespective of the integration scheme, the proposed procedure provides solution of acceptable accuracy. In this respect, it's not usually to adopt a mesh coarser than that shown in Figure (٤.٧). In case of sudden drawdown the time interval is increased gradually and the end of drawdown process reached after ٩٠ time steps. A constant time step was adopted for linear drawdown with Δt (٠.٠٢ day). The stability of the method is evident in Figures (٤.١٣) and (٤.١٤), the iterations required to obtain a solution for a typical time step are shown in these figures. Note that after five iterations, the maximum error was less than ٢٪ for gradually increased time.While the maximum error was less than ٢٪ after eleven iterations for constant increased time step.

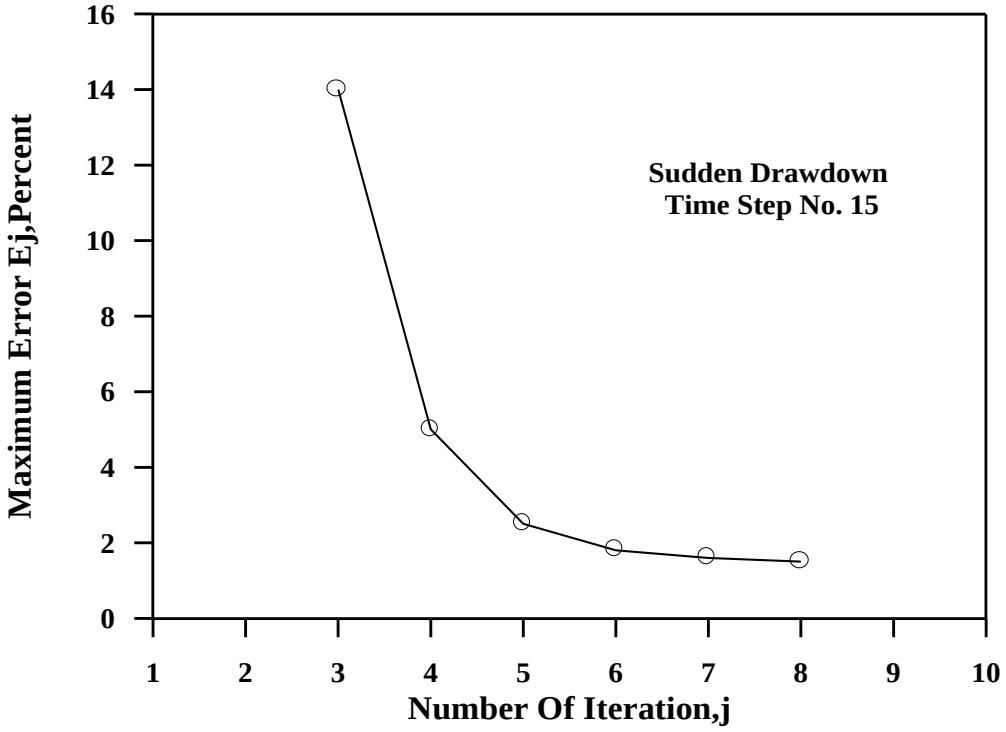

Figure (٤.١٣) Plot of Maximum Error E_j Versus Number of Iteration j for sudden drawdown process.

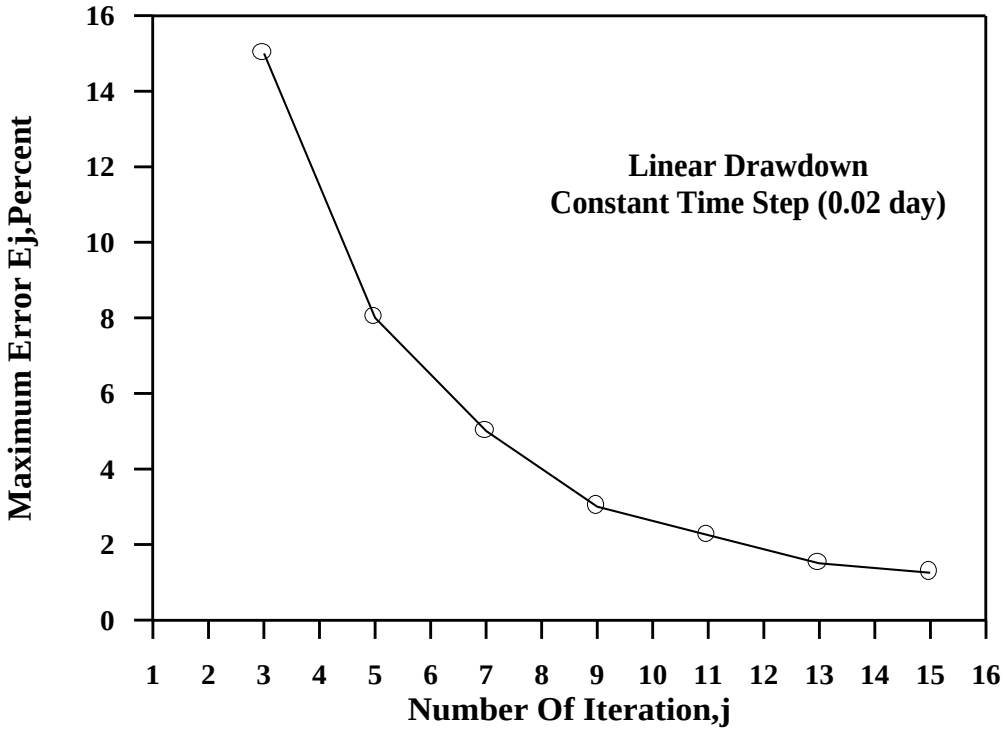

Figure (٤.١٤) Plot of Maximum Error E_j Versus Number of Iteration j for linear drawdown process.

٣. Effect of Magnitude of Permeability

Several investigators (**Desai**, ١٩٧٢; **Ching**, ١٩٨٨) had studied the effect of coefficients of permeability on the potential heads, and free surface movements. According to **Ching** (١٩٨٨) it is noted that the effect of hydraulic conductivity on the calculated potential heads is relatively insignificant. From an engineering point of view, it is desirable because the value of hydraulic conductivity in most field cases can only be determined approximately.

٤.٣.١.٢ Stability Analysis

The stability analysis performed here based on a limit equilibrium (Morgenstern – Price) method, with the following considerations:

١. Referring to Equation (٣.٤٤) in the preceding chapter, a wide range of $f(i)$ (which describes the variation of the angle of inclination of interslice forces) should be selected reasonably. **Al-Jorany** (١٩٩٦) considered three different functions of $f(i)$, and he noted that for the same slip surface the effect of function $f(i)$ on the value of factor of safety is almost insignificant. In addition **Muni** (٢٠٠٠) introduced $f(i)$ as a function $\approx$ ١, therefore; the adopted form of $f(i)$ in the present work is in (a constant form).

٢. The available information in the literature are mainly about the residual flow finite element procedure which, is used to analyze the Otter Brook dam, in which the behavior of construction materials are modeled on base of linear – elastic model, and on elastic – plastic model (stress – deformation analysis), also there are no more information about the failure surface corresponding the proposed rates of drawdown. While in the present analysis the soil skeleton is assumed to be incompressible, and no pore pressure occurs due to shear deformations.

Table (٤.٤) shows a comparison of values of factors of safety obtained by the present analysis and those obtained by **Li** and **Desai** (١٩٨٣). These values are

also plotted in Figures (٤.١٥) to (٤.١٧), it is noted that the present analysis yields lower factor of safety as compared to those by **Li** and **Desai**. For case of a sudden drawdown the factor of safety decreases first, with the lowest value around the end of drawdown, thereafter, the factor of safety increases. Figure (٤.١٨) display the comparison of the percentage of absolute error between the present analysis and those obtained by **Li** and **Desai**.

Table (٤.٤) Comparison of Factors of Safety Values Obtained by present Analysis and Those by **Li** and **Desai** (١٩٨٣).

Time (day)	Drawdown rate = ٣٠ m/day			Drawdown rate = ٣m/day			Drawdown rate = ٠.٣m/day		
	Present analysis	Li and Desai analysis	% Error	Present analysis	Li and Desai analysis	% Error	Present analysis	Li and Desai analysis	% Error
٠	٣.٨٧٣	٤.٣٧٣	١٢.٩	٣.٨٧٣	٤.٣٧٣	١٢.٩	٣.٨٧٣	٤.٣٧٣	١٢.٩
١	٣.٧٠١	٤.٢٣٦	١٤.٥	٣.٨٥	٤.٣٥١	١٢.٩	٣.٨٦٣	٤.٣٧٠	١٣.١
٢	٣.٧١٦	٤.٢٥٩	١٤.٦	٣.٨٥٧	٤.٣٧٠	١٣.٣	٣.٨٥٧	٤.٣٥٥	١٢.٩
٣	٣.٧٣٧	٤.٢٨١	١٤.٦	٣.٨٦٣	٤.٣٩٢	١٣.٦	٣.٨٦٣	٤.٣٧١	١٣.٢

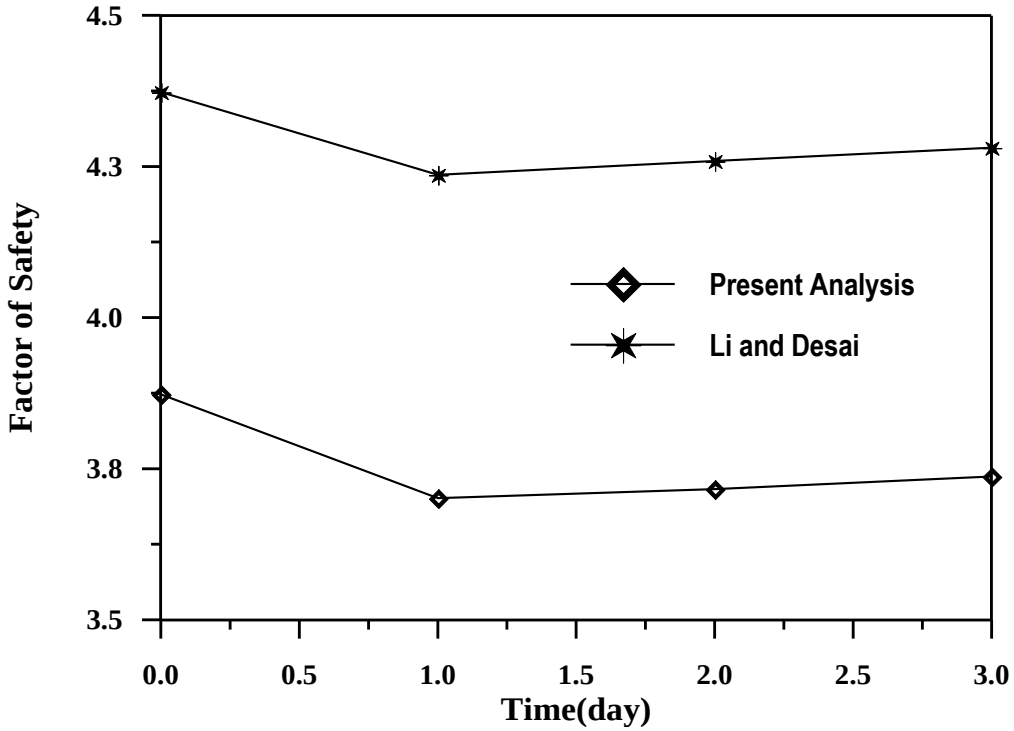

Figure (٤.١٥) Comparison of Factor of Safety Between Present Analysis and (**Li** and **Desai**) Results for Drawdown rate = ٣٠ m/day

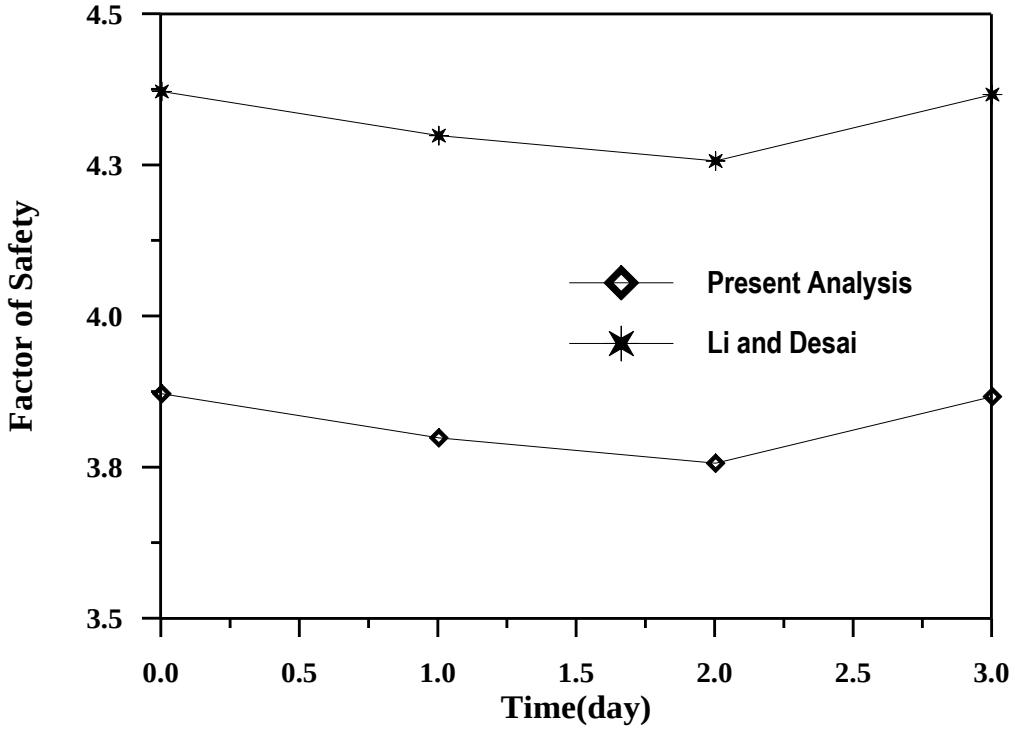

Figure (٤.١٦) Comparison of Factor of Safety Between Present Analysis and (**Li** and **Desai**) Results for Drawdown rate = ٣ m/day

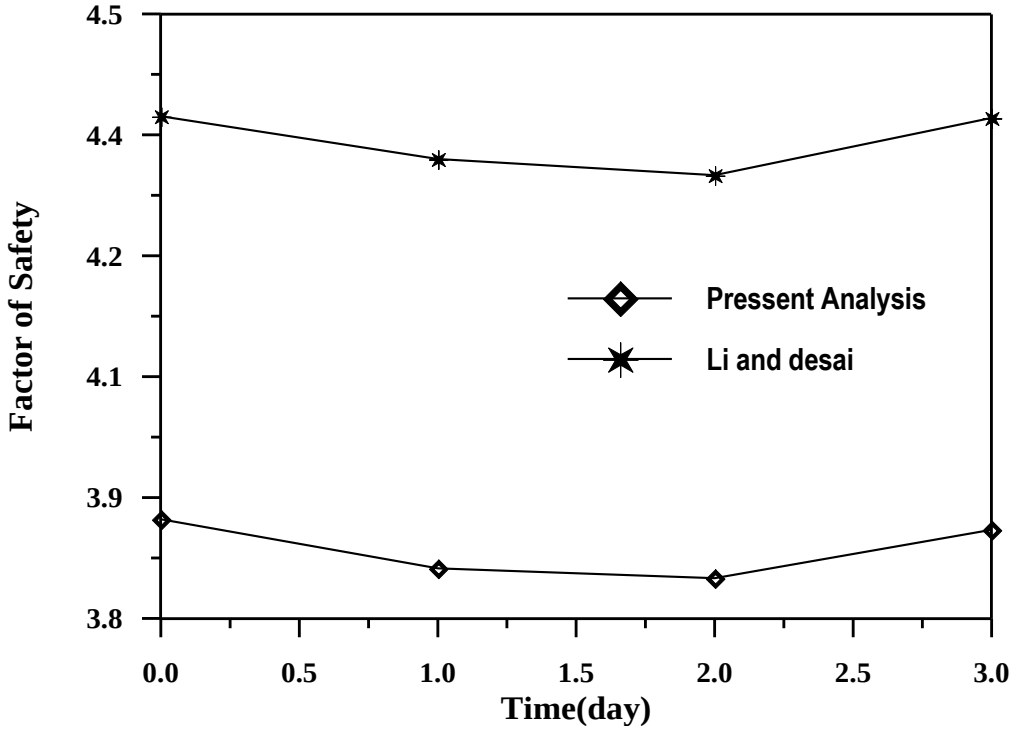

Figure (٤.١٧) Comparison of Factor of Safety Between Present Analysis and (**Li** and **Desai**) Results for Drawdown rate = ٠.٣ m/day

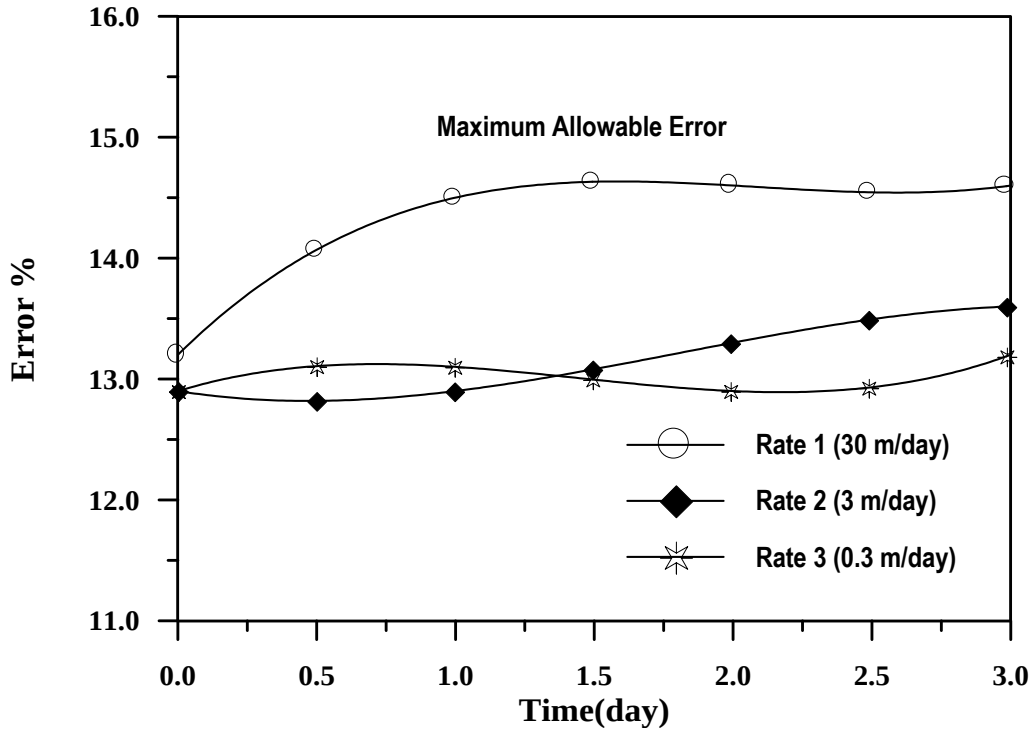

Figure (٤.١٨) Comparison of the percentage absolute error for present analysis and those by **Li** and **Desai**.

The paper by **Li** and **Desai** details a graphical comparison of factor of safety for both linear elastic model and elastic-plastic model. Table (٤.٥) gives the numeric comparison by mean of the percentage error.

Table (٤.٥) Comparison of Factor of Safety Values Obtained by Two Different Models.

Time (day)	Linear elastic model (١)	Elastic – plastic model (٢)	% Error of model (٢)
٠	٥.٢٦٨	٤.٣٧٣	٢٠.٥
١	٥.١٠٠	٤.٢٣٦	٢٠.٤
٢	٥.١٣٦	٤.٢٥٩	٢٠.٦
٣	٥.١٨٢	٤.٢٨١	٢١.٠

The preceding comparison indicates the following:

١. In spite of the completely different approach that is used in the present work and those by **Li** and **Desai**, the results show that maximum error is less than (١٥٪). The paper by **Yu *et al.***, (١٩٩٨) compares conventional limit-equilibrium results with rigorous upper and lower bound solutions for the stability of simple earth slopes. It is indicated that techniques that satisfy all conditions of global equilibrium gives similar results. Regardless of the different assumptions about the interslice forces, these methods (such as Bishop's simplified, Janbu, Spencer, and Morgenstern and Price) give values of safety factor that differ by no more than ٥٪. **Yu *et al***. (١٩٩٨) have been used Bishop's simplified method and they were concluded that for most cases it was found that the exact stability solution for both drained and undrained slopes can be predicted to within ٥-١٠٪ by the upper bound solutions.

٢. A fair correspondence between the present analysis and those by **Li** and **Desai**. Thus, the limit equilibrium method is a proper method to be used in the analysis and design of earth dam. A major advantage of this approach is that complex soil profiles, seepage, and a variety of loading conditions can be easily dealt with **Yu *et al.*** (١٩٩٨).

٣. The minimum factor of safety at the end of linear drawdown is about (٣.٥٪) higher than that from sudden drawdown, it was found that this percentage varied about (٢.٦٪) for **Li** and **Desai** analysis.

٤.٤ Investigation of Drawdown Ratios Effect on Stability of Dams

Prior to the lowering of the reservoir, the total head distribution or pore pressure in an earth dam is governed by the equilibrium conditions for the flow of water through porous media. Laplace's equation holds and the head may be determined readily by conventional or numerical methods. The effect of drawdown is twofold. First, it establishes new boundary conditions for the flow of water through the dam and an unsteady state is established while free surface adjusts to a new equilibrium position.

In case of free draining fills of low compressibility, such as clean sands and gravel, the head can be estimated by construction a flow net satisfying the new boundary conditions. The most critical distribution exists immediately after drawdown. With time, the pore pressure will decrease and the factor of safety of the upstream slope will increase.

In fill material with low permeability, considerable time must elapse for the pore pressure distribution to readjust the new conditions obtaining after drawdown.

A number of factors must be included and non-dimensional quantities be defined for easy interpretation. The significant factors included in analysis are:

(a) Angle of slope (β).
(b) Coefficient of permeability (k).
(c) Rate of drawdown (R).
(d) Strength parameters C and ϕ.

The safe function measured by mean of factor of safety is, therefore, seen to depend on several variables, an accurate and extensive general solution is made possible by these factors which has been discussed in detail by **Bishop** and **Morgenstern** (١٩٦٠). For a given value of dimensionless number (C / γH) the factor of safety depends only on the geometry of dam expressed by value of

(cot β), on the head within dam body and on the angle of internal friction ϕ. Only three values of ($C/\gamma H$) have been used (٠.٠١٢٥, ٠.٠٢٥, and ٠.٠٥) to simplify the presentation of data, these values have been selected as representing the range commonly encountered in effective stress analysis and also, a range within which a linear interpolation can be used without significant errors. Four slope inclinations have been selected for analysis and expressed in terms of cotangent of their inclination to horizontal (β); they are ٢:١, ٣:١, ٤:١, and ٥:١.

The factors of safety of these slopes at varying drawdown levels has been determined for a range of internal angle of friction ϕ with values ٤٠°, ٣٠°, and ٢٠°. These values represent most of the range encountered in drawdown problem [**Bishop** and **Morgenstern,** ١٩٦٠].

Referring to Figure (٤.١٩), introducing the drawdown ratio (H_d/H), where (H_d) is the drawdown head at given time, (H) is the height of slope or total height of drawdown; and (H_e) is the head of exit point of slope.

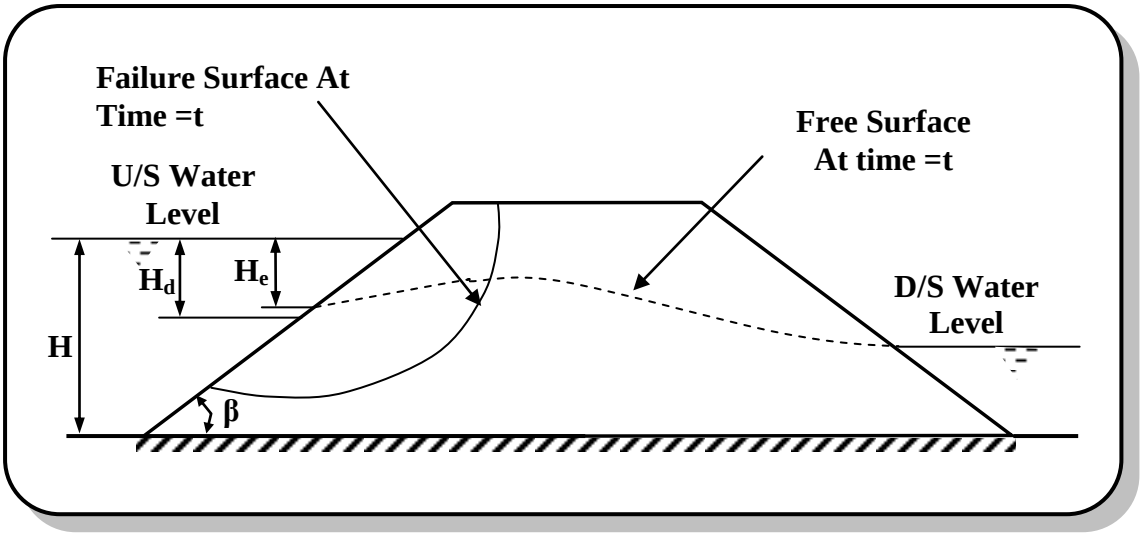

Figure (٤.١٩) Definition of Parameters.

The analysis used section shown in Figure (٤.١٩) with the following limitations:

١. The dam is homogenous and constructed of a single material with effective strength parameters C and ϕ.

٢. The dam is seated on rigid, impermeable base and before drawdown the reservoir is at crest level or full submergence conditions.

٣. The bulk density of the fill is taken to be twice that of water, i.e., $\gamma \approx ٢\gamma_w$.

In finite element analysis a consistent units and arbitrarily adopted a permeability of K = ٠.٠١ (cm/sec) and porosity of *n* = ٠.٤ were used. The value of permeability adopted here is to classify the soil into medium permeable soil according to the classification presented by **Lambe** and **Whitman** (١٩٦٩).

Typical value range of (*k*) for various soil types are shown in Table (٤.٦). Homogeneous clays are practically impervious. Two popular uses of impervious clays are in dam construction to curtail the flow of water through the dam and as barriers in land fills to prevent migration of effluent to the surrounding area. Clean sands and gravel are pervious and can be used as drainage materials or soil filters [**Muni**, ٢٠٠٠].

Figures (٢.٢٠) to (٤.٢١) show results from (H_e/H) versus drawdown ratio (H_d/H) for different (R/k). Such information allows location of exit point and determination of surface of seepage. A value of R/k = ١was adopted for final charts, the magnitude of R/k can influence the results significantly if its value is very small, i.e., the material is highly pervious. In such event, the finite element formulation used will need modifications, since the flow may no longer follow Darcy's law which is assumed in the formulation [**McCorquodale**, ١٩٧٠].

Table (٤.٦) Coefficient of Permeability for Common Soil Types [**Muni**, ٢٠٠٠].

Soil type	Value of K (cm/sec)
Clean gravel	> ١.٠
Clean sands, clean sand and gravel mixture	١.٠ to $١٠^{-٣}$
Fine sands, silts mixture comprising silts, and clays	$١٠^{-٣}$ to $١٠^{-٧}$
Homogenous clays	< $١٠^{-٧}$

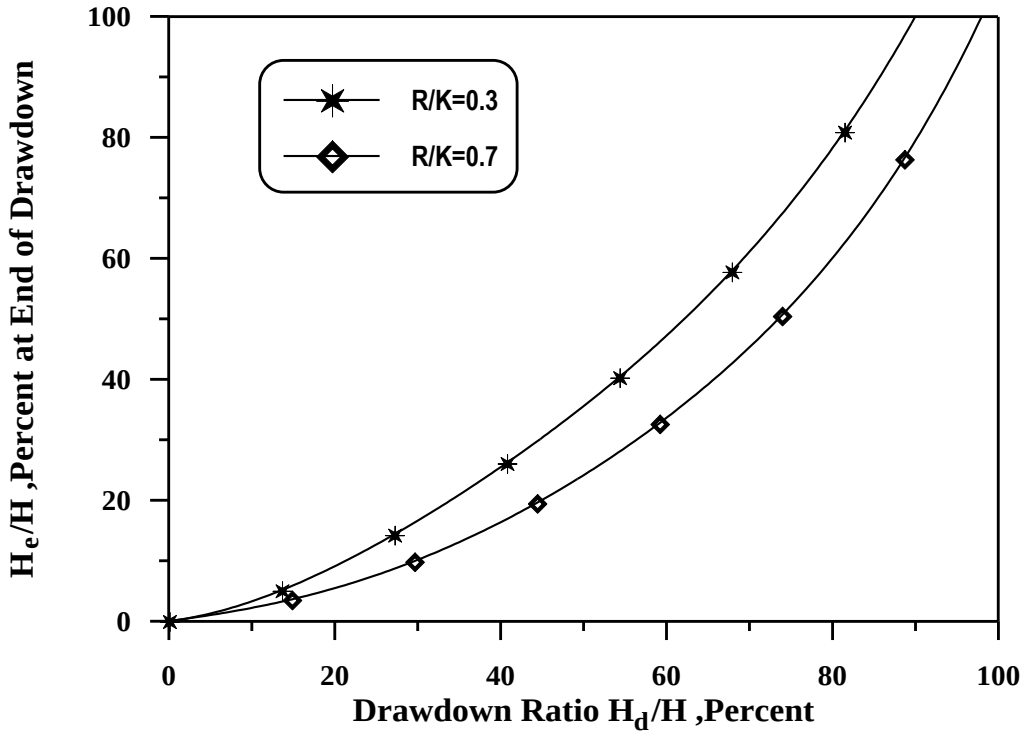

Figure (٤.٢٠) Plots for Drawdown Ratios (H_d/H) versus (H_e/H) for Linear Drawdown Rate.

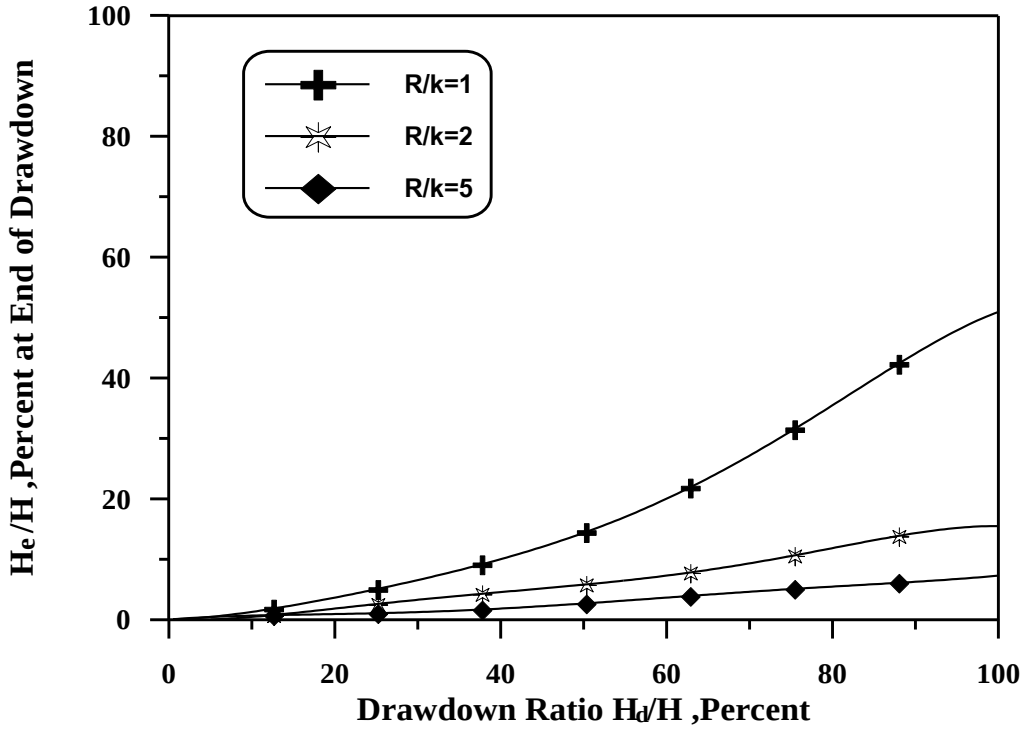

Figure (٤.٢١) Plots for Drawdown Ratios (H_d/H) versus (H_e/H) for Sudden Drawdown Rate.

The plots that showing the variation of the factor of safety with drawdown ratio are given in Figure (٤.٢٢) to (٤.٢٧). Figure (٤.٢٢) shows these relations for the value of (C / γH) equal to (٠.٠١٢٥) over a range of slope inclinations and angles of internal friction covered by solution, the factor of safety decreases as drawdown ratio increases, for the same strength parameters and water condition, the factor of safety increases as slope inclinations are decreases. For $C / \gamma H$ =٠.٠١٢٥ and ϕ=٢٠° the factor of safety corresponding to drawdown ratio = ٠.٥ increases about ٣٠٪ if slope inclinations varied from ٢:١ to ٣:١. Similarly, Figures (٤.٢٤) and (٤.٢٦) related to values of ($C / \gamma H$) of ٠.٠٢٥, and ٠.٠٥, respectively. These figures may be employed for computations of factors of safety at required times during drawdown. Note that the relations presented here in are meant only for those problems having conditions and properties similar to those considered in this work. Figures (٤.٢٨) and (٤.٢٩) show that for drawdown ratios (٠.٢٥, and ٠.٥) for typical cases with slope inclinations (٢:١ and ٤:١) and angles of internal friction of (٢٠°, and ٣٠°), the variation of the factor of safety with $C / \gamma H$ is almost linear. Extrapolation beyond the range of values of $C / \gamma H$ is allowed with a reasonable results.

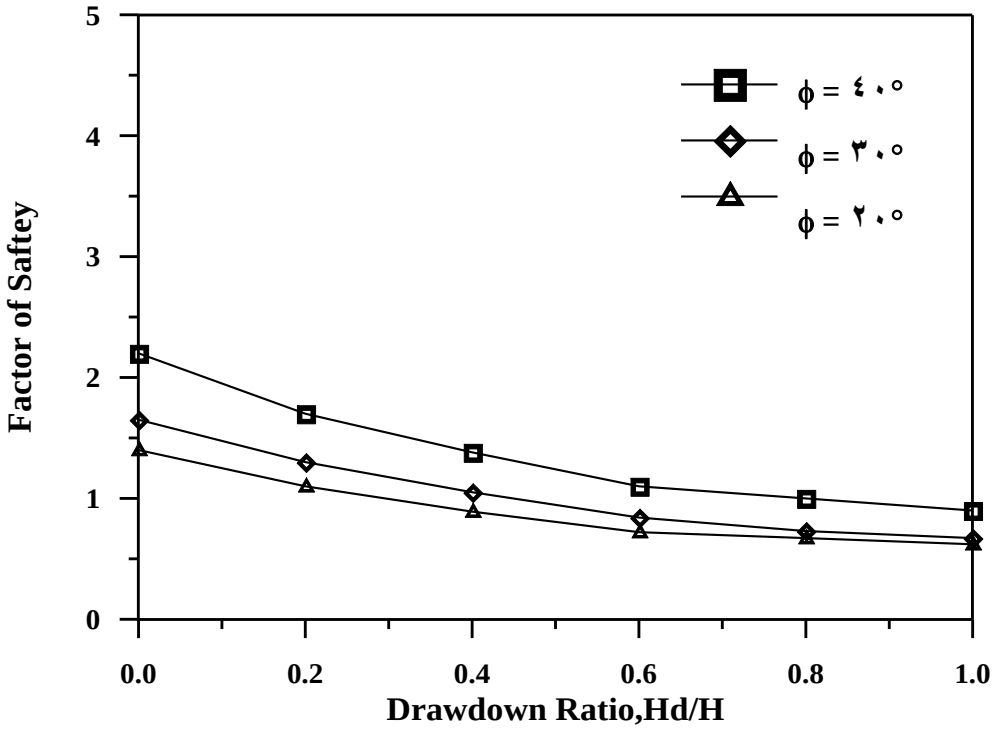
Factor of Saftey
Drawdown Ratio,Hd/H
ϕ = ٤٠°
ϕ = ٣٠°
ϕ = ٢٠°
0
1
2
3
4
5
0.0
0.2
0.4
0.6
0.8
1.0

β = ٢ : ١

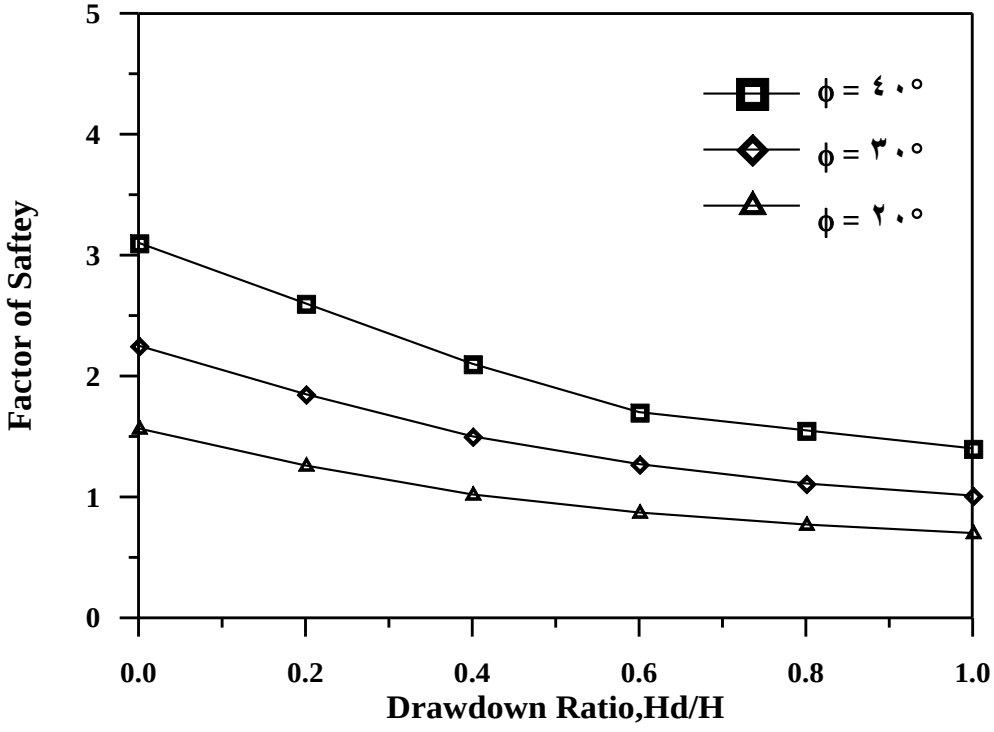
Factor of Saftey
Drawdown Ratio,Hd/H
ϕ = ٤٠°
ϕ = ٣٠°
ϕ = ٢٠°
0
1
2
3
4
5
0.0
0.2
0.4
0.6
0.8
1.0

β = ٣ : ١

Figure (٤.٢٢) Drawdown Stability Chart with (C / γ H = ٠.٠١٢٥).

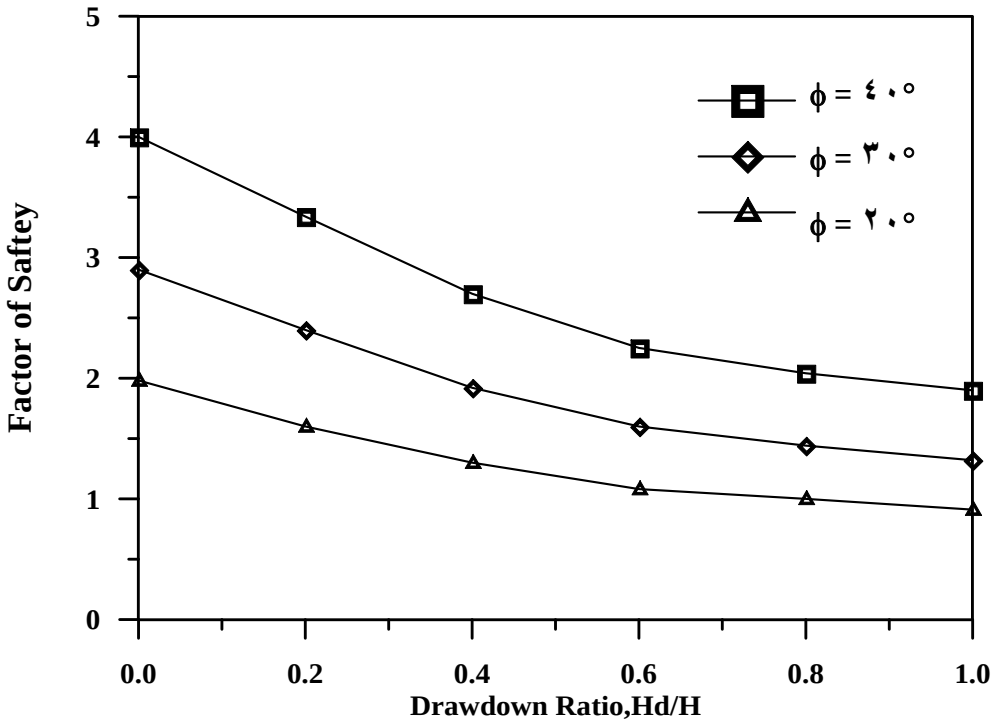

β = ٤ : ١

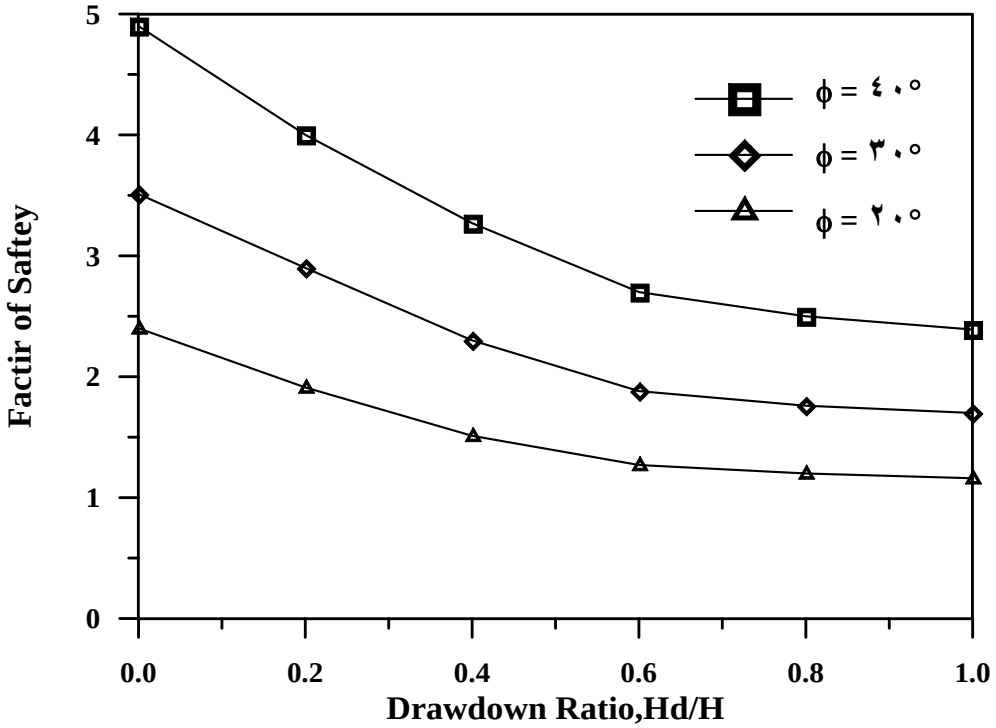

β = ٥: ١

Figure (٤.٢٣) Drawdown Stability Chart with (C / γ H = ٠.٠١٢٥).

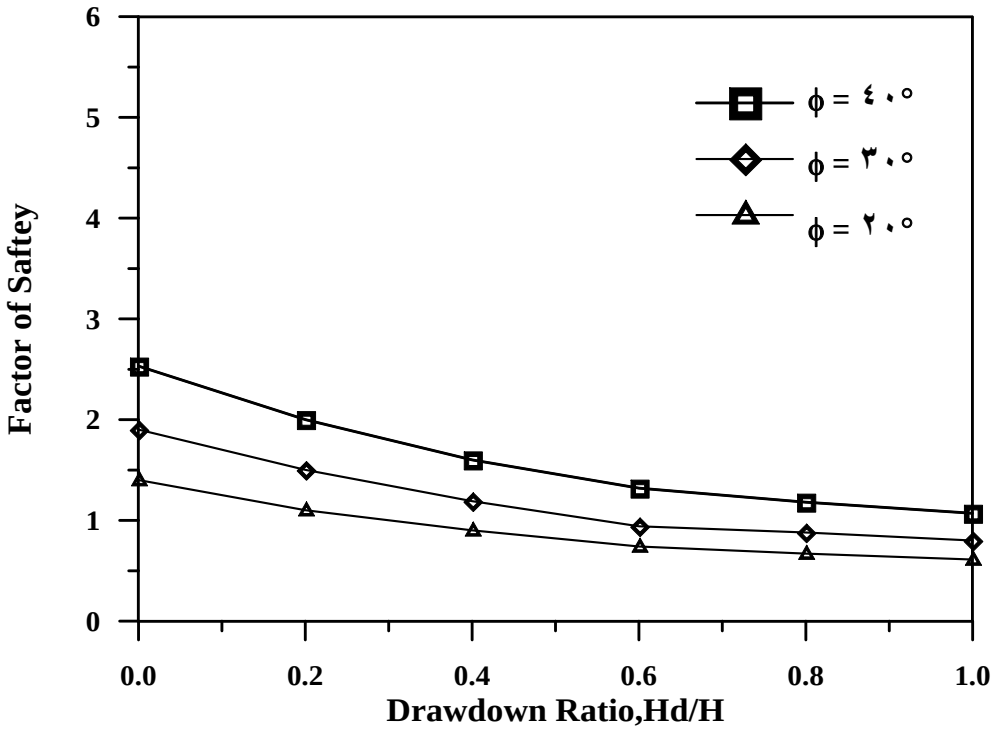

β = ٢ : ١

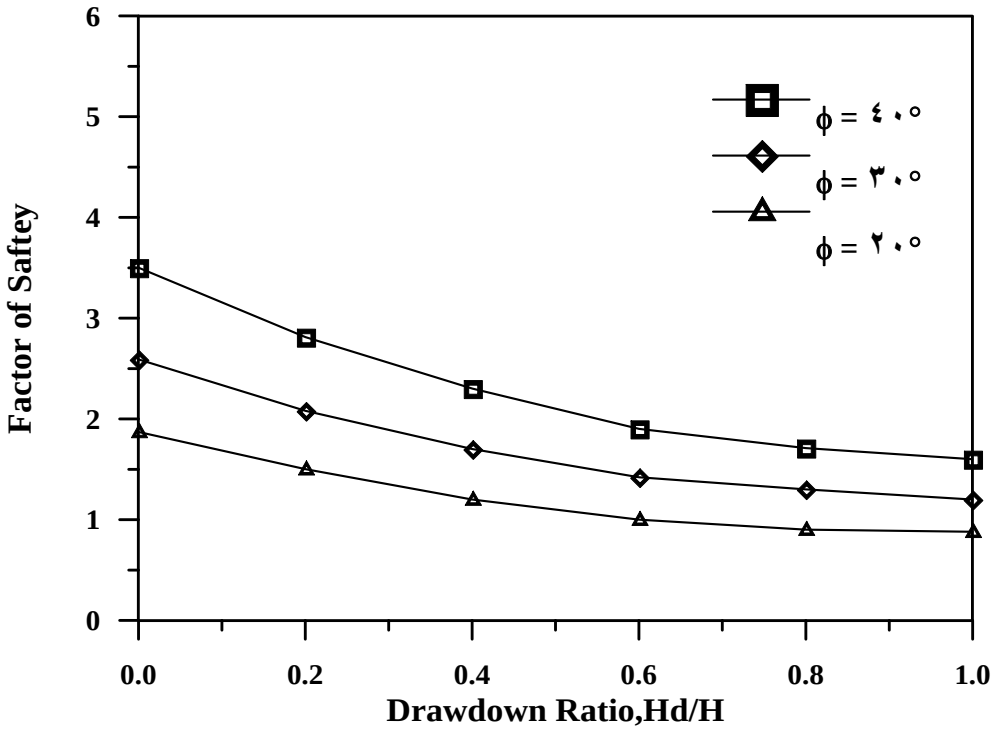

β = ٣ : ١

Figure (٤.٢٤) Drawdown Stability Chart with (C / γ H = ٠.٠٢٥).

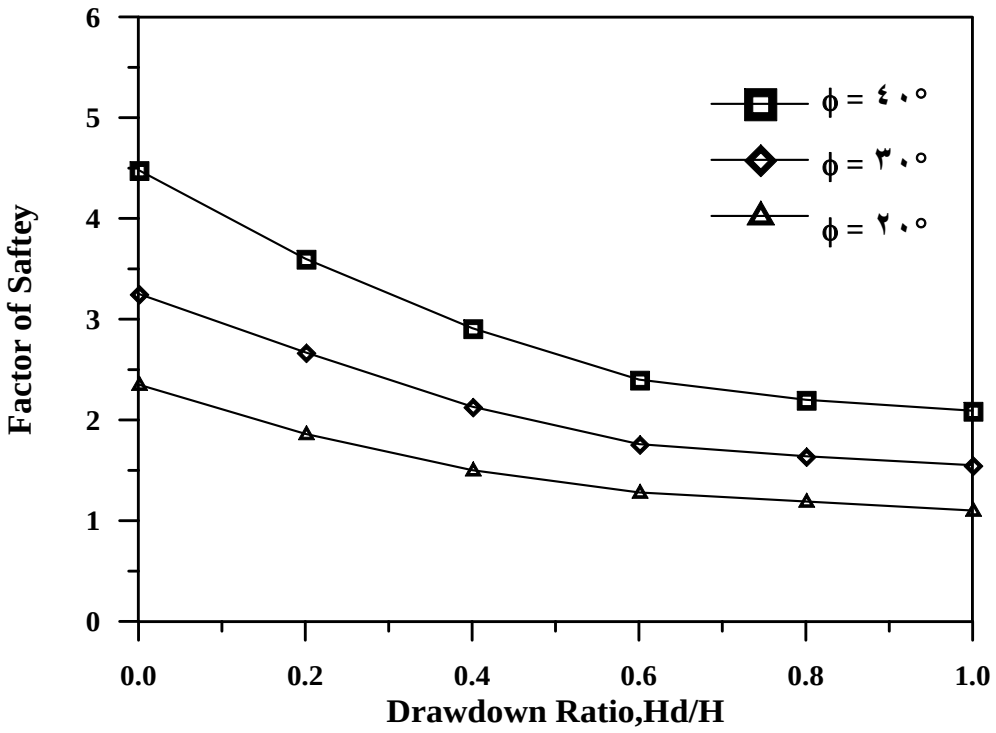

β = ٤ : ١

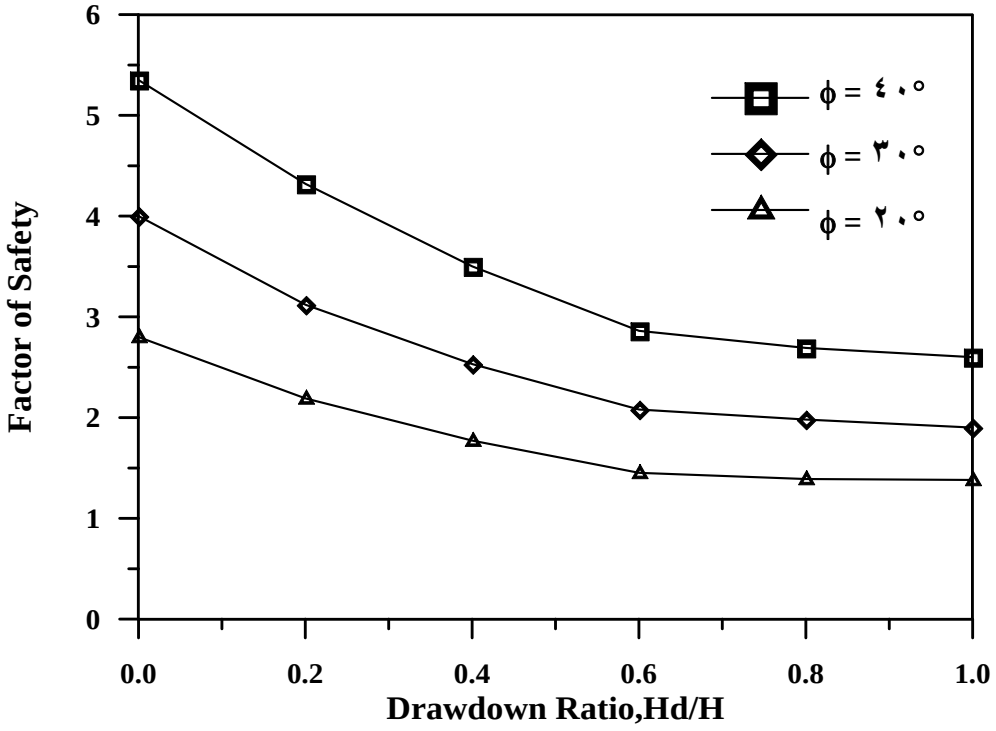

β = ٥ : ١

Figure (٤.٢٥) Drawdown Stability Chart with (C / γ H = ٠.٠٢٥).

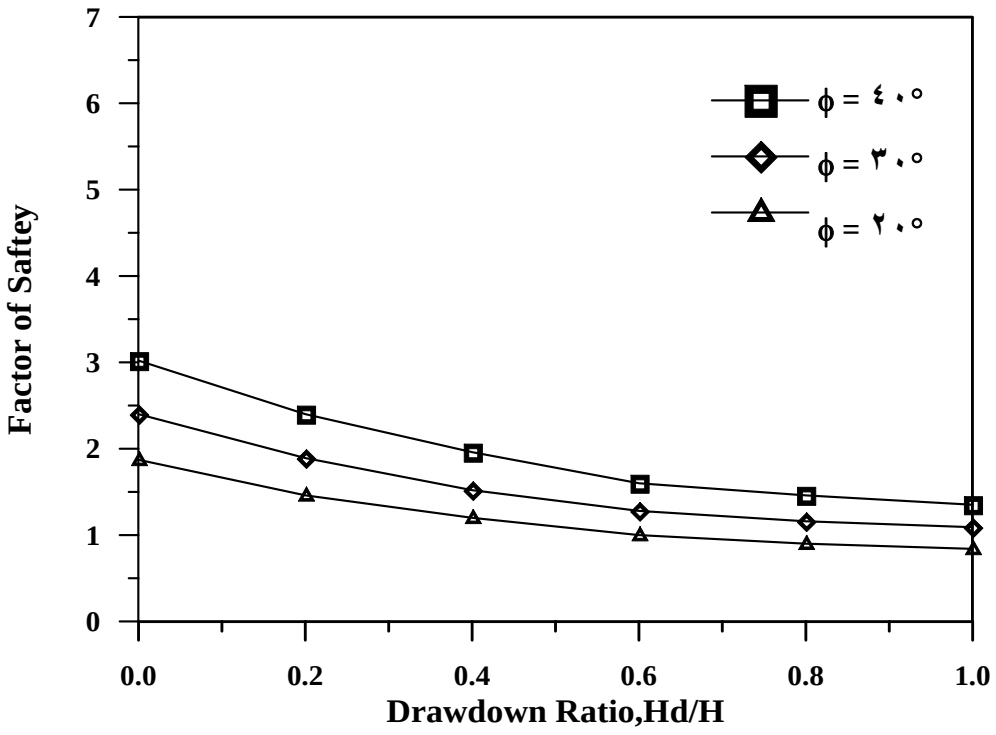

β = ٢ : ١

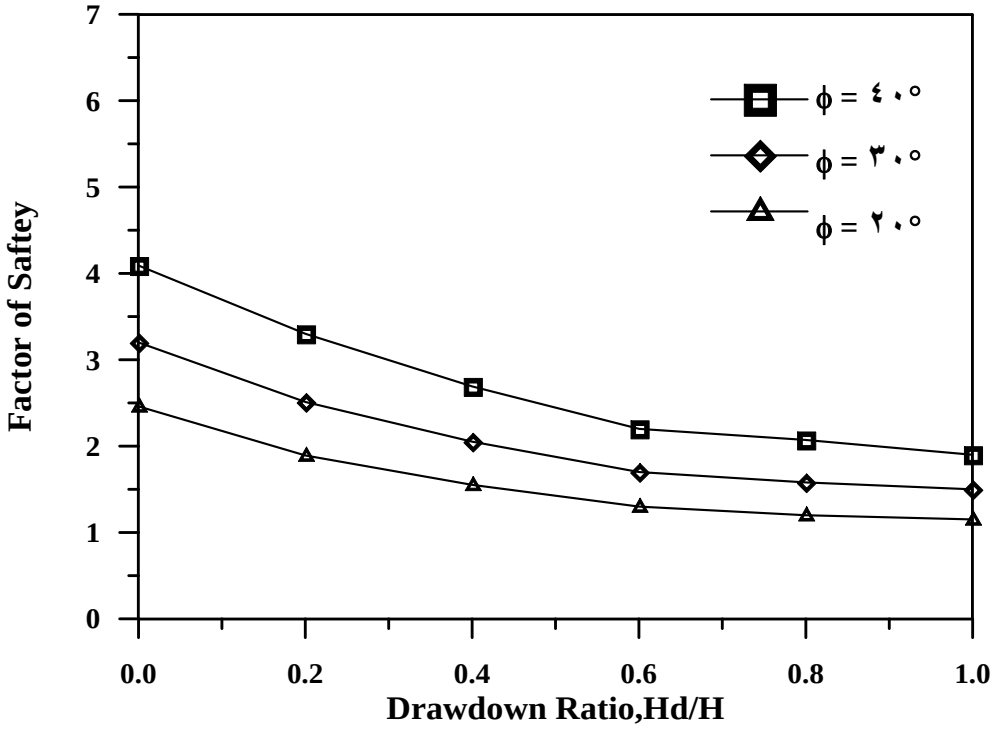

β = ٣ : ١

Figure (٤.٢٦) Drawdown Stability Chart with (C / γ H = ٠.٠٥).

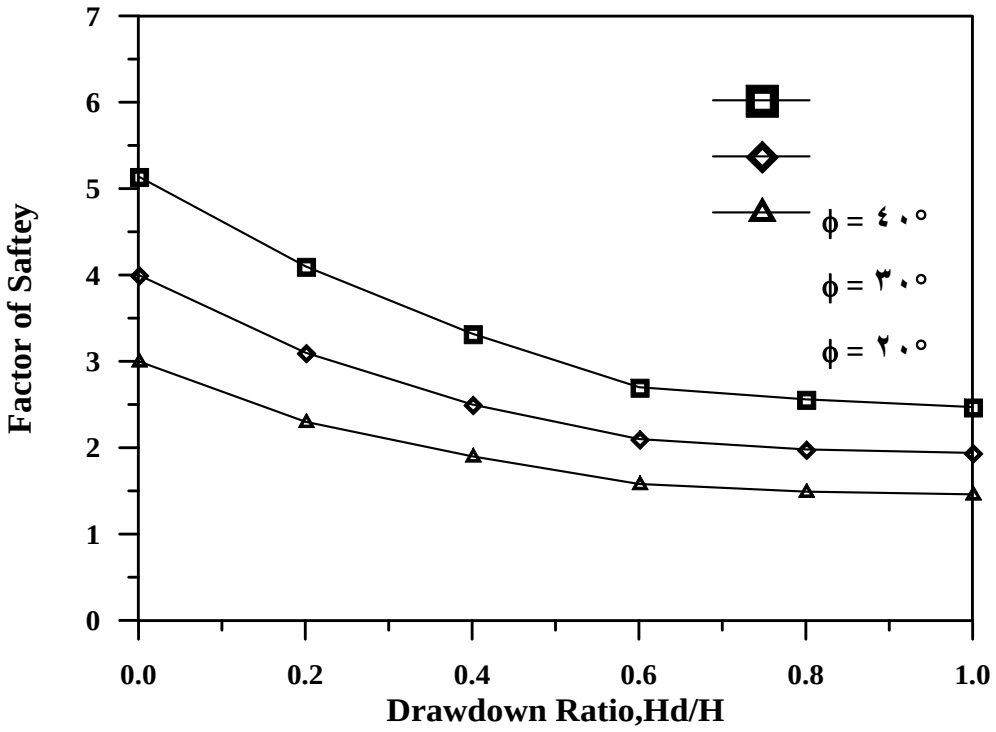

β = ٤ : ١

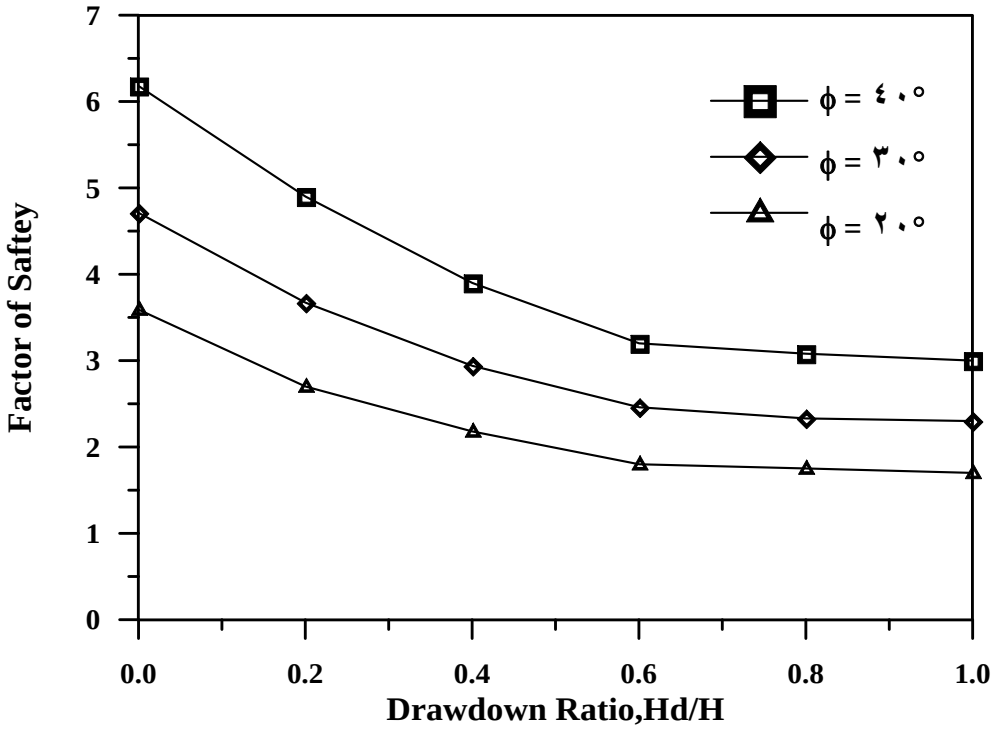

β = ٥ : ١

Figure (٤.٢٧) Drawdown Stability Chart with (C / γ H = ٠.٠٥).

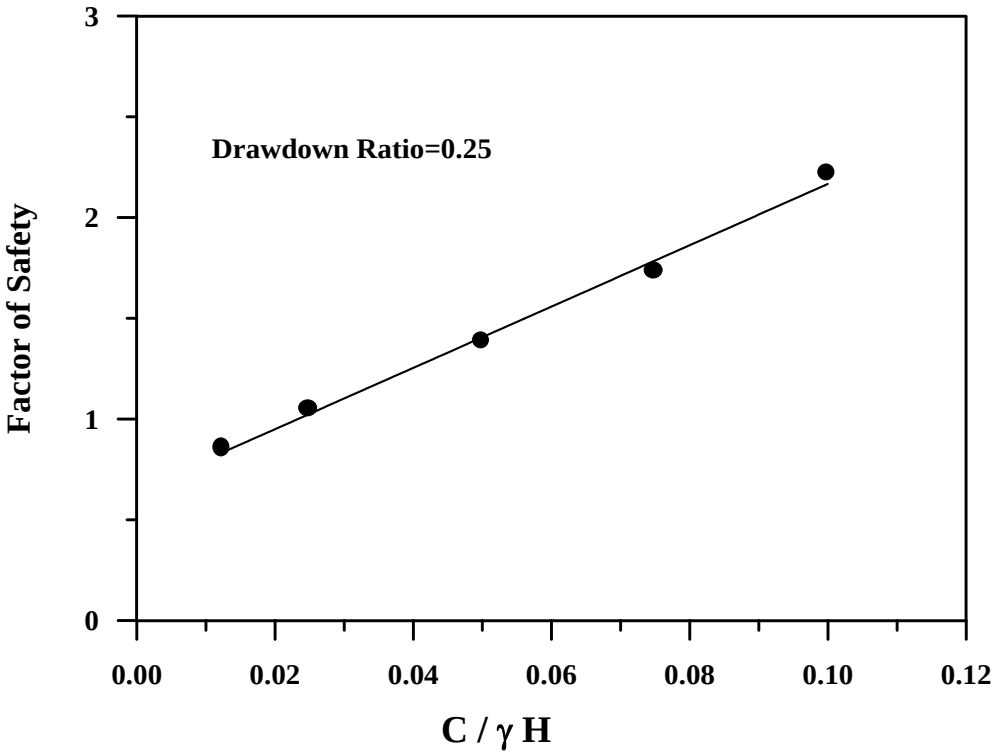

Figure (٤.٢٨) Linear Variation of Factor of Safety Versus (C / γ H) for β = ٢:١ and ϕ = ٢٠°.

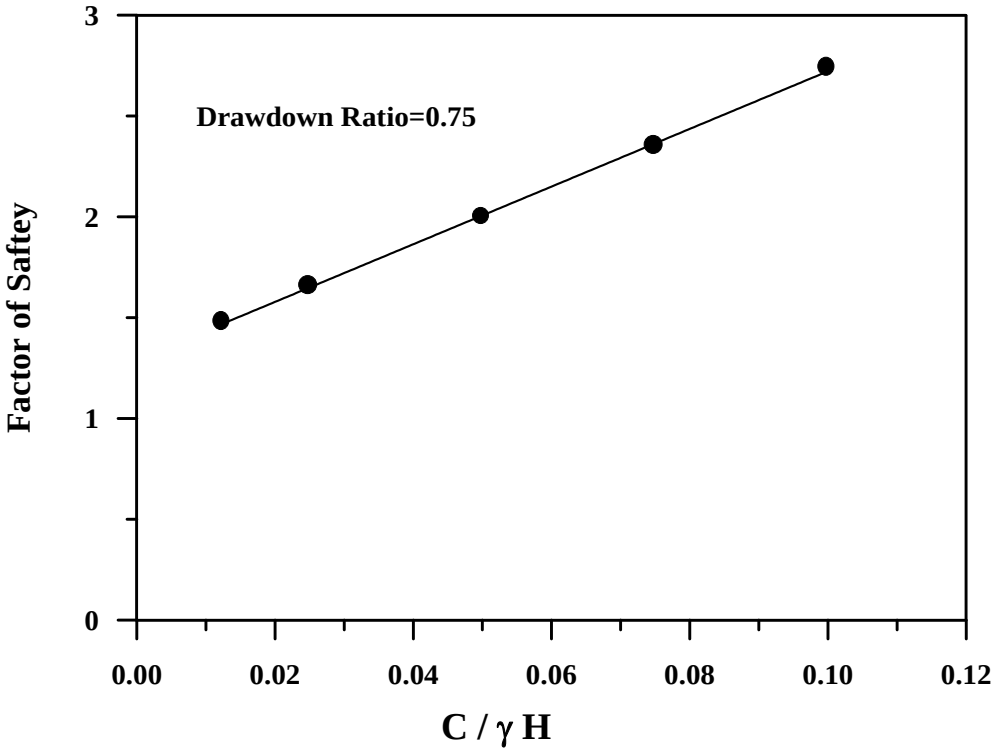

Figure (٤.٢٩) Linear Variation of Factor of Safety Versus (C / γ H) for β = ٤:١ and ϕ = ٣٠°.

Chapter Five

ANLAYSIS OF ZONED EARTH DAM

٥.١ General Review

Should through seepage in an embankment emerge on the downstream slope, it can soften fine grained fill in the vicinity of the downstream slope toe, cause sloughing of the slope, or even lead to piping (internal erasion) of fine sand or silt materials. Seepage exiting on the downstream slope would also result in the high seepage forces, decreasing the stability of the slope.

In many cases, high water stages do not act against the levee long enough for this happen, but the possibility of a combination of high water and a period of heavy precipitation may bring this about. If downstream slope stability berms or berms to control underseepage are required because of foundation conditions, they may be all that is necessary to prevent seepage emergence on the slope. On the other hand, if no berms are needed, downstream slopes are steep, and flood stages durations and other pertinent considerations indicate a potential problem of seepage emergence on the slope, provisions should be incorporated in the levee section such as horizontal and / or inclined downstream slop. These require select pervious granular material and graded filter layers to ensure continued functioning, and therefore add an appreciable cost to the levee construction, unless suitable materials are available in the borrow areas with only minimal processing required.

Where large quantities of pervious materials are available in the borrow areas, it may be more practicable to design a zoned dam with a large lad side pervious zone. This would provide an efficient means of through seepage

control and good utilization of available materials [**U.S. Army Crops. of Engineers**, ٢٠٠٠].

In this chapter, the effects of different water conditions in the reservoir of a zoned earth dam on the overall stability investigated.

٥.٢ A Zoned Earth Dam

٥.٢.١ General Description

The total length of the dam is about (٩km) and its maximum height is about (١٥٥m). The shell which is composed mainly of sand-gravel and / or rock muck and the central dolomite core are constructed by hydraulic filling. Due to reliability of the dolomite as an impervious core, an asphaltic concrete diaphragm was constructed inside the central core as an anti-seepage element. This vertical diaphragm is located (١٠ m) upstream the dam axis, and has a thickness of (١m) up to elevation (١٢٥.٠٠).

Above that level, the diaphragm thickness is reduced to only (٠.٥m). Figure (٥.١) shows a typical cross section of the central part of the dam at the channel portion where its constructed height is maximum [**Al-Jorany**, ١٩٩٦]. Table (٥.١) displays the most important properties of the different materials composing the dam.

Table (٥.١) Material Properties for Zoned Dam [Obtained from Al-Jorany, ١٩٩٦]

Material type	Parameter	Value
Mealy dolomite (Foundation)	Horizontal permeability, kx cm/sec	١.١٥×١٠^{-٥}
	Vertical permeability, ky cm/sec	١.١٥×١٠^{-٥}
	Total unit weight, γ_t kN/m^{٣}	٢٢
	Saturated unit weight, γ_s kN/m^{٢}	٢٢
	Cohesion, C kN/m^{٢}	٢٠-٤٠
	Angle of internal friction ϕ	٢٤-٢٨

Material type	Parameter	Value
Clay (Foundation)	Horizontal permeability, kx cm/sec	٢.٣١×١٠$^{-٦}$
	Vertical permeability, ky cm/sec	٢.٣١×١٠$^{-٦}$
	Total unit weight, γ_t kN/m^{٣}	١٨.٧
	Saturated unit weight, γ_s kN/m^{٢}	١٩.٠
	Cohesion, C kN/m^{٢}	٣٠-٥٠
	Angle of internal friction ϕ	١٤-١٦
Limestone (Foundation)	Horizontal permeability, kx cm/sec	١.١٥×١٠$^{-٦}$
	Vertical permeability, ky cm/sec	١.١٥×١٠$^{-٦}$
	Total unit weight, γ_t kN/m^{٣}	٢٢
	Saturated unit weight, γ_s kN/m^{٢}	٢٢
	Cohesion, C kN/m^{٢}	١٠٠-٢٠٠
	Angle of internal friction ϕ	٣٠-٣٥
Rock muck sandy gravel (shell)	Horizontal permeability, kx cm/sec	٢.٣١×١٠$^{-٤}$
	Vertical permeability, ky cm/sec	٢.٣١×١٠$^{-٤}$
	Total unit weight, γ_t kN/m^{٣}	١٧
	Saturated unit weight, γ_s kN/m^{٢}	٢٠.٣
	Cohesion, C kN/m^{٢}	٠
	Angle of internal friction ϕ	٢٧-٣٠
Dolomite (Core)	Horizontal permeability, kx cm/sec	١.١٥×١٠$^{-٦}$
	Vertical permeability, ky cm/sec	١.١٥×١٠$^{-٦}$
	Total unit weight, γ_t kN/m^{٣}	٢٠.٣
	Saturated unit weight, γ_s kN/m^{٢}	٢١.٤
	Cohesion, C kN/m^{٢}	٠
	Angle of internal friction ϕ	٣٠-٣٣

The finite element mesh used in this analysis is drawing in Figure (٥.٢). The mesh contains (٣٨٦) finite elements and (٤٢٦) nodal points.

٥.٣ Results and Discussion

٥.٣.١ Normal Reservoir Level

The water level in the upstream for case of normal operation is considered to be about ١٤٣.٠٠. Figure (٥.٣) shows location of free surface, its noticed from this figure that free surface is constructed form several discontinuous surfaces because the rate of water movement is different in each material within the dam body. Furthermore, the free surface elevation drops from (١٣٧.١٤m) to (١٣٠.١٨m) at the boundary of diaphragm which reflects the efficiency of the diaphragm as ani seepage device. Figure (٥.٤) and (٥.٥) show contour maps for total head and pressure head distributions throughout the dam body at normal operation conditions. The value of the factor of safety (F) for the upstream slope under this water condition is found to be ١.٧٧٣, while the designer factor of safety is ١.٦٠ according to ordinary method.

Figure (٥.٦) displays the shape and location of most critical slip surface according to present analysis which indicated by solid line. The shape and location of the critical slip surface in upstream slope is different from that obtained by the designer which indicated by dashed line. The shape of the present analysis slip surface is a non-circular arc that passes partially through the upstream shell.

٥.٣.٢ Maximum Reservoir Level

In this case, the water level in the upstream is considered to be maximum (i.e. ١٥٠.٢٠). Figure (٥.٧) shows computed locations of the free surface in the shell and core for this water condition. The head and pressure distributions are demonstrated in Figure (٥.٨) and (٥.٩) respectively. The value of the factor of safety presented by this work is ٢.١٨٦ which is lower than that obtained by the designer of (٢.٤٠) according to ordinary method. The shape and location of most critical slip surface are shown in Figure (٥.١٠).

The most critical surface as determined by the present analysis is a non-circular arc that passes close to the upper surface of the upstream slope. This slip surface which is denoted by solid line in Figure (٥.١٠), indicates that the mode of critical failure for this reservoir water level is almost a local failure in the upper face of upstream.

٥.٣.٣ Minimum Reservoir Level

The water level is considered to be about ١١٢.٠٠ in the upstream side. The computed location of free surface corresponding such a water condition is shown in Figure (٥.١١), it can be noticed that a free surface is relatively horizontal in the shell and extension of the free surface in core with a small drops near the junction of the core and diaphragm. Figure (٥.١٢) and (٥.١٣) display the total head and pressure head distributions due to the minimum water level in reservoir. From the present analysis, the critical slip surface in the upstream for this reservoir level is indicated by a solid lines in Figure (٥.١٤). The value of the factor of safety is ١.٥٠٥ which is clearly lower than that of ١.٦٣ obtained by the designer. The shape and location of present analysis are different from that presented by the designer.

٥.٣.٤ Rapid Drawdown Condition

The case of rapid drawdown of reservoir water level is considered to occur when water level drops from elevation ١٤٣.٠٠ to elevation ١١٣.٠٠. This rate of draowdown is similar to those considered previously of (٣٠ m/day) as rapid drawdown rate.

Two typical nodal points are selected with care to investigate the influence of the rapid drawdown process on the heads and pressures within the dam body, node ٥٨ which located at (١١٣.٥٤, ٩٥.٣٥) in the upstream side shell and node ٢٠١ which located at (٢٥١.٦٨, ٩٥.٣) in the downstream side shell. Figure (٥.١٥) shows the variation of heads in these nodes with time due to rapid drawdown process. For node ٥٨ the value of head is (١٤٢.٤ m) and decreases to the value of (١١٣.٦m) around the end of drawdown. For node ٢٠١ the value of head is (١٢٤.٩ m) and decreases to value of (١١٠.١m) around the end of drawdown. The computed results show that the rate of the change in heads depends greatly on the node location. The heads for node ٥٨ on the upstream side decreases in a rate of ٢٨.٨ /day) which is almost similar to the drawdown rate of reservoir. On the other hand, the heads for node ٢٠١ on the downstream side decreases at a rate of (١٤.٨ m/day) which is a much smaller rate than the drawdown rate of reservoir. Figure (٥.١٦) shows the variation of pressure head at nodes (٥٨ and ٢٠١) with time due to rapid drawdown process. The predication results agrees very well with trends of heads.

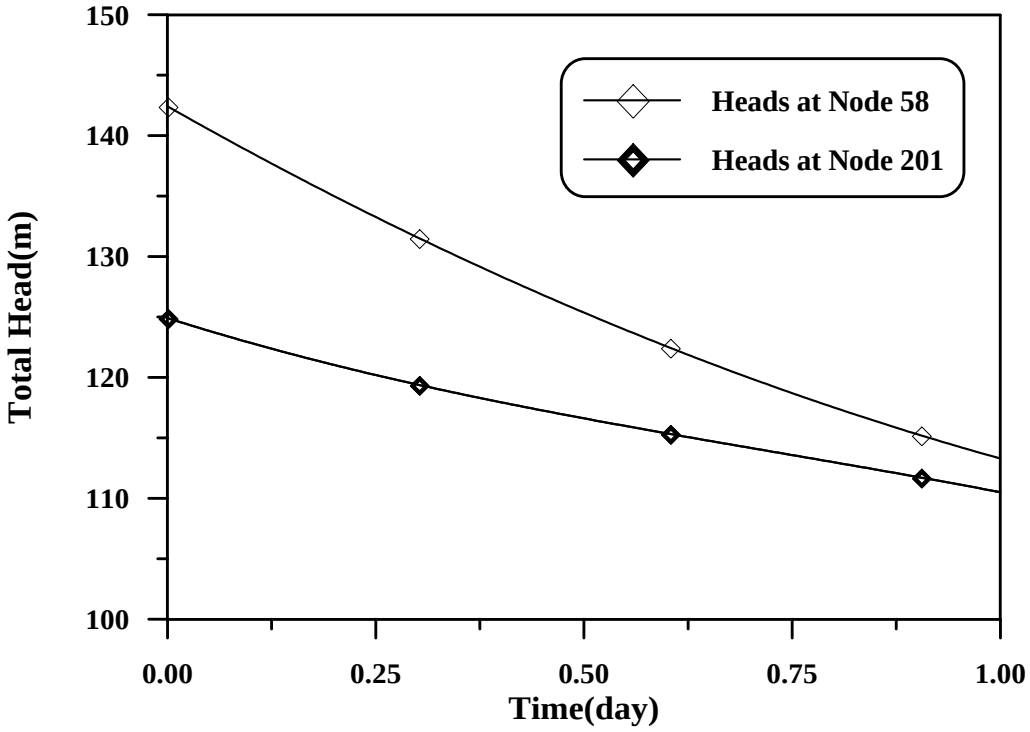

Figure (٥.١٥) Variation of Heads at Various Nodes (٥٨ and ٢٠١) with Time Due to Drawdown Conditions

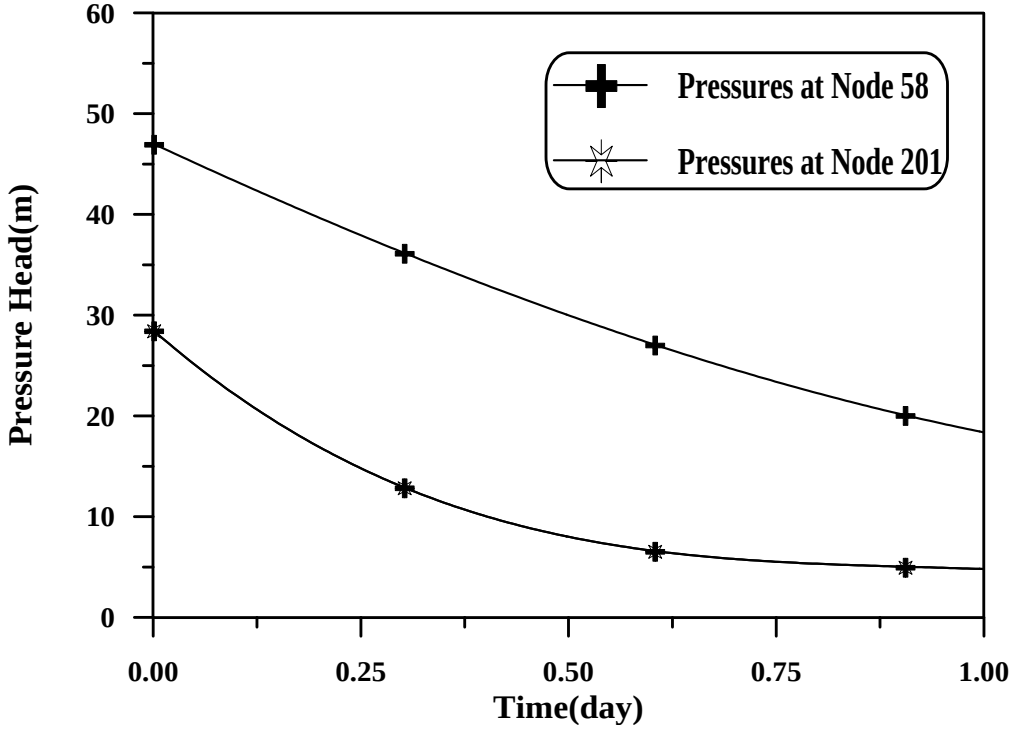

Figure (٥.١٦) Variation of Pressures at Various Nodes (٥٨ and ٢٠١) with Time Due to Drawdown Conditions

Figure (٥.١٧) displays the movement of the exit points at the entrance and seepage faces due to drawdown conditions. The location of the exit points allows introduction of proper boundary heads in the formulation. Moreover, it shows that it is not necessary that the free surface should follows the water level in the reservoir. For entrance face exit point the movement fasts down as the time increases while for seepage face exit point the movement slows down.

Figure (٥.١٨) shows the movement of the typical free surface points ($P_١$) with elevation of (١٣٧.٣٢ m) in the upstream side and point ($P_٢$) with elevation of (١٢٦.٦٨ m) in the downstream side, from this figure it is clear that the movement of free surface in upstream side is faster than those in downstream side.

The factor of safety obtained by designer is ١.٨٩ according to the ordinary method. This value is greater than that obtained by the designer himself for the case of normal water level of ١٤٣.٠٠ which is about ١.٦٠. These results are, therefore not fair since the designer implies that the case of rapid drawdown is safer than normal conditions. The value of factor of safety is ١.٥١٦ according to the present analysis method.

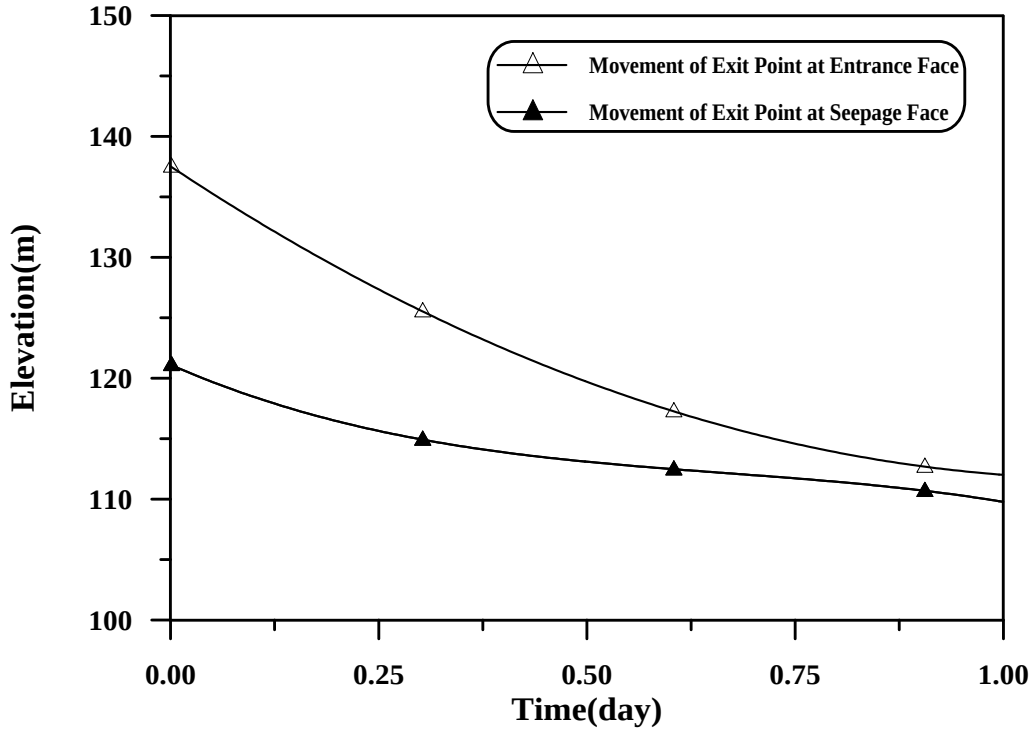

Figure (٥.١٧) Movement of Exit Points at Upstream and Downstream Sides with Time Due to Drawdown Conditions

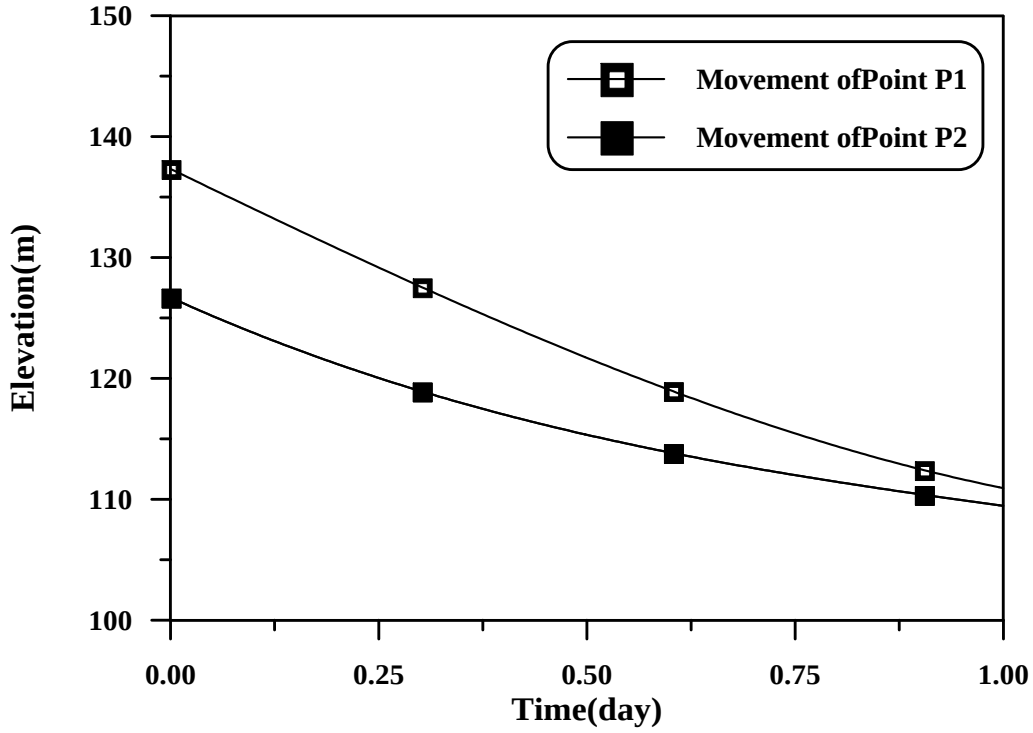

Figure (٥.١٨) Movement of Various Points (P_1 and P_2) with Time Due to Drawdown Conditions

Chapter Six

CONCLUSIONS AND SUGGESTIONS FOR FURTHER RESEARCHES

6

٦.١ Conclusions

The following main conclusions can be drawn from the results which are based on seepage and stability analysis.

١. The adopted analysis used in this work is considered to be a powerful one in dealing with seepage problem through earth dam under transient conditions. This is well demonstrated through the results obtained in this work as well as the convergence of them as compared with those reported in the literature.

٢. A forward difference scheme used in this work to perform the time integration, seem to be more suitable than the other procedures. Such a procedure is effected by a number of factors which should be taken into account.

a. The numerical instability beyond a certain range of discretization. Results indicate that if the size of the time step remains sufficiently small, the numerical solutions converge to approximately the same solution . However, as the magnitude of time step exceeds the certain value, oscillation about the true solution is observed. The true solution is assumed to be that using small Δt (Δt=٠.٠٢ day).

b. The type of mass matrix M of Equation (٣.١٨), lumped or consistent, did appear the exert significant influence on the stability and the accuracy of the solution. It was found that the mass matrix M had to be lumped (diagonalised) in order to improve its stability.

٣. The four noded quadrilateral element type that was used seems to give logical results especially in the estimation of the pore water pressure with no oscillations.

٤. Under drawdown condition, the rate of the change in the pressure heads depends not only on the drawdown rate of the reservoir level but also significantly on the locations where the pressure heads were measured within a dam.

٥. Pore-pressure heads in the downstream side of a dam usually decreases at a much slower rate than those in the upstream side of the dam.

٦. Although the change of the soil hydraulic conductivity due to the change of soil skeleton is neglected in the formulation, there are satisfactory correlations between the numerical solutions and field observations. For practical purposes, it may not be necessary to refine the analysis method to include the effects of time-dependent hydraulic conductivity. The present formulation of the seepage problem can be considered adequate for the problems under consideration.

٧. The adopted analysis also gives reasonable results when analyzing large zoned earth dams, thus the utilized analysis enables to study the behavior of the dam body and the foundation under various conditions.

٨. A detailed comparison of the present work with those from literature indicates that although the morgensten-price method gives reasonable solutions for homogeneous dams. It tends to underestimate the true stability solution for zoned dams with a low slope angle.

٩. In spite of the completely different theoretical espects on which the present limit equilibrium approach is based and those compared with, the values of factor of safety obtained by this work indicate fair correspondence. The percentage error in these values for most of cases studied are less than ١٥٪.

١٠. In case of zoned earth dam, the shape and location of the failure surface as determined by the present work are different from those proposed by the designer.

٦.٢ Suggestions for Further Researches

Further developments dealing the subject can be imposed on the present work. In this respect, the following points are suggested:

١. The analysis can be modified further if three dimensional analysis of the seepage problem under transient conditions is added. A Crank – Nicholson scheme to perform the time integration can be used to increase the accuracy of the numerical solution and improves its stability.

٢. The eight-noded isoparametric element can be added with further accuracy encountered.

٣. Anisotropic and nonhogeneous soil conditions can be added in the formulation by specifying different permeabilities in the x and y directions. Inclusion of the behavior of partially saturated soils, if the case is applicable.

٤. A reasonable dynamic analysis is essential, by such an analysis the actual dynamic response and the time dependent behavior of an earth dam due to realistic dynamic excitement are to be investigated. The pore water pressure generation due to such excitements is a very important factor that governs the stability of the whole structure.

- Amar, A.C., (١٩٧٥) "**Ground water recharge simulation**", Journal of the Hydraulics Division, ASCE, Vol.١٠١, No.Hy٩, pp.١٢٣٥-١٢٤٧.

- Anderson, P.F. and Woessner, W.W., (١٩٩٢), "**Applied groundwater modeling: simulation of flow and advective transport**", Academic Press, London.

- Al-Assady, A.M, (١٩٩٨) "**Effect of an isotropy on two dimensional consolidation of clayed soil**", M.Sc. Dissertation, Department of Civil Engineering, University of Baghdad.

- Al-Assaf, S., (١٩٩٨) "**Effect of stream fluctuations on aquifers**", Journal of Engineering and Technology, Vol.١٧, No.٨, Iraq, pp.٧٨٨-٧٩٨.

- Baker, R., (١٩٨٠) "**Determination of the critical slip surface in slope stability computations**", International Journal for Numerical and Analytical Methods in Geomechnics, Vol.٤ pp.٣٣٣-٣٥٩.

- Bear, J., and Verruijt A., (١٩٩٠) "**Modeling groundwater flow and pollution**", D.Reidal Publishing Company, Dordrecht. Holland.

- Bishop, A.W., and Morgenstern N., (١٩٦٠) "**Stability coefficients for earth slopes**", Geotechnique, Vol.١٠, No.٤, pp.١٢٩-١٥٠.

- Cedergren, H.R., (١٩٦٧), "**Seepage, drainage and flow nets**", ١st Edition, John Wiley and Sons, New York.

- Ching, S.C., (١٩٨٨), "**Boundary-element analysis for unconfined seepage problems**", Journal of Geotechnical Engineering, ASCE, Vol.١١٤, No.٥, pp.٥٥٦-٥٧١.

- Clough, R.W., and Woodward, R.J., (١٩٦٧), "**Analysis of embankment stresses and deformations**", Journal of the Soil Mechanics and Foundations Division, ASCE, Vol.٩٣, No.SM٤.

- Desai, C..S, and Sherman, W.C., (١٩٧١), "**Unconfined transient seepage in sloping banks**", Journal of the Soil Mechanics and Foundations Division, ASCE, Vol.٩٧, No.SM٢, pp.٣٥٧-٣٧٣.

- Desai, C.S., (١٩٧٢), "**Seepage analysis of earth banks under drawdown**", Journal of the soil Mechanics and Foundations Division, ASCE, Vol. ٩٨, No.SM١١, pp.١١٤٣-١١٦٠.

- Desai, C.S., and Abel, J.F. (١٩٧٢), "**Introduction to the finite element method**", Van Nostrand Reinhold Company.

- Finn, W.D.L., (١٩٦٧), "**Finite element analysis of seepage through dams**", Journal of the Soil Mechanics and Foundations Divisions, ASCE, Vol. ٩٣, No.SM٦, pp.٤١-٤٨.

- France, P.W., Parekh, C.J., Peters, J.C., and Taylor, C., (١٩٧١), "**Numerical analysis of free surface seepage problems**", Journal of the Irrigation and Drainage Division, ASCE, Vol.٩٧, No.-IR١, pp.١٦٥-١٧٩.

- Freeze, R.A., (١٩٧١a), "**Three dimensional, transient, saturated-unsaturated flow in a groundwater basic**", Water Resources Research, Vol.٧, No.٢, pp.٣٤٧-٣٦٦.

- Freeze, R.A., (١٩٧١b), "**Influence of the unsaturated flow domain on seepage through earth dams**", Water Resources Research, Vol.٧, No.٤, pp.٩٢٩-٩٤١.

- Freeze, R.A., and Cherry, J.A. (١٩٧٩), "**Groundwater**", Prentice-Hall, Inc. Englewood Cliffs, New Jersey.

- Garrg, S., (١٩٩٨), "**Soil mechanics and foundation engineering**", ٢nd edition, Sh. Romesh Chander Khanna, Delhi.

- Guvanasen, V., and Volker, R.E., (١٩٨٠), "**Numerical solutions for unsteady flow in unconfined aquifers**", International Journal for Numerical Methods in Engineering, Vol.١٥, No.١١, pp.١٦٤٣-١٦٥٧.

- Harr, M.E., (١٩٦٢), "**Ground water and seepage**", McGraw Hill, New York.
- Al-Jorany, A.N., (١٩٩٦), "**Slope Stability Analysis**", Ph.D. Dissertation, Department of Civil Engineering, University of Baghdad.
- Lambe, T.W., and Whitman, R.V., (١٩٦٩), "**Soil mechanics**", John Wily and Sons, New York.
- Li, G.C., and Desai, C.S., (١٩٨٣), "**Stress and seepage analysis of earth dams**", Journal of Geotechnical Engineering, ASCE, Vol.١٠٩, No.٧, pp.٩٤٦-٩٦٠.
- Liggett, J.A., (١٩٧٧), "**Location of free surface in porous media**", Journal of the Hydraulics Division, ASCE, Vol.١٠٣, No.HY٤, pp.٣٥٣-٣٦٥.
- McCorquodale, J.A., (١٩٧٠), "**Variation approach to non-Darcy flow**", Journal of the Hydraulics Division, ASCE, Vol.٩٦, No.HY١١, pp.٢٢٦٥-٢٢٧٨.
- Morgenstern, N.R., and Price, V.E., (١٩٦٥), "**The analysis of the stability of general slip surface**", Geotechnique, Vol.١٥, pp.٧٩-٩٣.
- Morgenstern, N.R., and Price, V.E., (١٩٦٧), "**A numerical method for solving the equations of stability of general slip surface**", Computer Journal, Vol.٩.
- Muni, B., (٢٠٠٠), "**Soil mechanics and foundations**", John Wily and Sons, New York.
- Neuman, S.P., and Witherspoon, P.A., (١٩٧١), "**Analysis of non-steady flow with a free surface using the finite element method**", Journal of Water Resources Research, Vol.٧, No.٣, pp.٦١١-٦٢٣.
- Norrie, D.H., and DeVries, G., (١٩٧٨), "**An introduction to finite element analysis**", Academic Press, Inc., London.
- Pinder, G.F., and Bredehoeft, J.D., (١٩٦٨), "**Application of the digital computer for aquifer evaluation**", Water Resources Research, Vol.٤, No.٥, pp.١٠٦٩-١٠٩٣.

- Al-Qaisi, K.A., (١٩٩٩), "**Analysis of earth dam by finite element method**", M.Sc. Dissertation, Department of Civil Engineering, University of Baghdad.

- Al-Qaisi, S.M.I., (١٩٩٥), "**Predictions of pore water pressure in cores of dams**", M.Sc. Dissertation, Department of Civil Engineering, University of Baghdad.

- Rank, E., and Werner, H., (١٩٨٦), "**An adaptive finite element approach for the free surface seepage problem**", International Journal for Numerical Methods in Engineering, Vol.٢٣, pp.١٢١٧-١٢٢٨.

- Segrlind, L.J., (١٩٨٤), "**Applied finite element analysis**", ٢nd. Edition, John Wily and Sons, Inc., New York.

- Sherard, J.L., Woodward, R.J., Gizienski, S.F., and Clevenger, W. A., (١٩٦٣), "**Earth and earth rock dams**", John Wily and Sons, Inc., New York.

- Smith, I.M., and Griffiths, D.V., (١٩٨٨), "**Programming the finite element method**", ٢nd edition, John Wiley and Sons, Inc., New York.

- Smith, I.M., and Griffiths, D.V., ١٩٩٨), "**Programming the finite element method**", ٣rd. edition, John Wily and Sons, Inc., New York.

- Spencer, E., (١٩٦٧), "**A method of analysis of the stability of embankments assuming parallel inter-slice forces**", Geotechnique, Vol.١٧, pp.١١-٢٦.

- Stephenson, D.,(١٩٧٨),"**Drawdown in embankments**", Geotechnique, Vol.٢٨, No.٣, pp.٢٧٣-٢٨٠.

- Suresh, P.B and Harr, M.E., (١٩٦٢), "**Transient development of the free surface in a homogeneous earth dam**", Geotechnique, Vol.١٢, pp.٢٨٣-٣٠٢.

- Taylor, R.L., and Brown, C.B., (١٩٦٧), "**Darcy flow solution with a free surface**". Journal of the Hydraulics Division, ASCE, Vol.٩٣, No.HY٢, pp.٢٥-٣٣.

- U.S. Army Crops. of Engineers, (١٩٨٦), "**Seepage principles**", Manual, EM١١١٠-٢-١٩٠١, Chapter ٤.
- U.S. Army Crops. of Engineers, (٢٠٠٠), "**Seepage control devices**", Manual, EM١١١٠-٢-١٩١٣, Chapter ٧.
- Verma, R.D., and Brutsaert, W., (١٩٧١), "**Unsteady free surface groundwater seepage**", Journal of the Hydraulics Division, ASCE, Vol.٩٧, No.HY٨, pp.١٢١٣-١٢٢٧.
- Wang, H.F., and Anderson, M.P., (١٩٨٢), "**Introduction to groundwater modeling: Finite difference and finite element methods**", W.H. Freeman, SanFracisco.
- Whitman, R.V., and Bailey, W.A., (١٩٦٧), "**Use of computers for slope stability**", Journal of Geotechnical Engineering, ASCE, Vol.٩٣, No.SM٤, pp.٤٧٥-٤٩٨.
- Yu, H.S., Salgado, R., Sloan, S.W., and Kim, J.M., (١٩٩٨), "**Limit analysis versus limit equilibrium for slope stability**", Journal of Geotechnical and Geoenvironmental Engineering, ASCE, Vol.١٢٤, No.١, pp.١-١١.
- Zienkiewicz, O.C., (١٩٧٧), "**The finite element method**", ٣rd. Edition, McGraw-Hill, London.
- Zienkiewicz, O.C., and Cheung, Y.K., (١٩٦٥), "**Finite element in the solution of field problems**", The Engineer, Sept. pp.٥٠٧-٥١٠.
- Zienkiewicz, O.C., Mayer, P., and Cheung, Y.K., (١٩٦٦), "**Solution of anisotropic seepage by finite elements**", Journal of the Engineering Mechanics Division, ASCE, Vol.٩٢, No.EM١, pp.١١١-١٢٠.

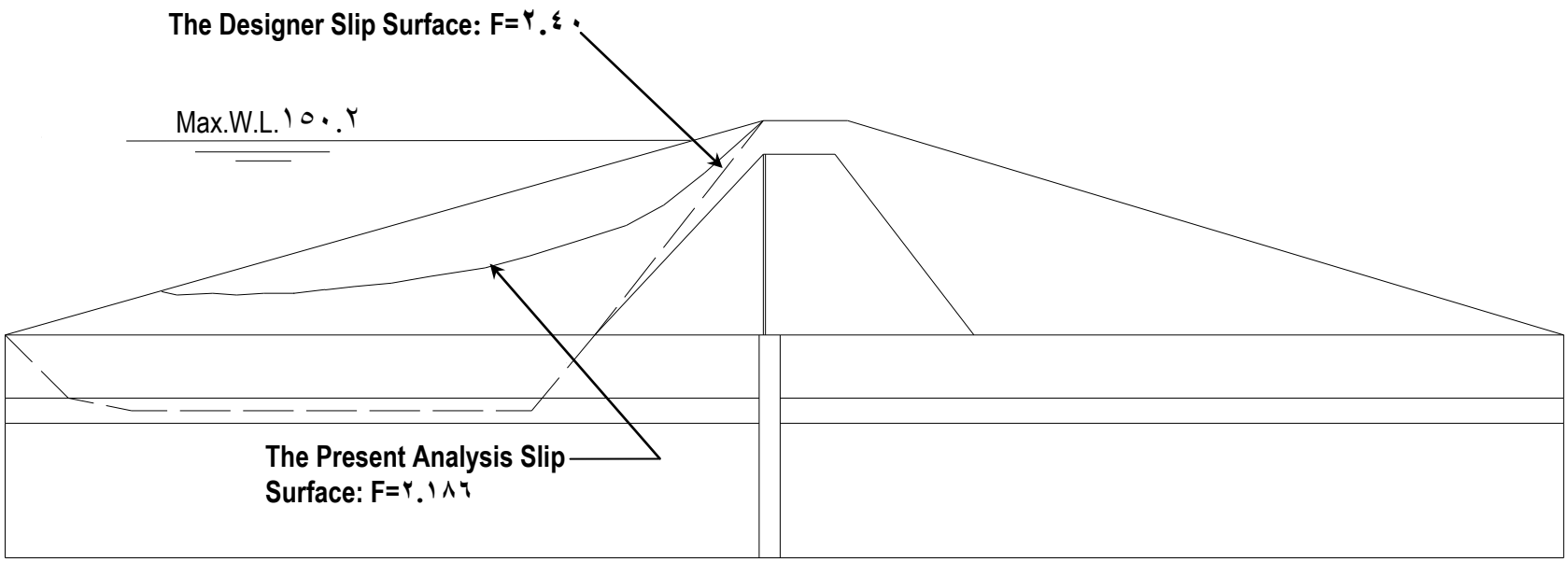

Figure (٥. ١٠) Results of the Present Analysis when Water at Maximum Level (Elevation ١٥٠.٢٠).

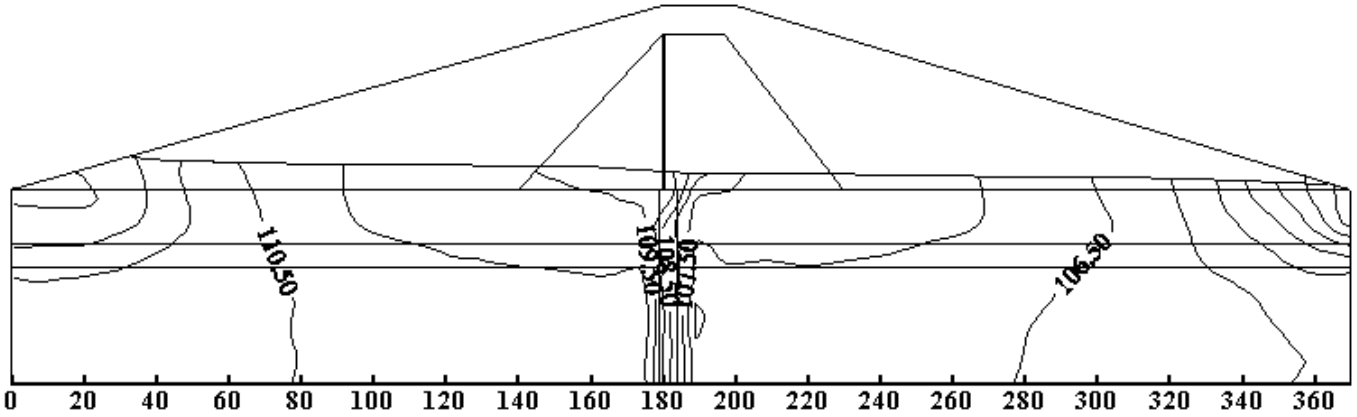

Figure (٥.١٢) Contour Map of Total Head Distribution for Minimum Water Level (Elevation ١١٢.٠٠).

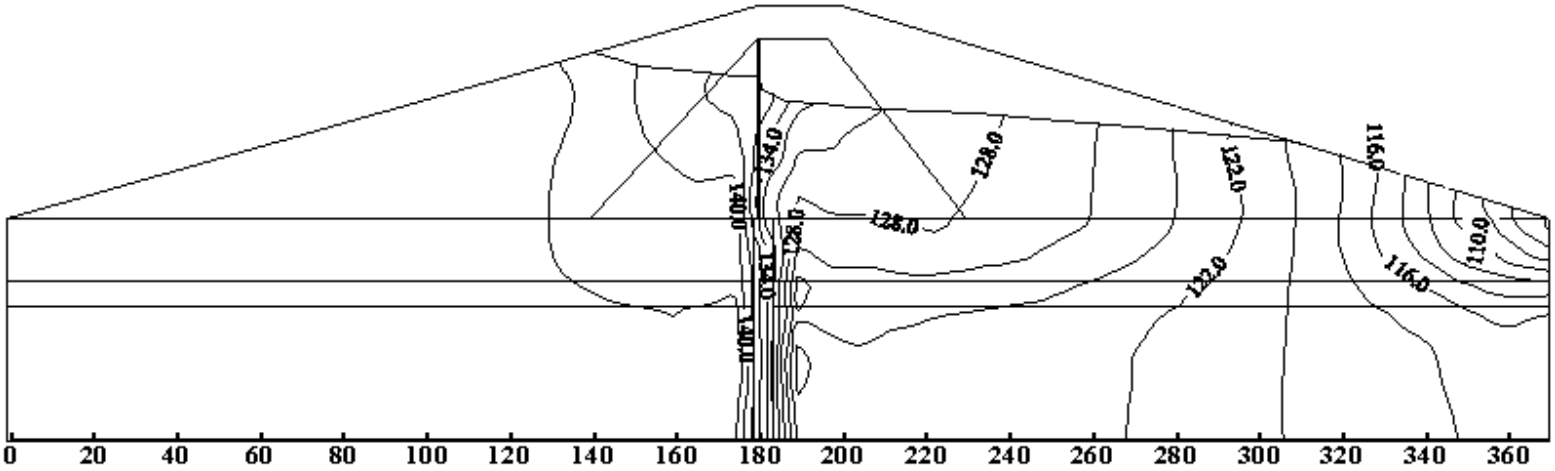

Figure (٥.٤) Contour Map of Total Head Distribution for Normal Water Level (Elevation ١٤٣.٠٠).

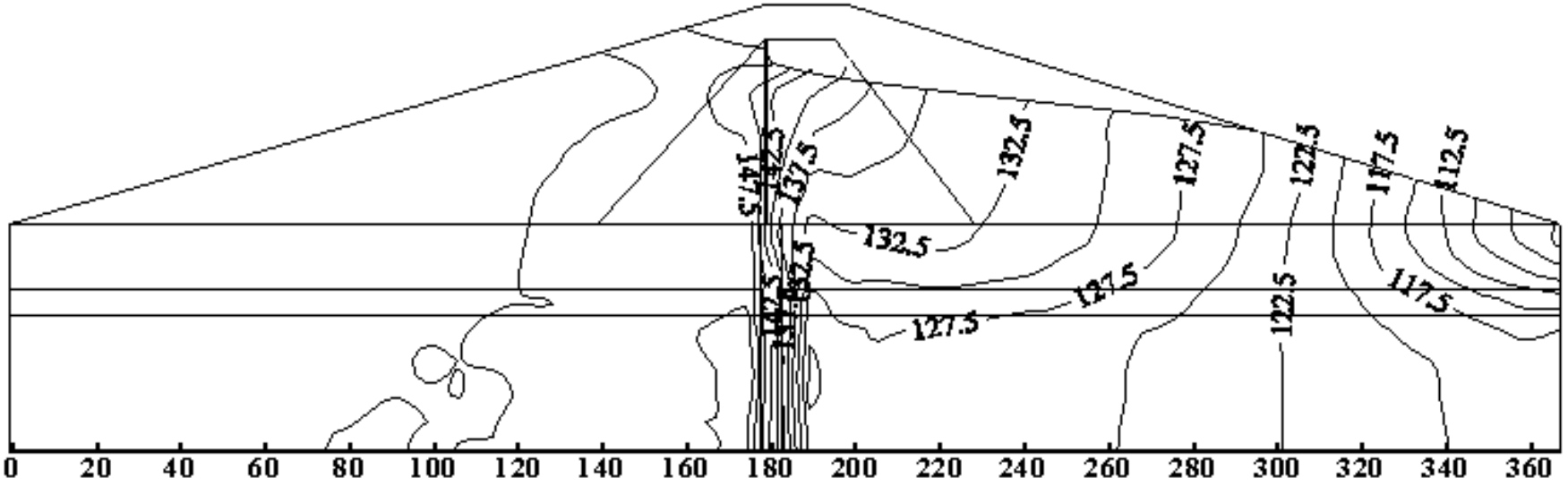

Figure (٥.٨) Contour Map of Total Head Distribution for Minimum Water Level (Elevation ١١٢.٠٠).

Total Number of Element =٣٦٨
Total Number of Nodes = ٤٢٦

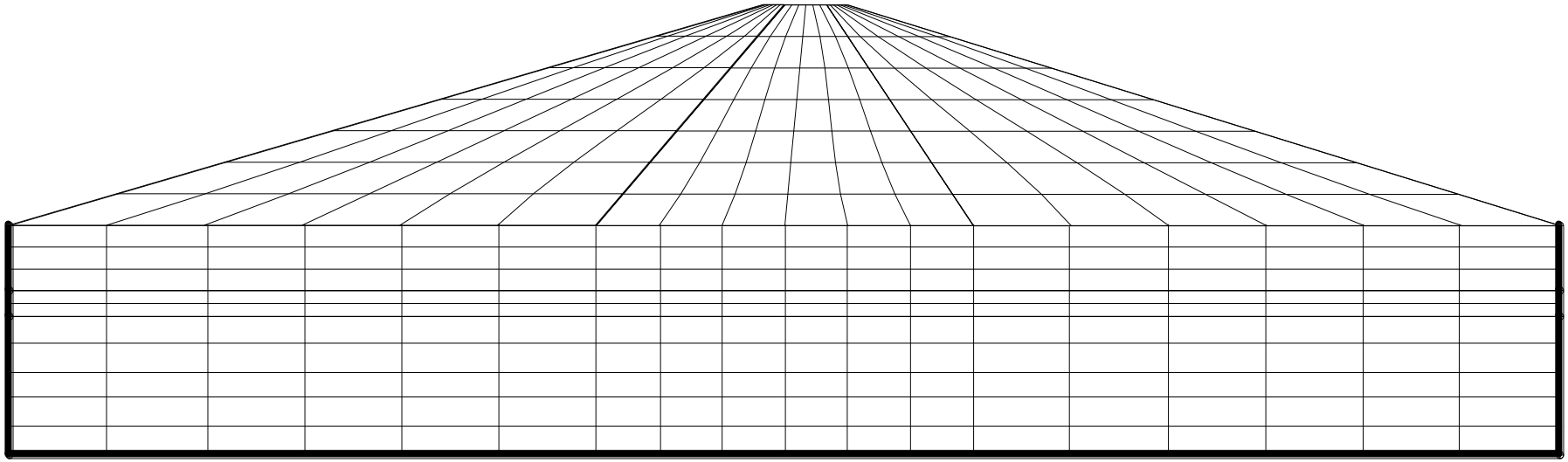

Figure (٥. ٢) Finite Element Mesh for Zoned Earth Dam

(Not to scale)

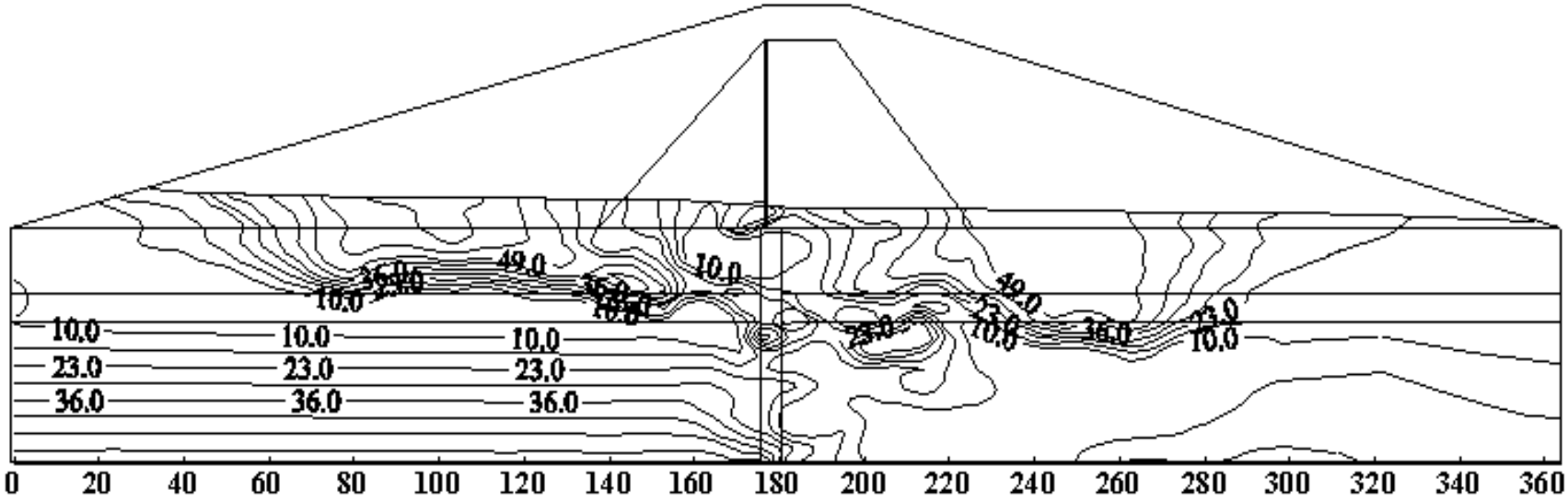

Figure (٥.١٣) Contour Map of Pressure Head Distribution for Minimum Water Level (Elevation ١١٢.٠٠).

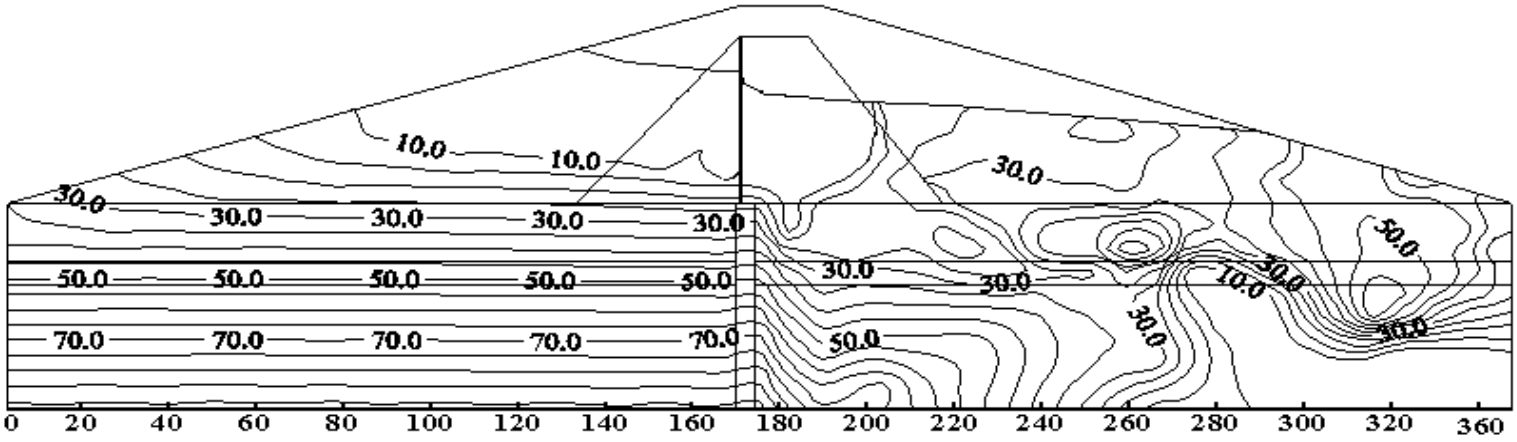

Figure (٥.٥) Contour Map of Pressure Head Distribution for Normal Water Level (Elevation ١٤٣.٠٠).

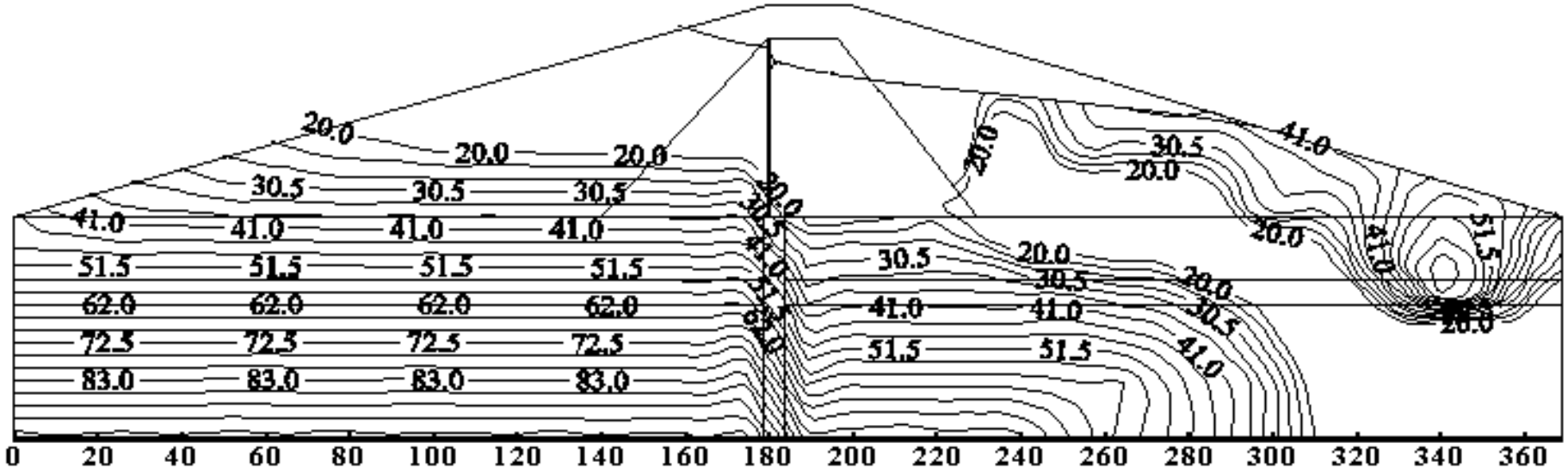

Figure (٥.٩) Contour Map of Pressure Head Distribution for Minimum Water Level (Elevation ١٥٠.٢٠).

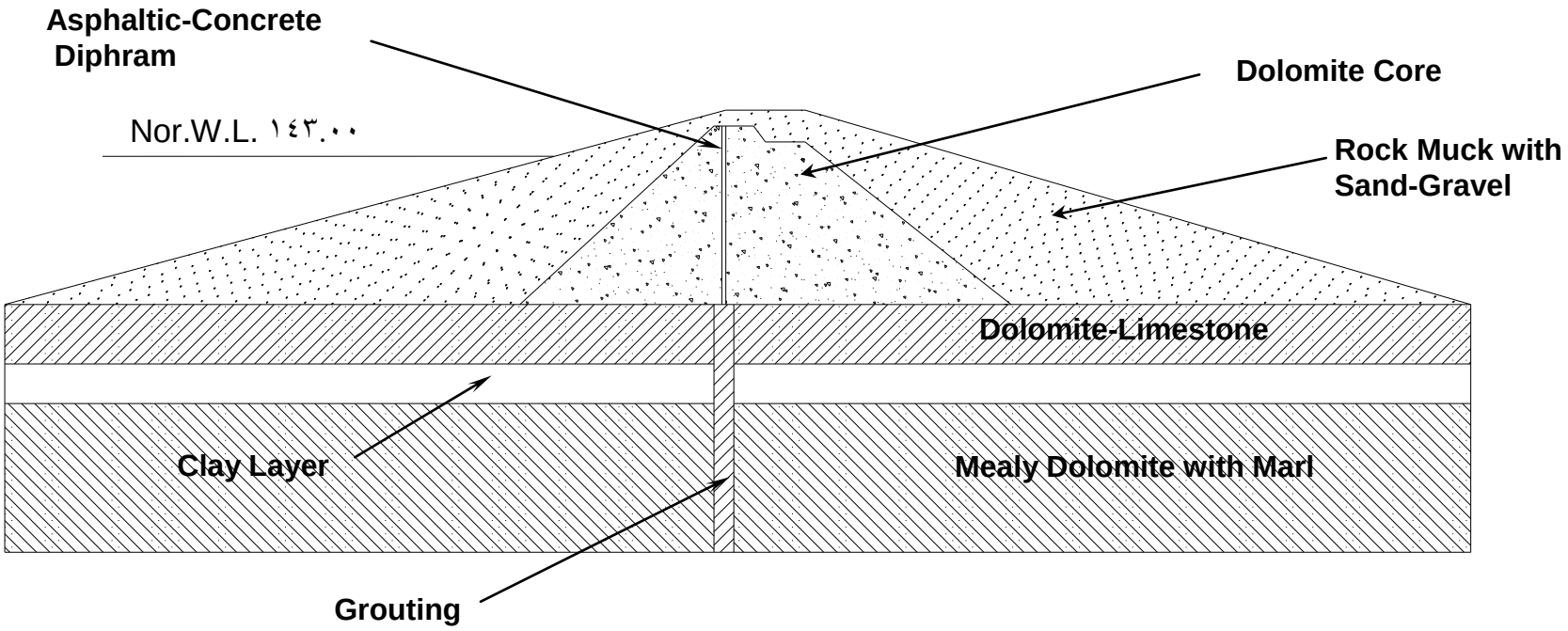

Figure (٥.١) A Typical Cross Section of The Dam [After Al-Jorany, ١٩٩٦].

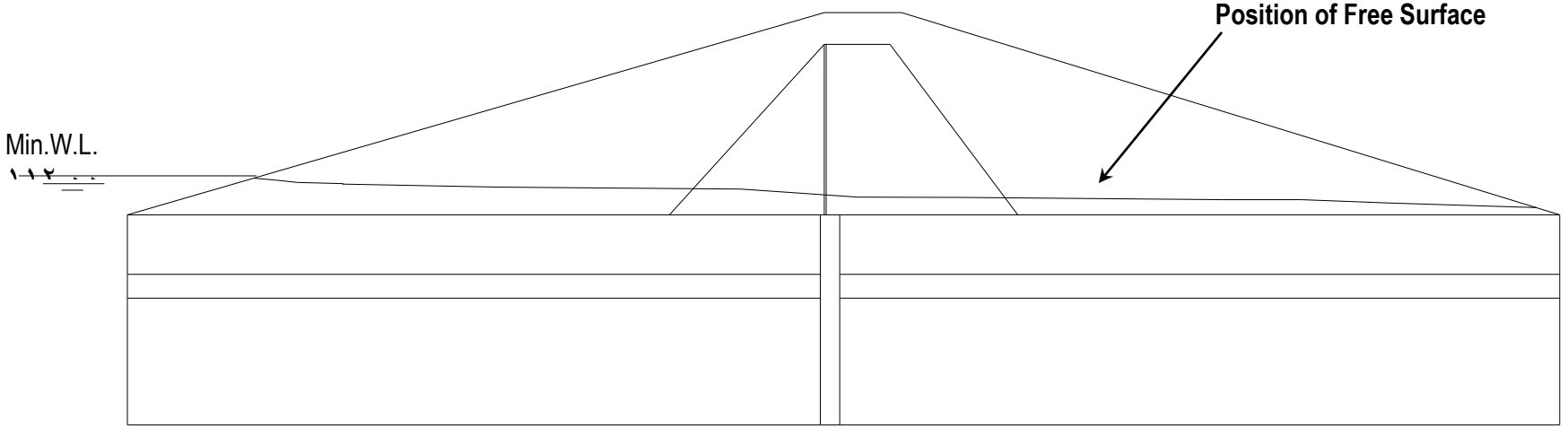

Figure(٥.١١) Location of Free Surface for Minimum Water Level(Elevation ١١٢.٠٠)

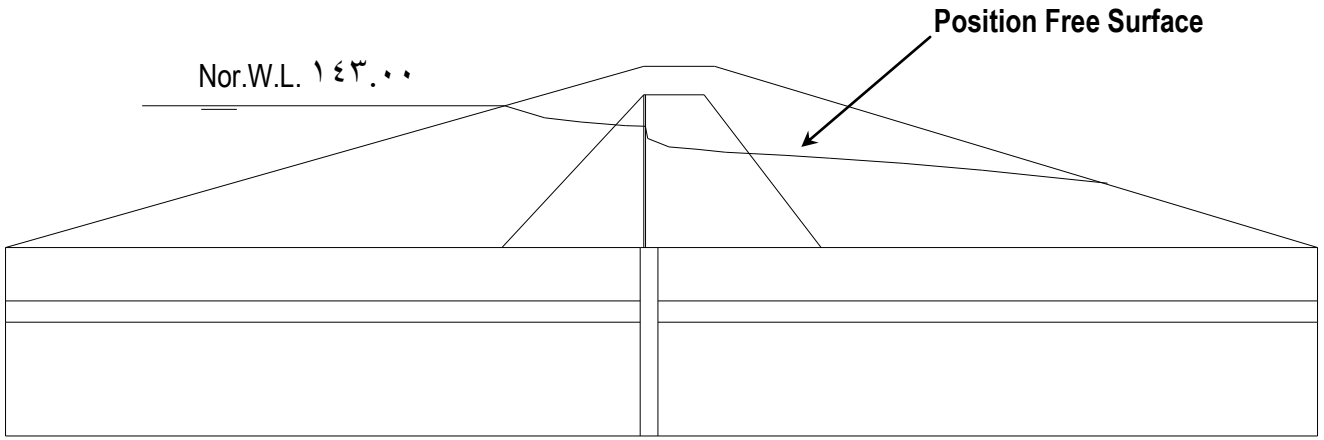

Figure (٥.٣) Location of Free Surface for Normal Water Level (Elevation ١٤٣.٠٠).

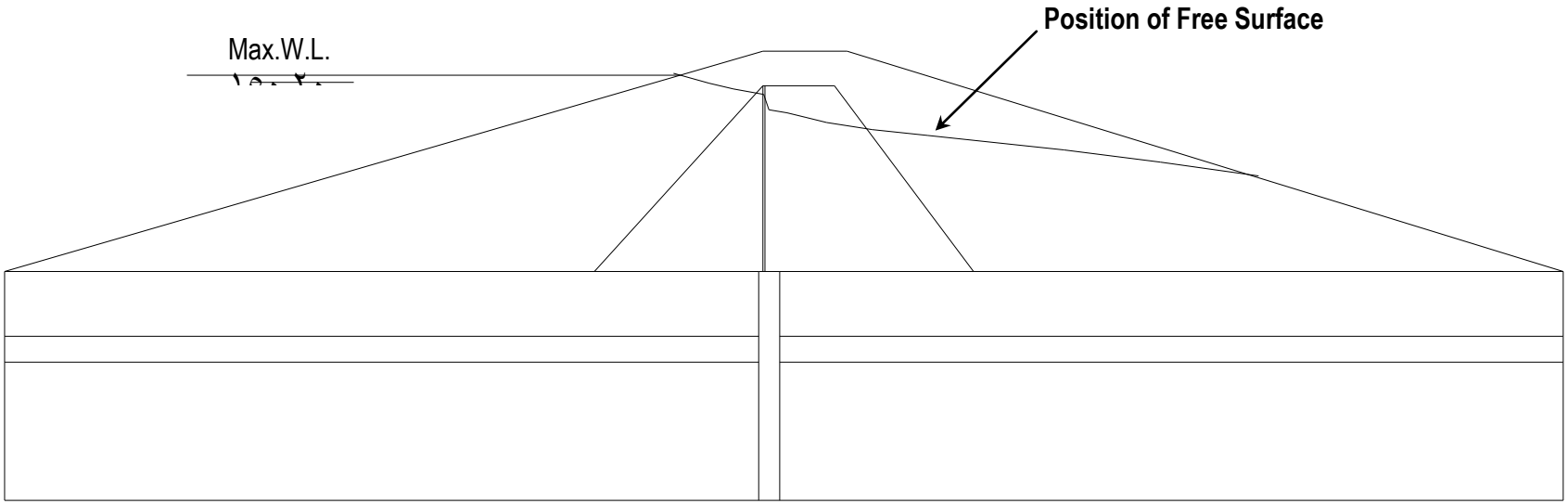

Figure (٥.٧) Location of Free Surface for Maximum Water Level (Elevation ١٥٠.٢٠).

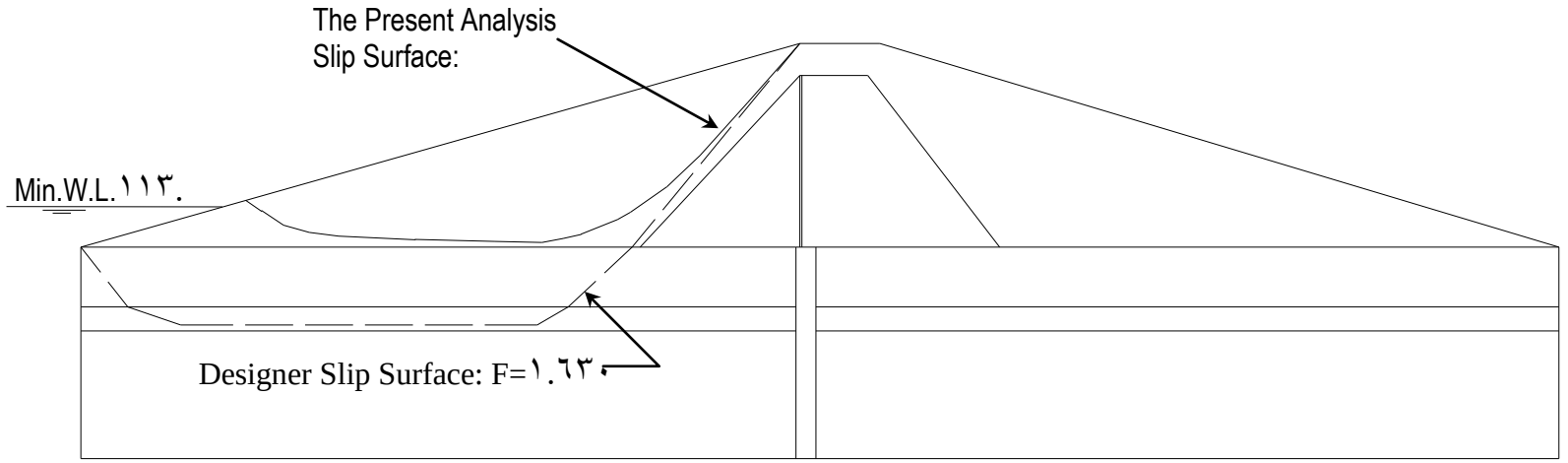

Figure (٥. ١٤) Results of the Present Analysis when Water at Minimum Level (Elevation ١١٣.٠٠).

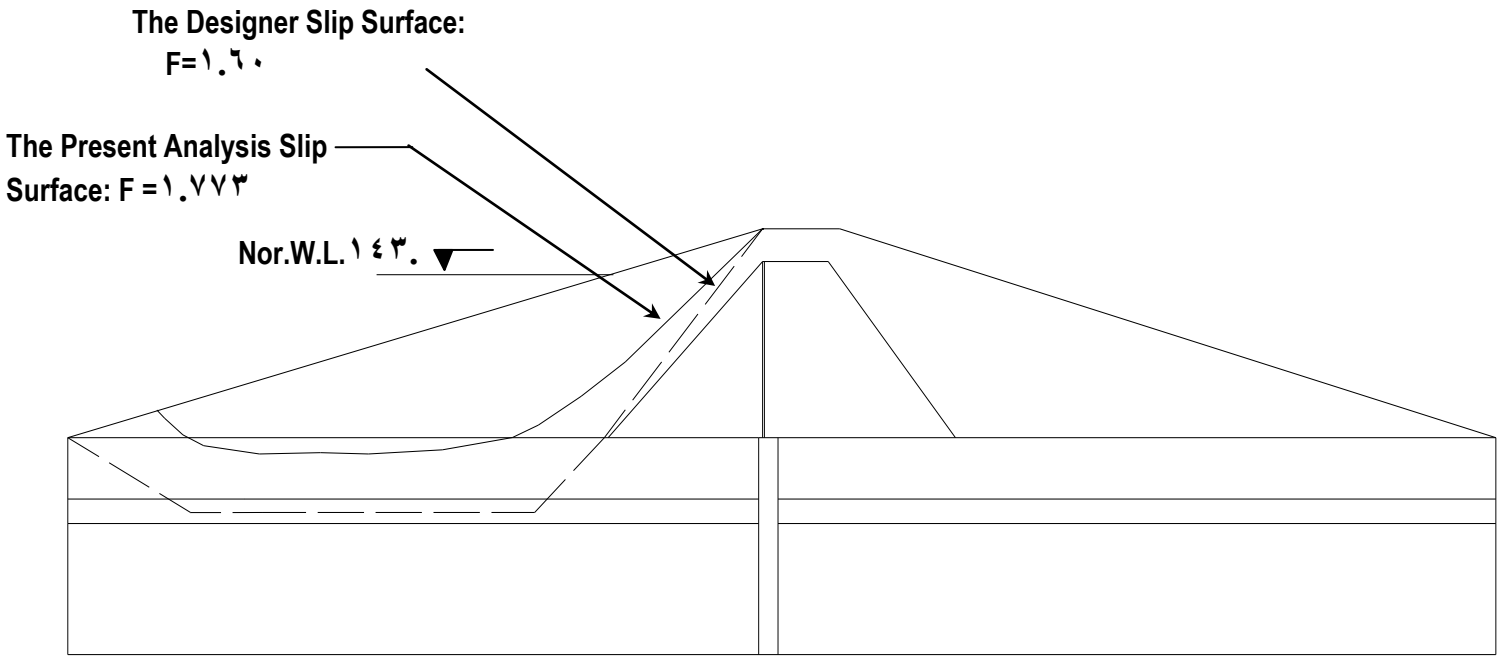

Figure (٥.٦) Results of the Present Analysis when Water at Normal Level (Elevation ١٤٣.٠٠).

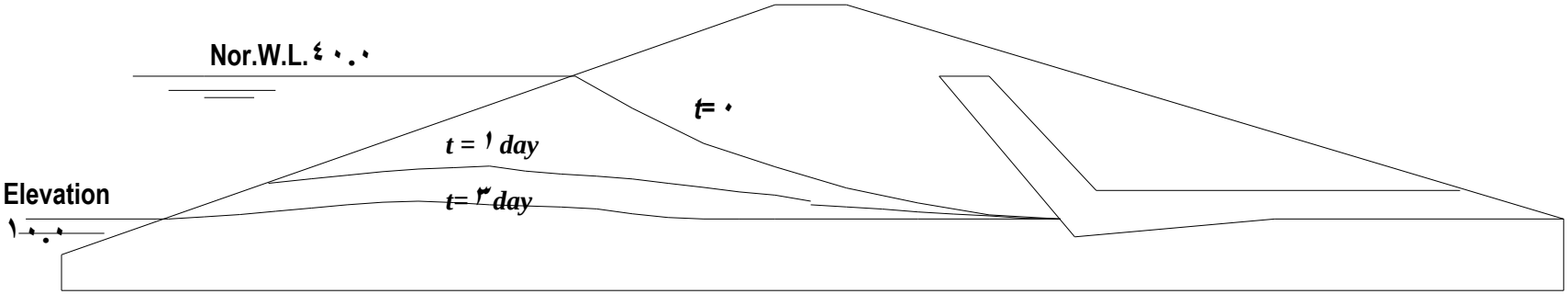

Figure (٤. ٩) Computed Successive Movements of Free Surface Due to Sudden Drawdown in Otter Brook Dam.

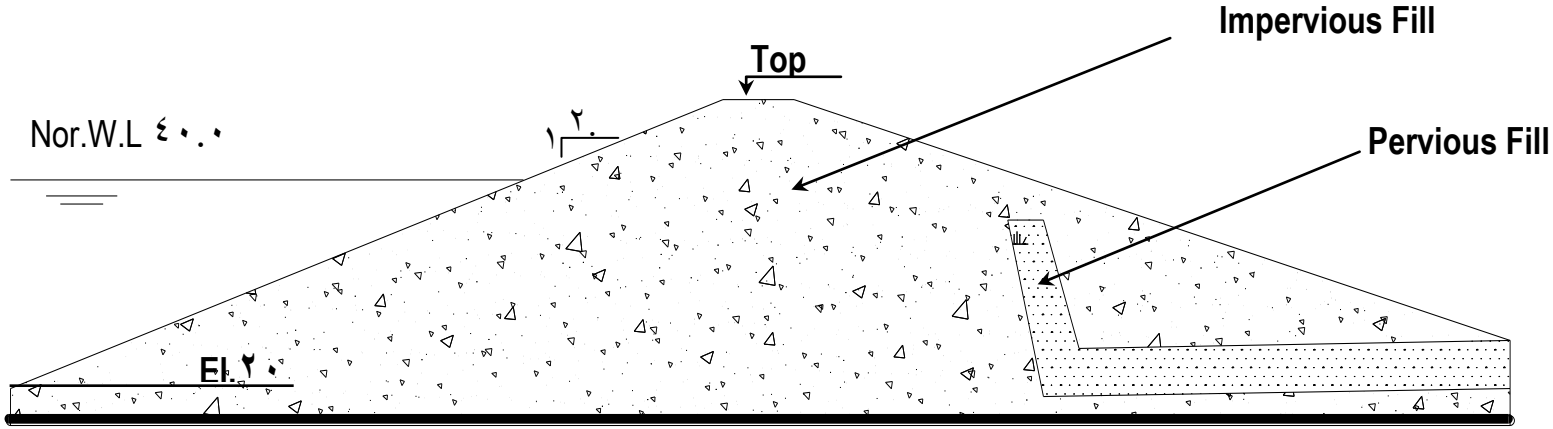

Figure (٤.٦) The Section of Otter Brook Dam (Desai and Abel, ١٩٧٢)

Number of Elements =٢٨٠

Number of Nodes =٣١٥

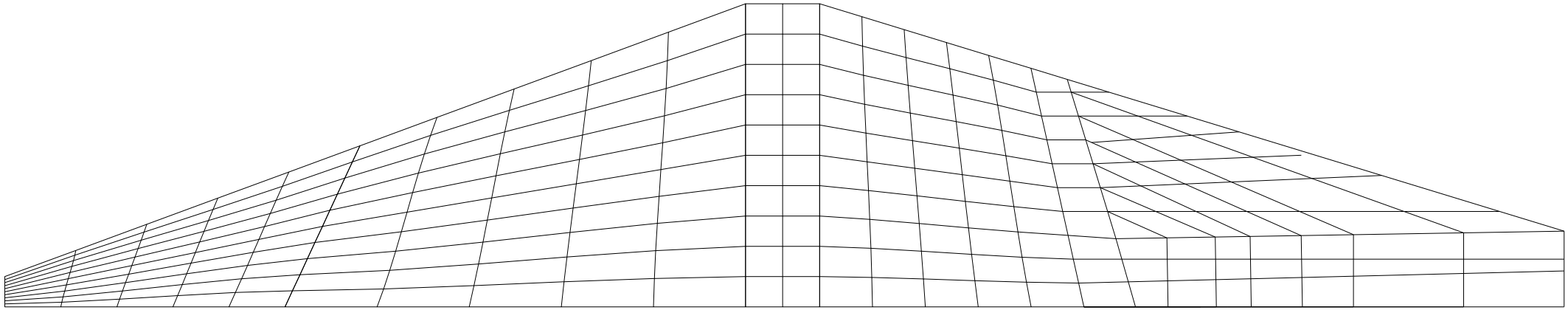

Figure(٤. ٧):The Finite Element Mesh Of The Otter Brook Dam (Not to scale).

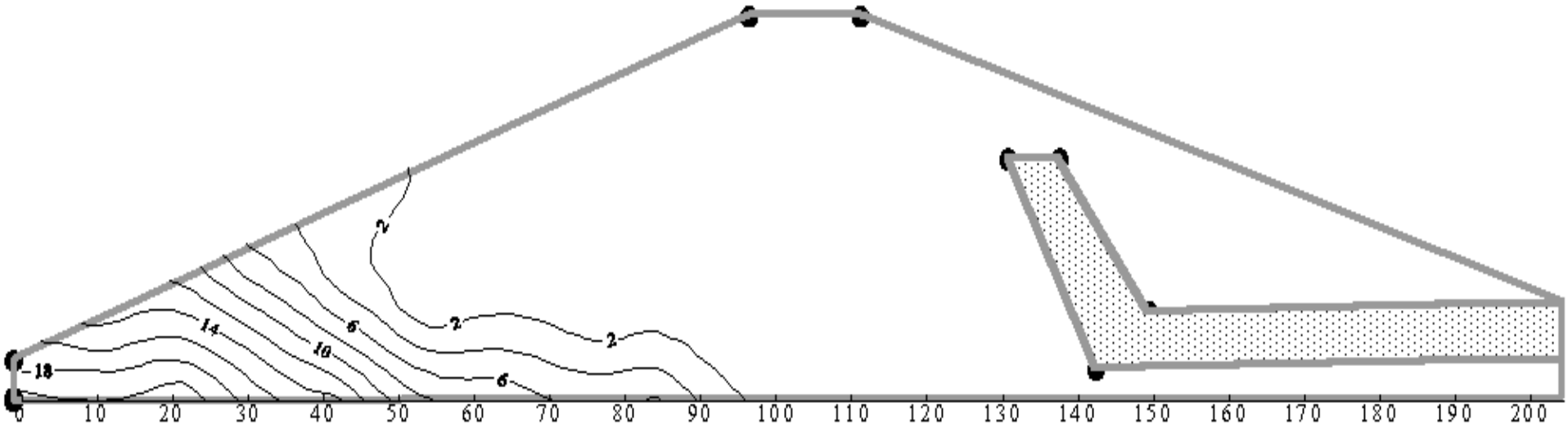

Figure (٤. ١٤) Contour Map of Pressure Head Distribution in Otter Brook Dam for Time=٣ Days and Drawdown Rate=٣m/day .

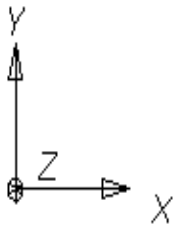

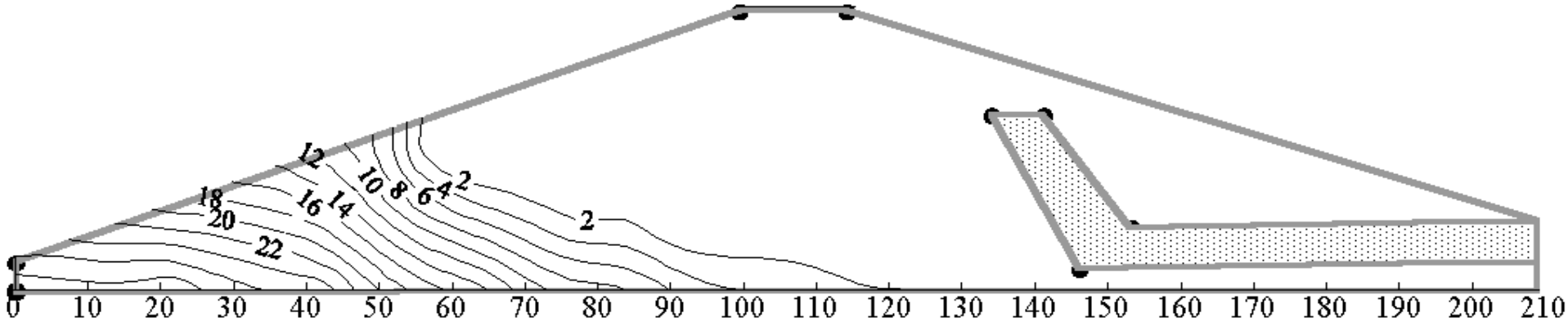

Figure (٤. ١٠) Contour Map of Pressure Head Distribution in Otter Brook Dam for Steady State Conditions.

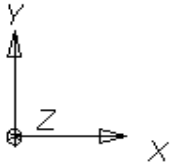

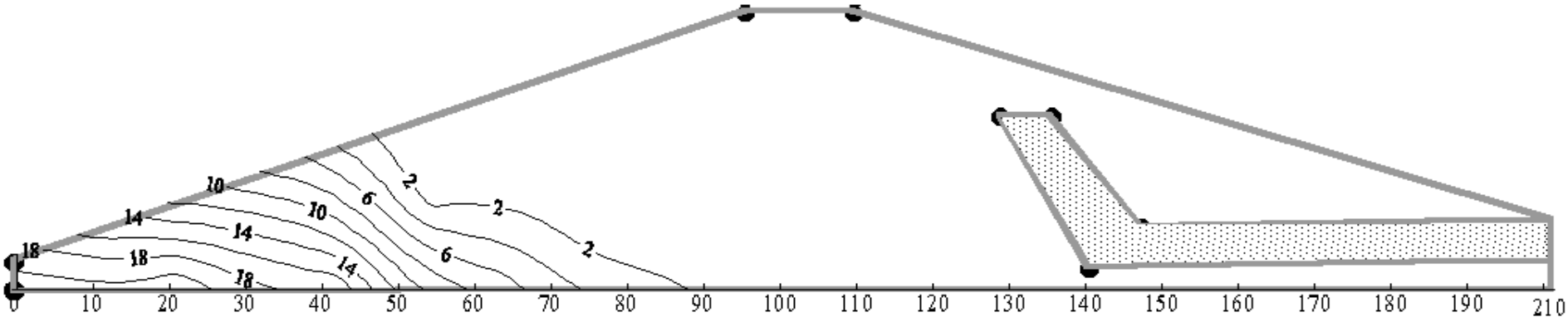

Figure (٤. ١١) Contour Map of Pressure Head Distribution in Otter Brook Dam for Time =٠.٥ day and Drawdown Rate=٣٠m/day .

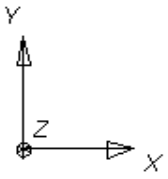

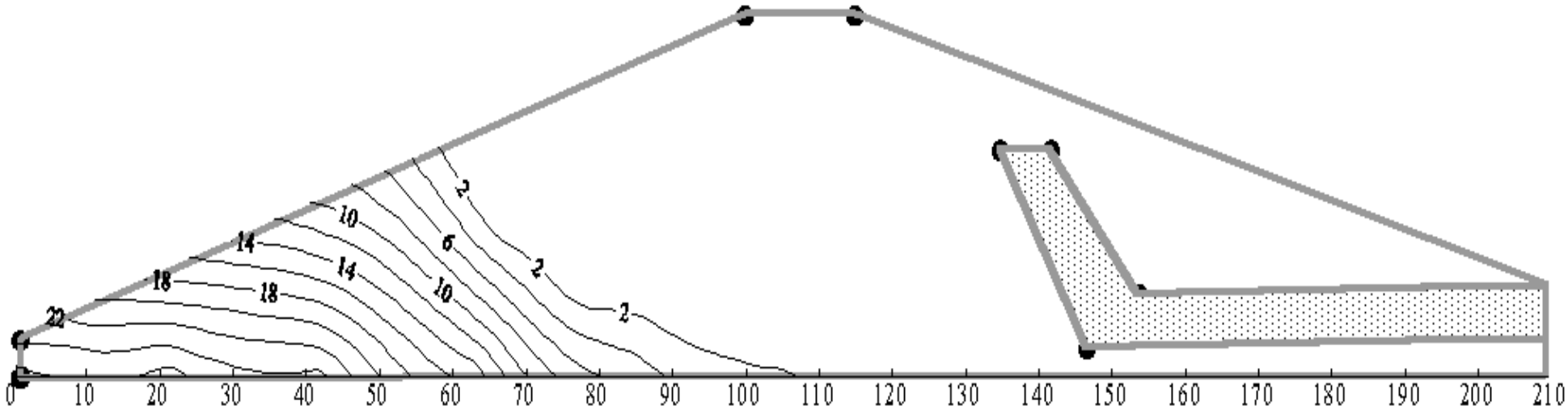

Figure (٤.١٣) Contour Map of Pressure Distribution in Otter Brook Dam for Time=١ day and Drawdown Rate=٣m/day .

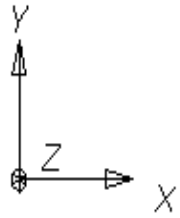

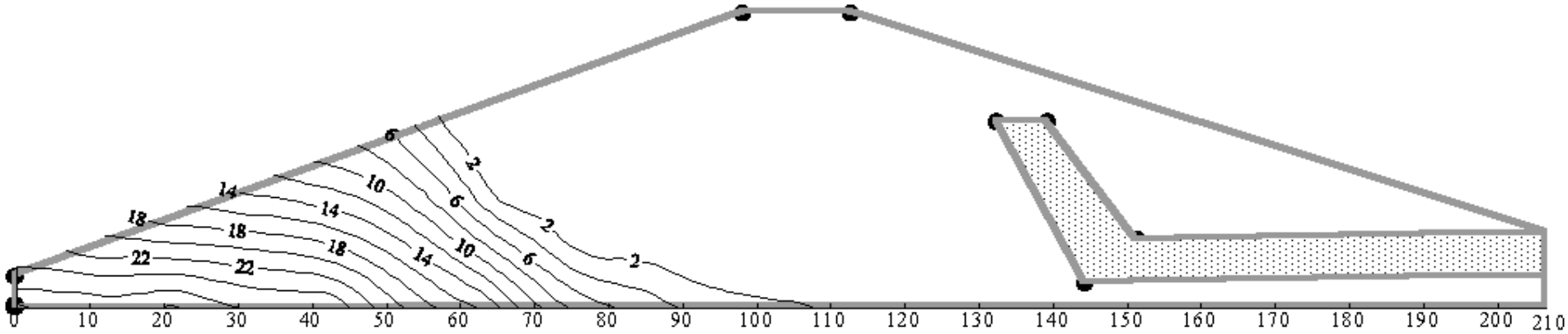

Figure (٤.١٢) Contour Map of Pressure Head Distribution in Otter Brook Dam for Time=٠.٥ day and Drawdown Rate =٣m/day.